Travail de fin d'études et stage[BR]- Travail de fin d'études : Investigation of different control algorithms for refrigeration cycle and evaluation of technical solutions for automation of refrigerant charge management[BR]- Stage

Auteur : Roemers, Quentin
Promoteur(s) : Lemort, Vincent
Faculté : Faculté des Sciences appliquées
Diplôme : Master en ingénieur civil électromécanicien, à finalité spécialisée en énergétique
Année académique : 2023-2024
URI/URL : http://hdl.handle.net/2268.2/20163

Institute of Thermodynamics (B49)
Allée de la Découverte 17
4000 Liège
Roemers Quentin

Investigation of different control algorithms for refrigeration cycle and evaluation of technical solutions for automation of refrigerant charge management

A case study at Copeland Welkenraedt

Master's Thesis

June 10. 2024
Travail de fin d'études réalisé en vue de l'obtention du grade de master Ingénieur Civil en Electromécanique
Ecrit par Quentin Roemers et supervisé par Vincent Lemort
Année académique 2023-2024
Université de Liège - Faculté des Sciences appliquées,
Institute of Thermodynamics (B49), Allée de la Découverte 17, 4000 Liège Belgium

Department of Engineering
Trois Bourdons 27. 4840 Welkenraedt
https://www.copeland.com/

Title:

Investigation of different control algorithms for refrigeration cycle and evaluation of technical solutions for automation of refrigerant charge management

Theme:

PID, System Identification, Refrigeration Cycle, Model Predictive Control, Control System, and Regulation of Charge Refrigerant

Project Period:

February 14, 2024 - June 10, 2024

Author:

Roemers Quentin

Supervisors:

Vincent Lemort

Simon Lenaerts

Pierre Poysat

Appendices: 6

Number of Pages: 122

Hand-in Date:

June 10. 2024

Abstract:

This thesis investigates control system improvements for Hot Gas By-Pass (HGBP) and gas cycle load stands at Copeland Welkenraedt. The current controllers struggle to reach the operating points of compressors efficiently, leading to a waste of time, energy, and resources.

To address these issues, a two-part approach is proposed. First, a data-driven modeling approach utilizing system identification with experimental data is used to represent the HGBP stands numerically. A Multi-Model PID control strategy with a piecewise linear model with gain scheduling is then developed to adjust PID parameters based on the identified model. The possibility of a Multi-Model Model Predictive Control (MPC) algorithm is also explored. The goal is to achieve faster transitions between operating points and reduce test time.

Second, the thesis investigates automatic refrigerant management for the HGBP and gas cycle systems. For the HGBP stands, level sensors are proposed to signal the need for adding or withdrawing refrigerant. A method to calculate the appropriate liquid receiver size is also presented. For the gas cycle stand, a solution suggests the utilization of a tank storing refrigerant with a coiled tube heat exchanger to manage refrigerant based on pressure changes induced by heating or cooling the tank.

The conclusion suggests further research on optimizing data acquisition methods for system identification and comparing different PID tuning techniques.

Nomenclature

Acronyms

A_3	Highly flammable/explosive
ADMM	Alternating Direction Method of Multipliers
AH	Alstrom and Hagglund
ARMA	AutoRegressive Moving Average
ARMAX	AutoRegressive Moving Average with eXogenous input
ARX	AutoRegressive with eXogenous input
ATEX	Atmospheres Explosives
CARIMA	Cross Correlation Autoregressive Integrated Moving Average
CC	Cohen-Cohen
CCS	Consistent Control Strategy
CFC	Continuous Function
CHR	Chien-Hrones-Reswick
COP	Coefficient of Performance
CV	Controlled Variables
EEV	Electronic Expansion Valve
EVI	Enhanced Vapor Injection
FBD	Function block diagram
FISTA	Fast Iterative Shrinking Threshold Algorithm
FOPTD	First Order Plus Time Delay
GPC	Generalized Predictive Control
HCR	Hrones-Chien-Renwick
HFC	Hydrofluorocarbon
HGBP	Hot Gas Bypass
HVAC	Heating, Ventilation, Air Conditioning
HX	Heat Exchanger
IAE	Integrated Absolute Error
IDE	Integrated Development Environment
IMC	Internal Model Control
LCN	Local Controller Network
LD	Ladder Diagram
LMI	Linear Matrix Inequality
LMN	Local Model Network
LPV	Linear Parameter Varying
LQG	Linear Quadratic Gaussian
LQR	Linear Quadratic Regulator
LSM	Least-squares Method
MISO	Multiple Inputs- Single Output
MIMO	Multiple Inputs- Multiple Outputs
MPC	Model Predictive control
MV	Manipulated Variables
OPC	Open Platform Control
P	Proportional
PI	Proportional Integral
PID	Proportional Integral Derivative
PLC	Programmable Logic Controllers
POU	Programmable Organisation Unit
PRBS	Pseudo Random Signal
R290	Propane
R744	Carbon dioxide
RHC	Receding Horizon Control
RMSE	Root Mean Square Error

SFC	Sequential function
SIMC	Skogestad Internal Model Control
SISO	Single Input- Single Output
SOPTD	Second Order Plus Time Delay
SSTO	Steady-State Target Optimization
ST	Structured Text
TV	Total Variation
VCC	Vapor Compression Cycle
ZN	Ziegler-Nichols
	Subscripts
bp	Bypass
cd	Condenser
d	Delay
displ	Displacement
ev	Evaporator
k	At current time k
ref	Refrigerant
sub	Subcooling
sr	Superheating
	Greek Letters
Γ	Nyquist Criterion stability
$\delta_{\text{cut off}}$	Cut off probability
ϵ(t)	Estimated residual
ϵ_{p,k,t_k}	Model error
θ	Delay of the system
τ	Relative Time constant
φ_m	Phase margin
φ	Regression vector
ω	Frequency
	Latin Letters
A	Dynamic matrix
a_c	Time delay fraction
A_V	Waterside valve of condenser
B	Controllability matrix
C	Observability matrix
C(s)	Transfer function of the controller
CS(s)	Noise sensitivity function
d	Disturbances
D	Load disturbance matrix
e(t)	Error of the system
EEV	Electronic expansion valve
G_c(s)	PID transfer function
g_m	Gain margin
h	Enthalpy (J/kg)
H(s)	Transfer Function
|H|	Amplitude of H
$\angle$ H	Phase of H
K	Feedback gain
K_p	Proportional gain
k_r	Feedforward gain
K_v	Valve coefficient
K_∞	Ultimate Gain (ZN)
L(s)	Loop transfer function
L	Apparent delay
m	Mass (g)
M	Convergence vector
$\dot{M}$	Mass flow rate (kg/s)
MM	Molar mass (g/mol)
m_{ref}	Mass of refrigerant (g)
M_s	Maximum of the sensitivity function
n	Number of moles (mol)
n	Noise
N	Number of measurements
N	Rotational speed (rpm)
P	Pressure (bar)
P(s)	Transfer function of the system
$P_{chiller}$	Condenser input power
P_{int}	Intermediate pressure
P_{mot}	Compressor input power (kW)
P_∞	Ultimate Period (ZN)
p_{r,k,t_k}	Bayesian probability
PS(S)	Load sensitivity function
P_1	Compressor inlet pressure
P_2	Compressor outlet pressure

$Q_{chiller}$	Refrigerating power of condenser (kW)
Q_{heater}	Heating power of evaporator (kW)
r	Reference
R	Gas constant (J/K mol)
s	Complex frequency $j\omega$
S(s)	Sensitivity function
s_m	Sensitivity margin
SP	Setpoint
T	Temperature (K)
T	Tonnes of refrigeration (U.S.)
T	Apparent time constant
T_i	Integral time (s)
T_d	Derivative time (s)
t_k	Current time k
T_m	Sampling time
T(s)	Complementary sensitivity function
T_1	Compressor inlet temperature
T_2	Compressor outlet temperature
T_{63}	63 % of rise time
T_{95}	Settling time
ΔT_{sr}	Superheating temperature
U(s)	Input Fourier transfer
u(t)	Input
v	Number of inputs
V	Volume (L)
V_{displ}	Volume displacement (cc)
V_N	Least squares criterion
v(t)	White noise vector
$w_{i,k}$	Specific weight
x	State vector
X_p	Proportional band (-)
Y(s)	Output Fourier transfer
y(t)	output
$\hat{y}$(t)	Estimated output
$\bar{y}$(t)	Mean output value

Table of Contents

List of Figures

Chapter 1

Introduction

The introduction of control systems in industry has developed into a vital role in integrating part of modern manufacturing, industrial processes, and testing. For most industrial processes, it is vital to control pressure, temperature, and flow in a fast efficient way to provide optimal operations in order to improve productivity and energy efficiency. To that extent, control systems have been thoroughly studied both in practice and in theory.
However, most systems include high-order dynamic behaviors or large time delays along with uncertainties and non-linearities making them sometimes hard to model based on physical laws alone. Henceforth, system identification on the specific process is commonly used in industry to represent the model numerically through experimental data.

With the help of a numerical representation of a process, advanced controller algorithms can be applied to the system to improve the performance, stability, and efficiency of a process. The simple PID control is the oldest and most well-known method of control and is still widely applied in industries. However, newly advanced control techniques offer more sophisticated approaches beyond simple PID control and can handle complex systems where traditional control struggles. Advanced control techniques consist of a wide range of different controller algorithm types.
Among the advanced control techniques, adaptive control has grown in popularity over recent years. This control method is used when the system dynamics or operating conditions of the process vary over time and continuously adjusts control parameters based on real-time measurements and feedback to maintain optimal performance. Model Predictive control can be included in the adaptive control technique which uses a mathematical model of the system to make predictions and optimize control actions over a future time horizon taking into account system dynamics and constraints.
In the case in which system behavior cannot be accurately described by mathematical knowledge, fuzzy logic control suggests the use of linguistic or fuzzy interference to handle systems with imprecise or uncertain information. It can incorporate human-like decision-making by using linguistic variables

and rules to handle non-linearities and complex relationships.
Another popular technique is the neural network control which uses a trained network of input-output of a system to approximate the system dynamics and determine the control actions.
A last advanced technique is the cascade control which involves a primary control loop and one or more secondary control loops. The primary loop controls a primary variable, while the secondary loops control other variables that directly affect the primary variable. Cascade control improves system response, disturbance rejection, and interactions between variables.
All the presented techniques can be combined partially together to produce the adequate controller algorithm for a specific system.

On another matter in recent years, the fight against climate change has extended to the world of refrigerant and HVAC & refrigeration systems. Traditionally, many refrigerants are composed of hydrofluorocarbon (HFC) such as R410A, boasting excellent performance but with a hidden cost which is a high Global Warming Potential.
To reduce the impact of HFC refrigerants, the Environmental Protection Agency has introduced a set of regulations aimed at reducing the usage of high global warming potential (GWP) refrigerants. Complying with the EPA regulations offers some advantages in the future as it ensures environmental sustainability, improves health and safety as well as long-term cost savings due to energy cost reduction. The HVAC industry is then pushed to transition to more natural refrigerants.
In the case of the company Copeland, development, testing, and production of new products working with natural low GWP refrigerants such R290 (propane) or R744 (CO_2) has been in place for several years already. Copeland is an industry specializing in the development and production of scroll compressors for HVAC and refrigeration systems. At Welkenraedt Copeland's site, a SoundRoom facility has been built to evaluate the sound of variable speed compressors working with different refrigerants with a specific focus on R290 and R744. The SoundRoom facility is equipped with two Hot Gas ByPass stands for 15 T and 50 T of refrigeration power and a gas cycle stand for 10 T.

1.1 Problem identification

The SoundRoom actual controller struggles to control the system of the HGPB accurately between nominal operating points. The effects of the non-optimized controller are even more critical for extreme points of the operating map of the compressor. As a result, tests take longer periods of time than needed to be carried out wasting energy in the process. The poor performance of the controller can be explained by the fixed parameters of the controller not being adapted to the whole operating range of the compressors. Models of refrigerant systems are non-linear. Furthermore, the spatial disposition of the HGBP stand induces a delay in the system exacerbated at low refrigerant volume rates.

Another problem can also be noticed concerning refrigerant management. During the tests of compressors, the desired output temperature of the compressor is often not met due to insufficient refrigerant in the system and manual injections of refrigerant in the refrigerant loop have to be performed in response.

1.2 Purpose and Goal

The main objective of this thesis is a case study at Copeland Welkenraedt in the sound laboratory to improve the current control systems of the 2 hot gas by-pass load stands working mostly with propane (R290) and a gas cycle load stand working with R744 (CO2) as refrigerant in order to reach nominal operating points of variable speed scroll compressors faster. In the case of the present work, the newly developed controller algorithm should be able to cover the whole operating map of compressors with power up to 50 tons. To that extent, a mix of advanced control techniques is used to produce an adequate controller algorithm specific to the vapor compression cycle of a hot gas by-pass stand. The improved controller algorithm of the stands is expected to be able to transition rapidly between operating conditions of the compressor in order to reduce the time and energy required to reach nominal operating points for sound measurements. To that extent, a Multi-model PID based on a gain scheduling approach applies an adaptive PID parameters algorithm using the neural network built of a bank of linear FOPTD models obtained from system identification to control the varying system dynamics required by the testing of compressors. The application of the algorithm is also presented for the use of Multi-model MPC algorithm replacing the PID control method. The control has to produce reliable and accurate data and take into account the large varying parameters of the stand such as different compressors' size, speed, refrigerant, evaporation temperature, and condensing temperature.

In addition to the primary goal of this thesis, an automatic management of charge refrigerant is also sought for the case of the HGBP and gas cycle systems.

1.3 Acknowledgements

I am deeply grateful to several individuals who supported me in completing this thesis.
First, I would like to thank Simon Lenaerts and Pierre Poysat at Copeland for providing me with the opportunity to conduct this research project within the company. Their knowledge of the scroll compressor and refrigeration cycles was invaluable in shaping the direction of my work.
My deepest gratitude also goes to Prof. Vincent Lemort, my university supervisor for his expertise in thermodynamics and his eagerness to meet with me and discuss my ideas were crucial to the successful completion of this thesis.
I would be remiss not to acknowledge Dr. Hernandez Andres, a researcher at the Institute of Thermodynamics of Liège. His willingness to share his knowledge and insights on system identification significantly improved my understanding and helped me refine my research approach.
Finally, I extend my sincere thanks to the technicians at Copeland for their invaluable assistance during the experimental phase of this research. Their expertise and willingness to help ensured the smooth running of the experiments.
Of course, none of this would have been possible without the unwavering support and encouragement of my family and friends. To them, I express my deepest gratitude.

Chapter 2

Problem formulation

As stated in the purpose and goal, this thesis presents an advanced method of control to accurately control hot-gas bypass stands that can be applied to any refrigeration system as well as an automatic charge refrigerant management. The method of control presented in the thesis is applied to a case study at Copeland Welkenraedt in the Sound Laboratory. The objective behind the case study is to improve the current control systems of 2 hot gas by-pass load stands working most of the time with propane (R290) and a gas cycle load stand working with R744 (CO_2) as refrigerant in order to reach nominal operating points of variable speed scroll compressors faster and introduce an automatic regulation of refrigerant charge in the stand.
The first part of the problem formulation consists of an introduction to the different load stands implemented at Copeland Welkenraedt. A second step involves the investigation of the current controller and functionalities. The two first steps result in the identification of the problem.
In the second part of the problem formulation, the actual management of charge refrigerant for both stand types is introduced.

To begin with, a little reminder of the working principle of the Vapor Compression Cycle (VCC) is presented to understand the more complex stand implemented at Copeland. As can be observed in Figure 2.1, the essential components of a VCC are the compressor, the condenser, the evaporator, and the expansion valve.

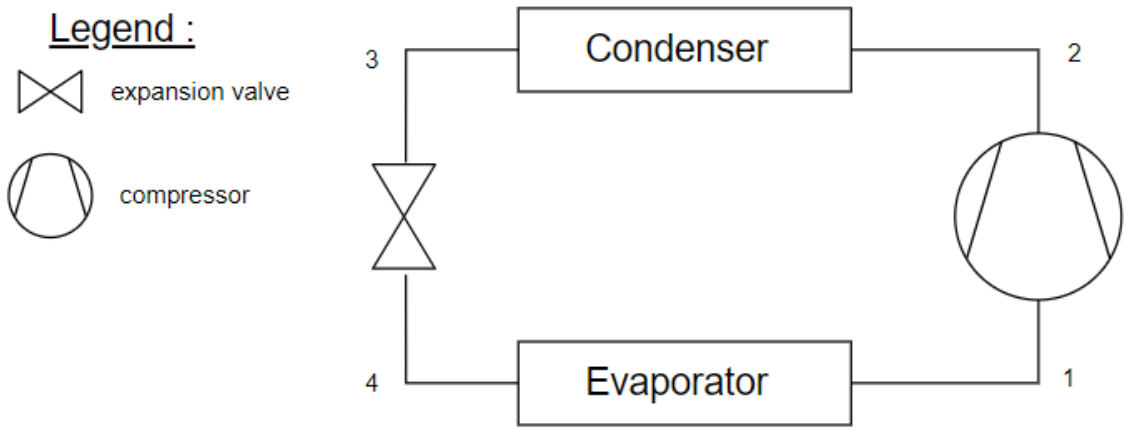

Figure 2.1: Model of a Vapor Compression Cycle

The system is characterized by two pressure levels called low pressure P_1 corresponding to the evaporating pressure and high pressure P_2 corresponding to the condensing pressure. The evaporator has the function of bringing the refrigerant to a vapor state with a margin ΔT_{sr} to ensure that all the refrigerant is in a vapor state. To that extent, a suction accumulator is often placed between the evaporator and the compressor to prevent liquid from entering the compressor by storing refrigerant and thus ensuring the safe operation of the compressor. The vapor superheating then enters the inlet of the compressor at a specific temperature T_1 and pressure P_1. The compressor then provides the work to bring the superheated refrigerant to a higher pressure P_2 and higher temperature T_2. The flow of refrigerant enters the condenser and is brought to a liquid state with a margin ΔT_{sub} to ensure a liquid state at the outlet. A liquid receiver is often placed in the system after the condenser to store refrigerant and ensure that no liquid refrigerant builds up in the condenser. The last component is an expansion valve and as the name indicates it expands the refrigerant back from high pressure P_2 to low pressure P_1. The refrigerant is then ready to start a new vapor compression cycle.

When a simple model of the system is sought, the evaporator and condenser are assumed ideal (e.g. without pressure losses and at constant temperature) as the losses are considered small enough to be neglected. The compressor is considered isentropic and the expansion valve is on the other hand considered isenthalpic. A simple model representing a vapor compression cycle is modeled in EES and the corresponding P-h diagram is represented in Figure 2.2.

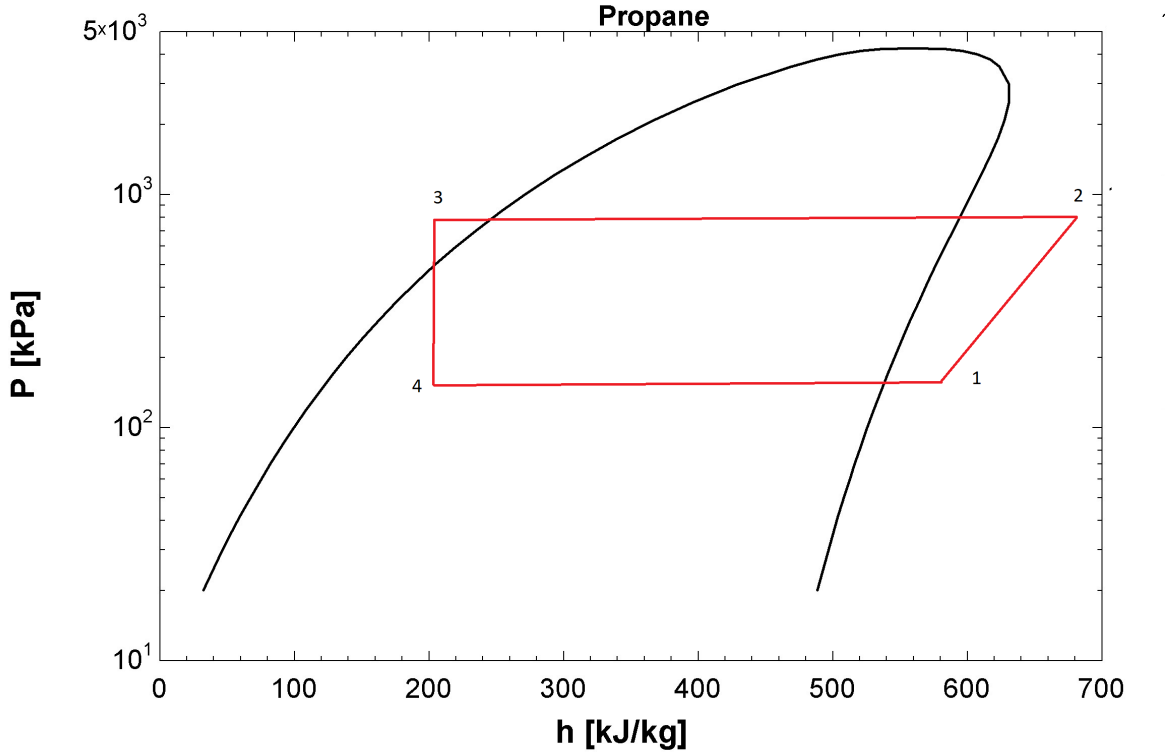

Figure 2.2: P-h diagram of thevapor-compression cycle

Controlled Variables :

First, one can identify the variables determining the nominal operating points of the compressor. These variables are varied in order to gather data to compute the operating maps relative to one specific compressor including efficiency and COP. In this simple case, the inlet and outlet temperature and pressure of the compressor are to be monitored. As a matter of fact, one can observe that:

- P_1 can be controlled using the expansion valve
- T_1 can be controlled by the heat rate furnished in the evaporator to the system
- P_2 can be controlled by the heat rate given in the condenser by the system
- T_2 cannot be controlled directly but depends on the three other parameters and the mass of refrigerant in the system

These variables P_1, T_1, P_2 T_2 represent the outputs of the system controlled or the Controlled Variables (CV). Other variables influencing the work of a compressor are the rotation speed, the refrigerant, the

volume displacement, the amount of refrigerant, the temperature inlet of the cold side of the condenser, the superheating and subcooling temperature margins. These other variables represent disturbances of the system as they can influence the system but are not directly meant to be controlled.
A simple black box model with inputs and outputs of the compressor can be seen in Figure 2.3.

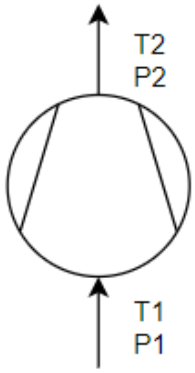

Figure 2.3: Black box of the compressor

In the case study, the compressor characteristics are not fixed and can vary depending on the application such as rotation speed, or refrigerant used and the volume displacement. The hot gas by-pass load stands have been built so that any refrigerant can be used. However, only two refrigerants are to be evaluated which are R744 also called carbon dioxide for the gas cycle and R290 called propane or C_3H_8 for the hot gas by-pass.

A sufficient point to notice is that R744 pressure can rise up to 130 bar and for his counterpart, R290 pressure to 35 bar which makes the system's pressure vary a lot depending on the refrigerant and the type of stand.

Concerning safety as R290 is highly flammable (A_3), the laboratory has to be equipped with strict safety types of equipment including gas detectors used as a preventive measure and ATEX fans. Once the concentration of R290 has reached 10 % of the lower flammability concentration, a fan is activated and once 20% is reached, the test bench is shut down to prevent risks from combustion from occurring.

2.1 The Different Load Stands

In this section, The 3 different load stands are presented and their relative components are also presented with technical descriptions.

To test compressors, several test equipment using different refrigeration circuits can be used to control the operating conditions of a compressor in order to evaluate the characteristics of a specific compressor and to perform experimental tests. The different methods are briefly described but further information on the different testing methods can be read in the section methods 7 or in the manual handbook [3] from the company ASHRAE.

The first method is the calorimeter which consists of electrically heating the refrigerant to act as an evaporator but is not to be analyzed further in this work.

A second method consists of using a hot gas bypass (HGBP) to save energy. The evaporator is totally withdrawn from the process and by the use of a bypass, superheated gas from the exit of the compressor is mixed with liquid refrigerant to produce superheating vapor fed to the compressor. This method of testing saves energy as the cooling power required in the system is reduced to equal the work of the compressor.

The last method is the gas cycle in which the refrigerant only stays in a vapor state and is used with R744 refrigerant. The system is composed of a compressor building the high pressure, an expansion valve following to expand until an intermediate pressure, a condenser to cool down the fluid at constant pressure, and a second expansion valve to expand refrigerant to the low pressure for the inlet of the compressor. The energy saving is further enhanced as the refrigerant does not need to cool down to a liquid state.

In the studied case, 2 hot gas by-pass stands function with a refrigeration power of 15 T and 50 T and a gas cycle stand for R744 functions with a refrigeration power of 10 kW. Note that a refrigeration power in T is an American unit and the equivalence of 1 T of refrigeration equals 3.51685 kW.

The different load stands also present an EVI injection system used for specific applications of some compressors.

2.1.1 Hot gas bypass stand 15 T

The first load stand analyzed is a hot gas bypass system composed of a variable speed scroll compressor, a plate condenser, electronic expansion valves, a filter dryer, a liquid receiver, and 2 mixing chambers. As previously mentioned, a hot gas bypass system is characterized in comparison to a classical refrigeration cycle by the use of a bypass which uses the discharge gas from the output of the compressor to provide the energy required for evaporation. Therefore, the condenser only needs to provide an energy equivalent to the power of the compressor. A representation of the system can be seen in Figure 2.4.

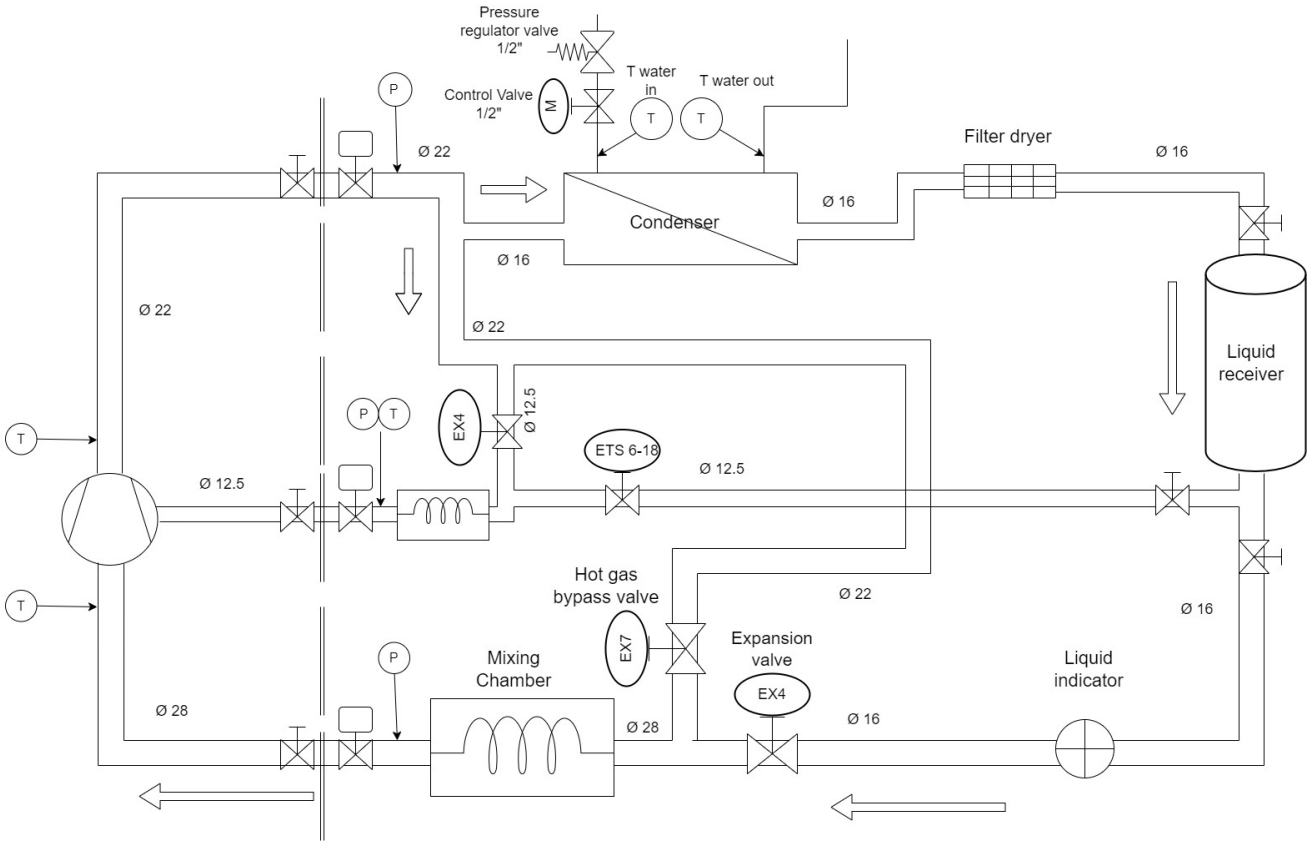

Figure 2.4: Load stand of the hot gas bypass stand 15 T

The description of the components of the load stand starts after the compressor and follows the flow of refrigerant in the system. The compressor is not described as it is not fixed. The pipes from the system are all made from Copper with varying diameters as can be seen in Figure 2.4.

The condenser ensures that the refrigerant returns to a liquid state by withdrawing energy from the refrigerant side. The flow of water in the condenser is controlled by a pressure regulator valve (Bellimo

1/2) and a control valve (1/2). The control of the flow of water and temperature inlet-outlet of the condenser is crucial as it controls the high pressure side of the system. The condenser is a plate heat exchanger functioning in a counter-current mode.

A filter dryer is placed after the condenser to remove the moisture from the refrigerant.

A refrigerant receiver of 3.9 L with a pressure of 45 bar follows to partially manage the charge of refrigerant in the system.

For the injection of vapor and for the inlet of the compressor, the system consists of the following a first electric expansion valve controls the amount of cooled refrigerant and a second one controls the amount of refrigerant bypassed from the outlet of the compressor.

A mixing chamber is situated after the connection to ensure an ideal mix of vapor refrigerant .

Specific electric expansion valves are used in the stand Figure 2.4 and Table 2.1 include the technical description of those valves.

Table 2.1: Technical description of Electric expansion valves (*EX4 low-pressure drops correspond to a liquid use)

Types	Flow	Valve coefficient K_v [m^3/h]	Pressure drop [bar] [-]	Isentropic efficiency	Total number of steps [-]	Maximum pressure difference [bar]
EX4	Uniflow	0.21	0.35-0.5*	80 %	750	30
EX5	Uniflow	0.68	0.5	80 %	750	30
EX6	Uniflow	1.57	0.35	80 %	750	30
EX7	Uniflow	5.58	0.5	80 %	1600	35
EX8	Uniflow	16.95	0.5	80 %	2600	30
ETS 6 -18	Bi-flow	0.082	0	100 %	480	47

2.1.2 Hot gas bypass stand 50 T

The second hot gas by-pass load stand of 50 T is composed of the same components with different sizes than the stand 15 T. This is explained by the fact that both stands are used to test compressors but for different ranges of refrigerating power. The electronic expansion valves are different and the diameter of the pipes is larger for the stand of 50 T as the mass flow of refrigerant is higher. The diameter of the pipes and valves used can be found in Figure 2.5 and the characteristics of the valve can be found in Table 2.1. The representation of the stand can be seen in Figure 2.5.

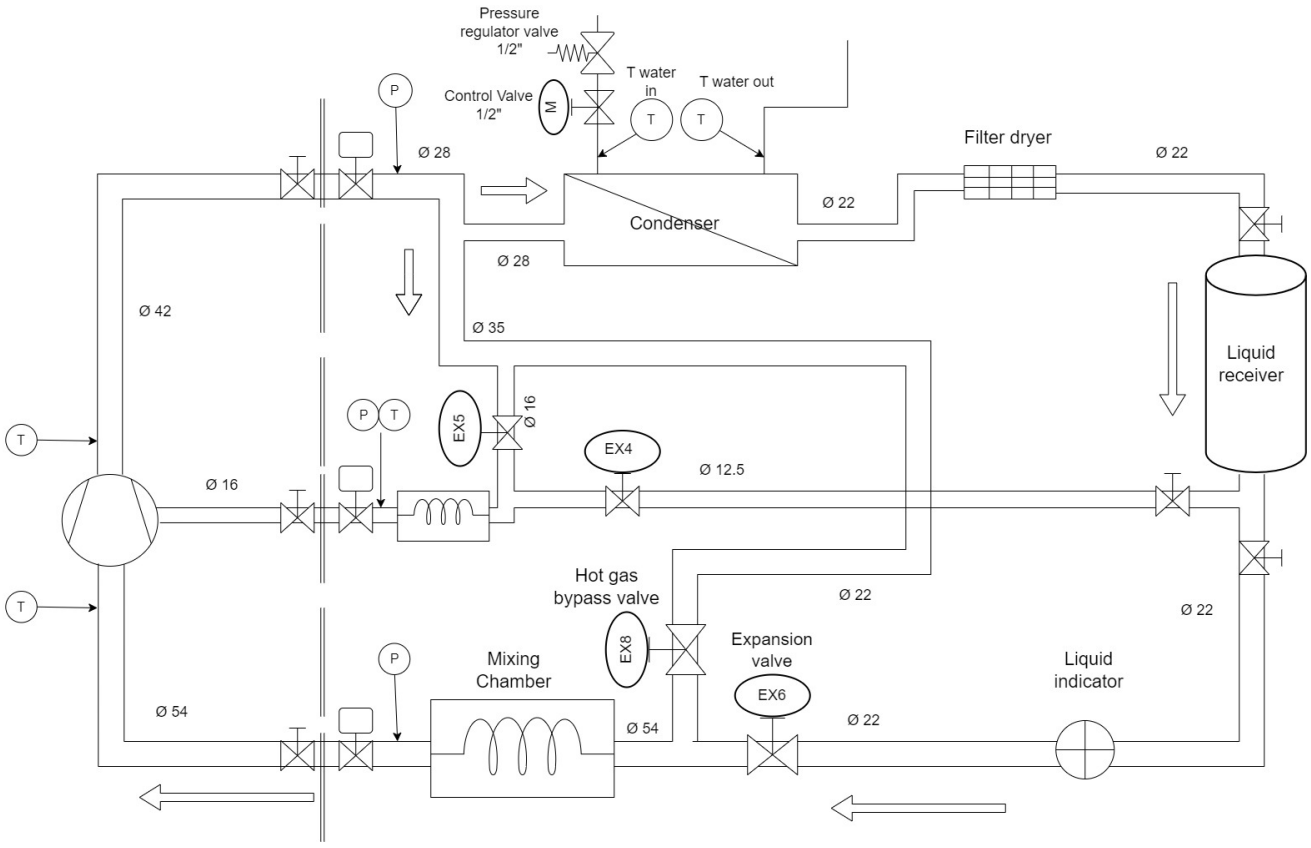

Figure 2.5: Load stand of the hot gas bypass stand 50 T

2.1.3 Gas Cycle stand 10 kW

The last load stand implemented in Copeland at Welkenraedt is a gas cycle working with R744 refrigerant also known as CO_2. The stand is composed of a compressor, a filter dryer, electronic expansion valves, and a condenser. As the name indicates the gas cycle is a method in which the refrigerant stays in a vapor state throughout the cycle. The first expansion valve expands the refrigerant to an intermediate pressure. The condenser is situated at this intermediate pressure and provides the cooling required before another expansion valve expands the fluid to the inlet of the compressor. This method as can be read in Methods 7 works on a very small range of power (10kW) and therefore it consumes less energy than the HGBP stand. A representation of the system can be seen in Figure 2.6.

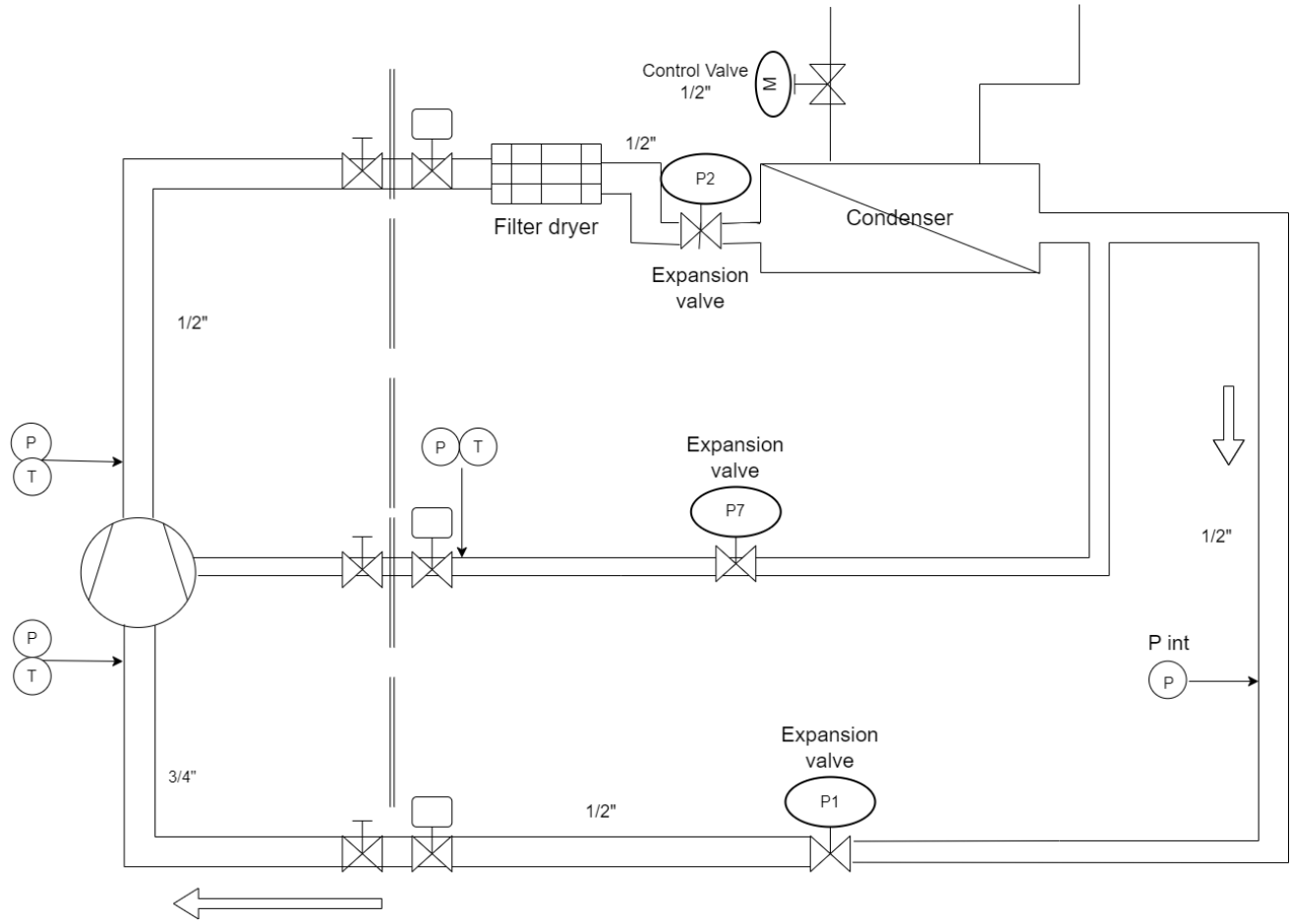

Figure 2.6: Load stand of the gas cycle stand 10 kW

There is also an EVI path to inject vapor refrigerant to cool down the compressor during the compression of the refrigerant. The components of the gas cycle are not described in further detail as the main focus is the HGBP stands.

2.1.4 Sensors

Each load stand is equipped with a variety of sensors to measure the desired variables. The sensors' main function is to measure data for the sake of adjusting and testing the compressor's characteristics. In the case of the HGBP stands, these sensors consist of 2 pressure transducers (+1 for vapor injection), 4 thermocouples Type T (+1 for vapor injection), and a pressure switch for measurements of temperature and pressure. The pressure transducers are composed of a compressor suction pressure sensor PT4 measuring a relative pressure from 0 to 18 bar with an accuracy of 0.2 bar, and a compressor discharge pressure sensor PT4 measuring relative pressure from 0 to 50 bar with an accuracy of 0.2 bar. The thermocouples consist of PT100 4 wires 2 mm sensors to measure the suction and discharge tem-

perature of the compressor. A pressure switch KPS47 is also present with a setting range of 6-60 bar and an accuracy of 6 bar to regulate pressure and safeguard equipment from damage or running at low efficiency. A liquid indicator is also present to check if the refrigerant after the condenser is in the liquid phase. On the other hand, the gas cycle stand is composed of 3 pressure sensors (+1 for EVI), and 2 temperature sensors (+1 for EVI). No further information on the sensors is given as the main focus is on the HGBP stands.

2.1.5 Controlled & Manipulated Variables

In this subsection, only the controlled and manipulated variables for the HGBP stands are presented.

Concerning the control of the HGB stands more specifically of the compressor's performance, three essential parameters are required to be manipulated during compressor testing. In order to obtain the full range of a compressor's operation maps, the suction temperature, suction pressure and discharge pressure of the compressor have to be controlled.
The outlet pressure of the compressor P_2 is controlled by the amount of cooling water provided to the condenser. Therefore, the opening of the valve A_v and the inlet temperature of water from the condenser circuit control the pressure in the condenser. Even though, the temperature of the condenser inlet is supposed fixed, thus only the valve of the water side of the condenser A_v controls the amount of water.
The second manipulated variable is the inlet pressure P_1 of the compressor which is controlled mainly by the expansion valve of the bypass EEV_{bp}.
The last parameter, the inlet temperature T_1 of the compressor is highly dependent on the previous controlling parameters. Nevertheless, it can be controlled through the opening of the electronic expansion valve (EEV) after the condenser EEV_{cd} as it controls the quantity of liquid refrigerant to be mixed with hot gas and therefore, the temperature inlet of the compressor.

To sum up the case of the HGBP stand, the Controlled Variables (CV) are the inlet temperature T_1, inlet and outlet pressure P_1 and P_2. These CV are controlled by the use of the Manipulated Variables (MV). The MV are the valve from the waterside of the condenser A_v, the EEV of the bypass EEV_{bp} and the EEV after the condenser EEV_{cd}.

2.1.6 Problem identification

The main problem occurring during the test of HGBP stands is the slow convergence of CV between setpoints (SP). In other words, the controller is not able to quickly and accurately transition from one nominal operating point to another. These slow convergence effects impact the time required to test compressors and therefore result in a loss of time and resources. The inlet and outlet pressure of the compressor P_1 and P_2 still converge in a reasonable time.

However, the change in the opening of EEV after the condenser EEV_{cd} takes long time delays to affect the inlet temperature of the compressor (T_1). The long settling time is explained by the geometry of the stand. In reality, the stand is characterized by very long pipes (up to 5 meters) between the temperature sensor of T_1 and the EEV after the condenser EEV_{cd}. As a result, the heated refrigerant takes time to travel to the temperature sensor. The geometry of the stand cannot be modified to shorten the length of the pipes as both HGBP stands share the same isolated sound room to test the sound of compressors. The room is isolated to exclude any sound interference from components of the system apart from the compressor.

In the case of a low-speed compressor with a low volume of refrigerant, the effects of the valve opening EEV_{cd} take an even longer time to be sensed by the temperature sensor of T_1. Even though the temperature sensor is situated far away from the control valve, the loss of heat to the ambient is negligible as the pipes are encapsulated in insulation pipes.

The delayed response time of sensors can be seen in the output responses of the sensors relative to each CV whenever a step change (change in MV) is applied in the system but is not taken into account by the controller parameters. Therefore, the controller is not able to adapt correctly to the change of MV and tries to correct the error of measurement faster than the system can respond. As a result, oscillations of the CV can be observed around the reference and the error is rectified slowly over time to reduce the oscillations.

With the help of the example of the controlled variable T_1, one can easily understand that the actual implementation of the controller is not optimal and improvements are needed to better control the dynamics of the system.

In addition, the dynamics of the system are time-varying and can greatly change depending on the compressor size and speed, the refrigerant used, and the low and high pressure conditions.

With the help of a HGBP EES code, Figure 2.7 represents some nominal operating points in the operating map of the variable speed compressor **YHV046HG** with R290 as the working fluid and a volume displacement of 46 cc. The operating map is built for 196 points with a liquid subcooling of 4 K and a suction superheat of 10 K at a compressor speed of 4500 rpm. Each point is characterized by a different evaporation temperature and a different condensing temperature and therefore a specific low and high pressure. Figure 2.7 represents 7 extreme and 1 middle points of the operating map.

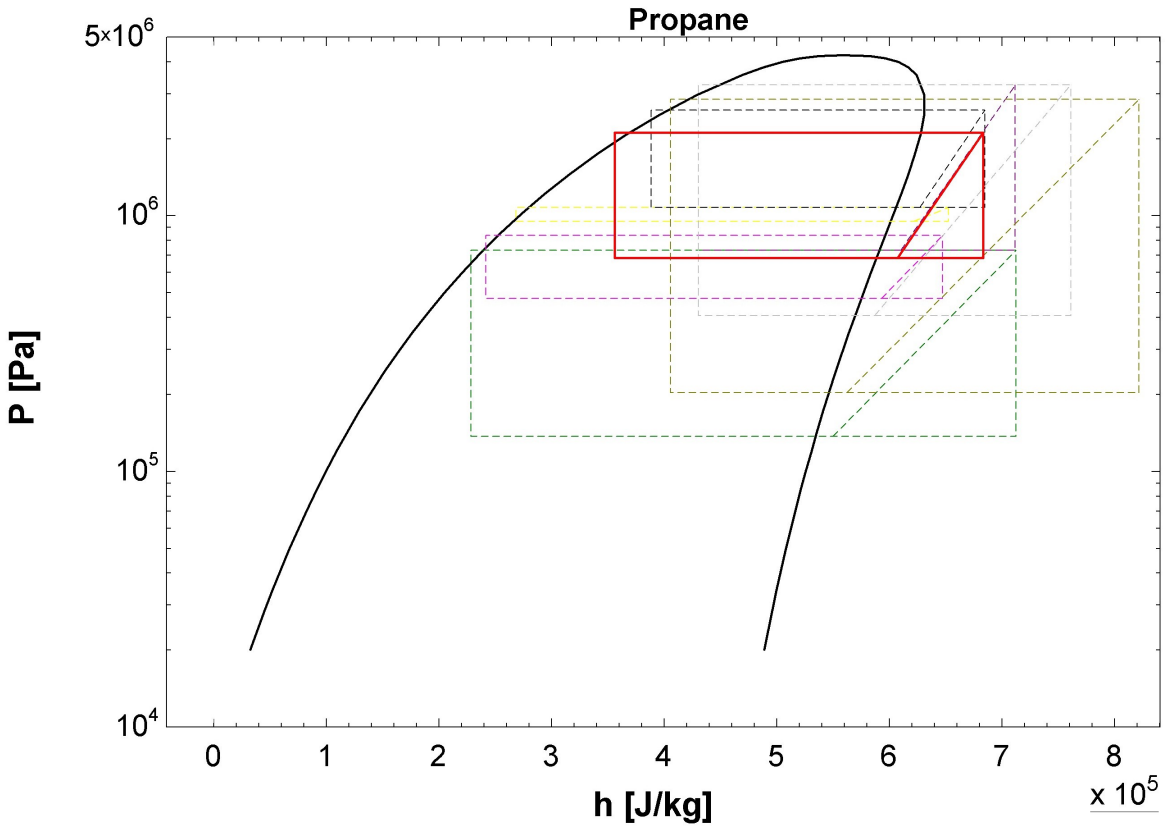

Figure 2.7: Diagram P-h of 7 points from the operating map of YHV046HG

The characteristics associated with each point can be found in Table 2.2. A middle point of the operating map is represented in a red line and the extreme points are in dotted lines.

Line	T_{ev} [°C]	T_{cd} [°C]	Isentropic efficiency [%]
Red	12.5	60	73.21
Purple	15	82	71.35
Grey	-5	82	58.57
Orange	-25	75	50.66
Green	-35	15	50.07
Pink	0	20	50.78
Yellow	25	30	19.76
Black	30	70	72.62

Table 2.2: Nominal operating points of compressor **YHV046HG** for fixed speed at 4500 rpm

As can be observed from Figure 2.7, the conditions of the system can vary a lot even when the speed, the size of the compressor, the type of refrigerant, the temperature difference of superheat and subcooling are fixed. The problem is extremely complex to tackle with simple control systems. The representation of the compressor with already specific rotation speed, fluid, compressor type, subcooling and superheating temperature for different points in the operating map in Figure 2.7 shows the complexity of the wide range of applications in which the control is required to function efficiently.

The actual control is done by the use of a PID controller further described in the subsection of the actual controller. Nevertheless, the actual control is not efficient to control the non-linear refrigeration system with its wide range of applications in which the compressor is expected to vary in size, speed, and type of refrigerant.

2.2 Actual controller

In industrial control, Programming Logic Controllers (PLC) have become a key part of modern industry to provide monitoring and control for a variety of industrial systems. A controller can first be defined as a feedback or closed-loop control that compares a measurement (CV) to the desired value (setpoint or reference) and generates a correction signal applied to the controlled output (MV). The goal of the controller is to effectively eliminate the error which is the difference between the setpoint and the output measurement. By definition, a PLC has the function to control a system's parameters using internal logic programmed into it. PLC can be programmed through the use of the standard support IEC 61131-3 including Function Block Diagram (FBD), Structured Text (ST), Sequential function (SFC),

Ladder Diagram (LD), and Continuous Function (CFC). Among those programming languages, FBD, LD, and SFC are graphical ones compared to ST, IL, and SFC which are textual. The general composition of a PLC code typically consists of several Programmable Organisation Units (POU) written in IEC 61131-3 and communicating with each other. Using an IDE (Integrated Development Environment), PLC code can be parsed, compiled, and executed. An example of IDE is CODESYS, developed by Smart Software Solutions. CODESYS therefore supports the above IEC 61121-3 code.

In this case study, the stand of the sound room is equipped with the m Tron T system provided by the manufacturer JUMO GmbH & Co technology for monitoring and control. More precisely, the automation and control systems are performed by the m Tron T system through the use of an Integrated Development Environment (IDE) called CODESYS. Moreover, the m Tron T integrates sensors, controllers, and actuators to provide efficient process control and monitoring. The data acquisition and analysis are also performed by the same device. The system enables real-time monitoring, data logging, and analysis, allowing users to meet specific set points, and make informed decisions based on the collected data.

2.2.1 CODESYS

As mentioned above, the controller m Tron t uses a flexible and programmable platform called CODESYS, an Integrated Development Environment (IDE) for programming controller applications. The programming language consists of the international industrial standard programming language IEC 61131-3 and provides automation solutions to control processes or plants. However, the programming language Python can be supported provided the package " Python editor" by CODESYS allowing script importation and running.

The use of the programming interface Codesys provides the user with a user-friendly configuration, an optional full PLC function with automatic transfer of the hardware configuration to PLC, and the option to create personalized PLC applications in the user-defined part. In the user-defined part, it is possible to create a custom PLC application in standard IEC 61131-3 Structured Text to meet specific application requirements.

2.2.2 Actual PID controller

The actual control consists of 3 PID controllers with basic parameters of a PID controller respective to each pair of main input-output for an industrial process and can be observed in table 2.3. These parameters are sometimes changed by the technicians operating the stand to reach convergence faster. However, those technicians are not specialized in the control of system and PID tuning. As a result, they avoid as much as possible to interfere with the actual controllers.

Table 2.3: Parameters of the PID controllers

Controller	X_p [-]	T_i [s]	T_d [s]	T_n [s]
$T1 - EEV_{cd}$	400	300	0	20
$P1 - EEV_{bp}$	18	5	0	20
$P2 - A_v$	20	120	0	20

The term X_p is the proportional band and represents the proportional term. T_i is the integral time and represents the integration of previous errors in the control. T_d is the derivative time and is used to predict future errors to improve convergence. Even though, no derivative time is used in the current controllers.
It can be noted that the proportional band of the controller $T1 - EEV_{cd}$ is set very high to reach a slow but steady convergence without an overshoot as the temperature T_1 is highly influenced by the two other inputs valves (EEV_{bp} and A_v).

The different parameters of a PID controller are explained theoretically in the section of theory 6.2. To resume, a PID controller acts upon a system based on the input u(t) and the error e(t) (the difference between the output and the estimated output) and is of the following general form:

$$u(t) = K_p \left(e(t) + \frac{1}{T_i} \int_0^t e(\tau) d\tau + T_d \frac{de(t)}{dt} \right) \tag{2.1}$$

2.2.3 Self-optimization

The general controller system used is not well-suited to the specific application as it is the default parameter from the manufacturer. However, a function called "auto-tune" is already implemented in the m Tron t system and can be used to provide more suitable PID gains to the compressors' nominal operating points. However, these points will be optimal only for specific operating points of the compressor and not throughout the whole testing range.

The first method has for working principle to apply self-optimization around the reference provided that the reference is already reached.
Once the controller has reached the reference value, an optimization is launched and a modulation rate of 0% and 100% is applied alternatively.
The controller optimizes then the choice of the parameters from the signal oscillating around the reference value and saves it automatically.
This method assures that the overshoot does not lead to material destruction of the sensors. The self-optimization function likely uses the Ziegler-Nichols method to compute the optimal parameters of the PID controller.

A second type of self-optimization also exists.
When the measured value is below the reference value, self-optimization is launched. The system calculates the dead time of the system from the first reaction of the measured value. From the dead time and the slope of the first reaction, a commutation line is drawn. Depending on the linearity of the system, the commutation line prevents the measured value from oscillating above the reference if linear or the overshoot is decreased if non-linear. The controller applies in total two times the modulation rate of 100 % punctuated with a rate of 0 %. After that, the controller takes into account the optimal parameters and adjusts the error.

Another thing to take into consideration is that to determine the parameters of optimization, JUMO supposes that the system is not affected by a time delay. Time delays can cause the system to operate slower and have to be taken into account in the design.

The technicians have tested the self-optimization function at different nominal operating points to

have the optimal tuning parameters for a specific point with no satisfactory results. The use of the self-optimization function can take several hours depending on the operating point. In addition, the tuning parameters are then optimized to stay at a specific nominal operating point. The resulting problem is that the tuning parameters are not optimized for setpoint changes which is the main problem to improve at the load stand.

2.3 Charge management of refrigerant

In the second part of the thesis, an evaluation of the charge management of refrigerant is also investigated. This section underlines the need for management of charge refrigerant and presents the actual manual regulation of charge refrigerant in the case of the HGBP stand and the gas cycle stand.

One important subject when designing refrigerating machines is the appropriate refrigerant mass charge in the system as it is directly linked to performance and stability. Despite the well-known phenomenon, the evaluation of optimal refrigerant heavily relies on trial and error which is time and resource-consuming. Depending on the size and speed rotation of the compressor, the optimal amount of refrigerant in the system varies. As a result, in the case of a variable-speed compressor, automatic management of charge refrigerant is needed to cover the full operation map of the compressor.

Apart from the gas cycle, in most of the refrigeration cycle [3] and [6], the management of charge refrigerant is handled by a liquid receiver placed after the condenser whose main function is to hold liquid refrigerant as a storage tank, to ensure that only liquid is sent to the expansion valve and to prevent liquid refrigerant from backing up into the condenser. The liquid receiver functions as a charge of refrigerant regulator in the case of the hot gas by-pass stand. Accumulators can also be placed before the compressor to prevent liquid refrigerant from flooding the compressor and causing damage and to act as a second storage tank.
However, in the case of the gas cycle, the refrigerant does not enter a liquid state. Therefore, another management method of charge refrigerant is necessary to avoid slow manual interactions by technicians to find the optimal charge of the system at each speed rotation.

Troubles in the management of charge refrigerant can impact the performance, stability, and durability of the compressor. Figure 2.8 shows the impact of the variation of charge refrigerant over a

general refrigeration cycle.

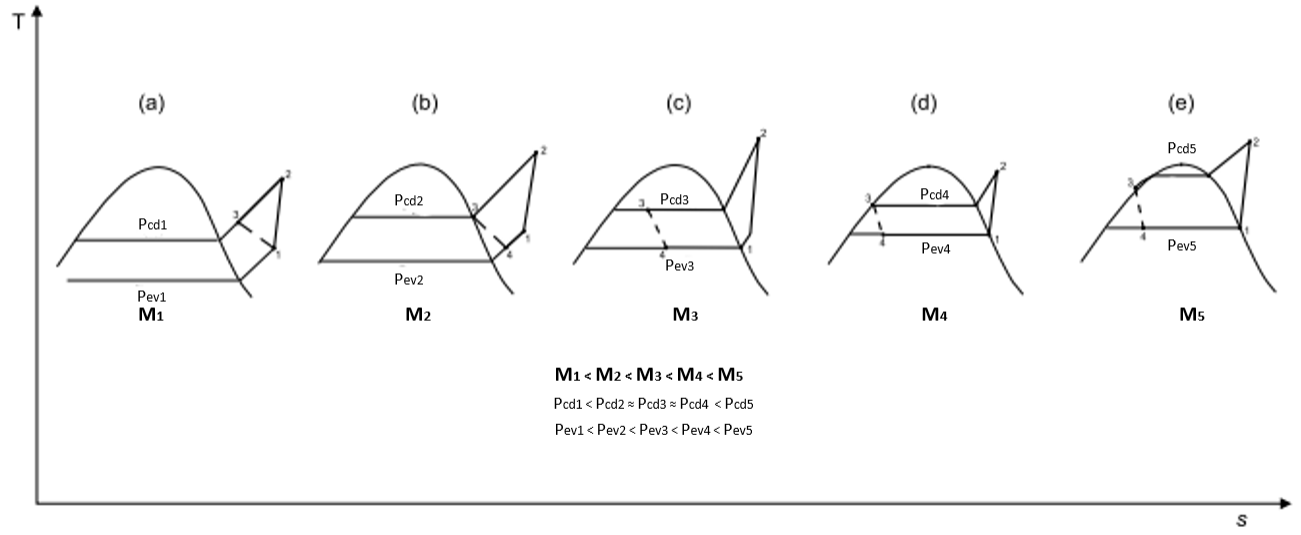

Figure 2.8: Influence of charge refrigerant over a general refrigeration cycle

Starting with case a where an initial small amount of refrigerant M_1 is introduced into the system, a "triangular" cycle first appears in which the compressor cannot bring the refrigerant to the desired pressure. The result is that the condenser cannot provide enough cooling and the refrigerant stays in a vapor state at a temperature close to the ambient temperature. After the expansion valve, the temperature of the refrigerant is already at a much higher value than the design temperature of the evaporator. The evaporator is then not used at all, resulting in the "triangular" cycle. In other words, the refrigerant is already at a higher temperature than the desired temperature for the inlet of the compressor.

For the case b, an increase in the mass of refrigerant in the system $M_2 = M_1 + \Delta M$ such that the refrigerant state at the end of the condenser reaches the saturated vapor line but results in the same case as before with a refrigerant staying in vapor state. However, the evaporator pressure and condenser pressure increase compared to case a according to the ideal gas law ($PV = nRT$).

Increasing the mass of refrigerant further leads to case c for which the outlet of the condenser is in the two-phase region but not fully condensed. The passage through the expansion valve with a two-phase refrigerant leads to a larger decrease in temperature and pressure in the evaporator. The evaporator is partially composed of vapor and liquid refrigerant. The evaporator pressure is however still below the designed value as a too great proportion of vapor enters the evaporator.

In case d, another increase in the mass of refrigerant leads to an almost optimal charge of refrigerant.

Case d corresponds to a fully condensed state at the outlet of the condenser with subsequent throttling to the designed pressure value of the evaporator. The system tends to be unstable but can still function properly. Instability comes from disturbances in the ambient temperature that can cause the refrigerant outlet at the condenser to move back into the two-phase region.
Increasing the mass of refrigerant even further stabilizes the operation of the refrigeration cycle with a subcooling temperature difference which ensures stability of the system with a condensed state at the outlet of the condenser. The case e corresponds to the optimal charge of refrigerant in the system. In a usual nominal operating mode, 10 % of the condenser should be composed of fully condensed refrigerant.
Increasing the refrigerant charge even further will increase the proportion of condensed refrigerant in the condenser reducing the heat exchange area of the condenser and increasing the pressure of the condenser up until the compressor is not able to pump the refrigerant to the condenser pressure anymore. The presence of a liquid receiver can mitigate the surplus of mass refrigerant until the liquid receiver is full.

In the case of the hot gas by-pass, the charge of refrigerant will have a similar impact as presented for the general refrigeration system.
In the case of the gas cycle, a liquid receiver cannot be used as the refrigerant stays only in a vapor state. As a result, the management of charge refrigerant is even more critical. Deviations from the optimal charge refrigerant have an impact on the intermediate pressure corresponding to the pressure of the condenser and the work of the compressor. In a gas cycle as described in methods, the intermediate pressure of the condenser in a gas cycle is always situated between the low pressure and the high pressure in the gas cycle. In the case of too much refrigerant in the system, vapor refrigerant is going to build up in the condenser therefore reducing the heat exchanger area of the condenser. The reduction of the area of heat exchange leads to insufficient cooling power and an increase in the pressure of the condenser until the point for which the compressor is not able to provide the difference in pressure from low to high pressure.
The case with an insufficient amount of refrigerant results in a compressor working at loss with not enough refrigerant entering the compressor, the temperature outlet of the refrigerant is lower than required and so is the pressure of the condenser.

2.3.1 Charging a system

The method of charging refrigerant in a stand is explained in paper [3]. The charging of the compressor with refrigerant is done to avoid an accumulation of liquid in the compressor (flooded start) and to prevent potential wet return at the inlet of the compressor. To avoid these complications, the refrigerant is charged at the high pressure side using the pressure of the bottle of refrigerant until the system is at the same pressure as the bottle of refrigerant. Once the system is fully injected with refrigerant, the technician usually starts the compressor until the high pressure side is high and low pressure side is low. The technician is then able to charge even more refrigerant in the system at the low pressure side as the pressure in the bottle is higher than the low pressure side. However, the spatial disposition of the pipes and valves has to be taken into account to avoid the migration of refrigerant to unwanted areas.

To measure the amount of refrigerant fed to the system, the technician charges the stand and through a weighting scale, the amount of refrigerant injected in the system is known. For the specific case of the SoundRoom hot gas bypass stands, a recovery bottle of refrigerant can be used to add or withdraw refrigerant in the system as detailed performances of the power are not required. The gas cycle on the opposite cannot recover the refrigerant from the stand. Generally, more refrigerant is added than withdrawn as to change a compressor, the system withdraws refrigerant until void using an aspiration tube. Nevertheless, a small amount of refrigerant is still left in the compressor but can be neglected in the calculation of mass refrigerant in the system.
The testing order of the different compressors starts with the smaller compressor and ends with the bigger compressors. Taking the case of the compressor with the highest volume (or refrigerating power), the maximal amount of charge in the system can be calculated by accounting for all the refrigerant inputs/outputs occurring in the system over the testing operation of the stand.

2.3.2 Actual charge management

In the case of a hot gas bypass, the management of charge refrigerant in a system is done by a liquid receiver. However, in practice, the capacity of the liquid receiver is not enough to cover the whole operating map of the compressor. To not take any risks, the technicians charge the system filling half the liquid receiver with refrigerant. To cover the operating map, a charge management manual method has been developed.

In the actual configuration, two gas cylinders have been added to the hot gas by-pass to add or recover refrigerant. As the flow of refrigerant follows the pressure difference, a cylinder of refrigerant is placed before the compressor at low pressure and is regulated manually by a technician through a valve to add refrigerant to the system. Inversely, another cylinder is placed after the compressor to withdraw the excess refrigerant from the cycle manually also through a valve. Figure 2.9 is a representation of the actual charge regulation in the hot gas by-pass which is regulated manually by technicians.

The quantity of refrigerant to add or recover is done by trial and error by looking at the exhaust temperature of the compressor. If T_2 is too high compared to the reference value, more refrigerant is added to the cycle through the valves. Inversely, if T_2 is lower than expected, refrigerant is withdrawn from the system.

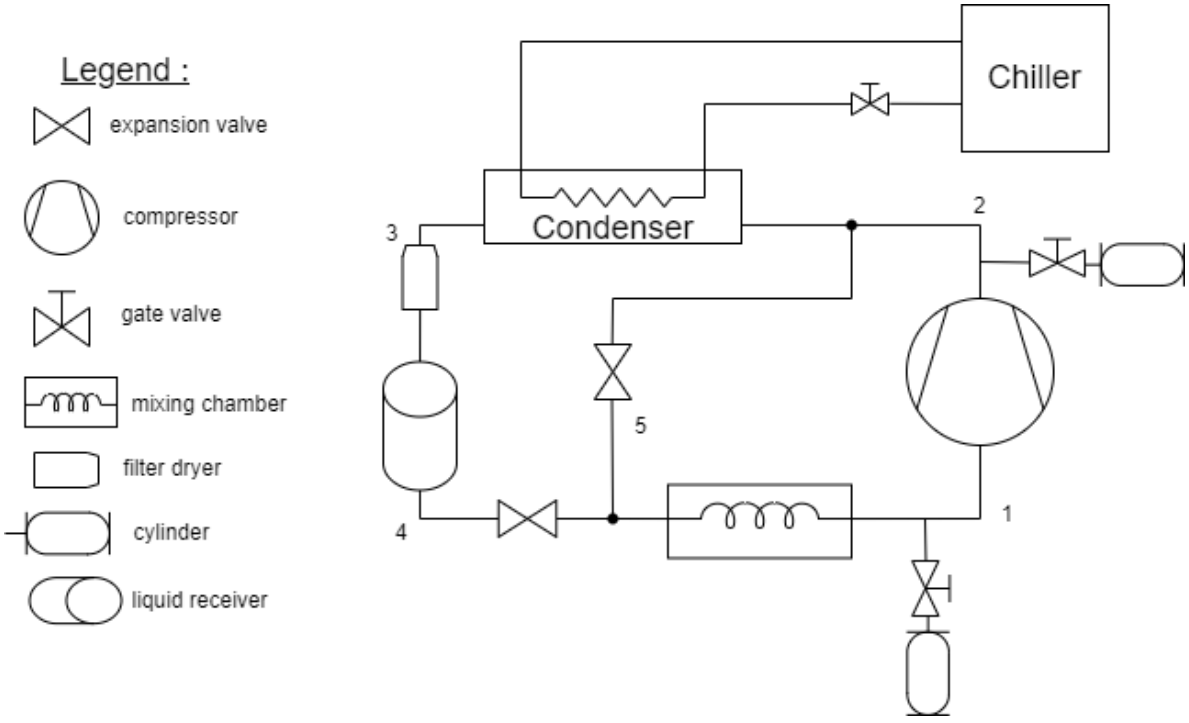

Figure 2.9: Model of the actual charge regulation in the hot gas by-pass

In the case of the gas cycle, the same method of manual charge management is in place. However, the automatic charge management of refrigerant is even more crucial to the gas cycle stand as the stand cannot use a liquid receiver as a regulator for storing refrigerant.

Chapter 3

Literature review

In this section, an overview of different articles and books will be presented based on earlier academic works on control systems and charge management of refrigerant for Vapor Compression Cycles (VCC). The review is based on a broad search process, making use of mainly Science Direct, ResearchGate, Uliège Library, and ORBI as the scientific database. Articles and books are not limited to recent years but are limited to the theoretical presentation of algorithms of control or the specific cases of vapor compression systems. The literature review starts with the presentation of control systems and similar study papers applying control systems algorithms to VCC are afterwards investigated. Based on the previous papers, a numerical model of the stand is required. To that extent, several articles are detailed explaining the modelization of components of a VCC and the different possibilities to represent a physical stand numerically. Once further information is known on the model representation, different control algorithms such as PID, predictive control, and MPC are further researched in papers. The last part of the literature review focuses on charge management of refrigerant in VCC as it represents the second focus of the thesis.

The literature review starts with two books [33] and [20] acting as a reminder on Control Systems which is later used in theory to introduce control systems to the reader of the thesis. The book [33] written by Katshuko Ogata uses the software Matlab to perform design, control, and analysis of systems by applying the theoretical approach to simple examples. The material presented in the book is taught to senior and first-year graduate students on control systems at the University of Minnesota. In the first chapters, the theory behind control systems can be read such as the use of Laplace transforms, state-space representation, transfer functions, and transient responses. Starting from Chapter 5, basic control actions are introduced along with stability criterion and root locus method of design including lead, lag, and lag-lead compensators. In the following chapters, the analysis of control systems is done in the frequency domain and introduces the concept of Bode diagrams, and Nyquist stability

criterion in closed loop frequency. Afterward, the PID tuning method is presented in theory under the form of state-space representation and transfer function through the use of Matlab. Concepts such as observability and controllability matrices are introduced along with the use of state-observers. Lastly, the final chapter presents the Liapunov stability analysis applied to a quadratic optimal control problem. The second book [20] written by Ioan Landau and Gianluca Zito targets an audience that aims to acquire the methodology for system identification, control design, and implementation using a digital computer. The structure of the book on Digital Control Systems follows the same construction as the previous book with an introduction of the theory behind the control systems and how to analyze the performances of a controller. In the following chapters, the author presents system identification with the related methods that can be applied to a system. The book provides some practical examples of applications of processes. It also considered some practical aspects of the design of a model representation to obtain maximally informative data and avoid oversampling. At the end of the book, by the analysis of the closed-loop, ways to reduce the controller complexity are presented.

3.1 Similar works

An extensive literature on the control of refrigeration systems can be found using a variety of methods to accurately represent and control of a VCC. Most of literature shows the first analysis with a first principle approach to understand the dynamics of the system and calibration with performance maps of experimental data before switching to a data-driven approach with system identification; The system identification method is able to accurately represent the stand under a state-space or transfer function form using a wide variety of methods. Among those methods, the local linear models of simple FOPTD seem to be applied in most papers than other regressions methods such ARMAX structure, and MIMO state-space representation. Even though, different algorithms are investigated in this literature review. In the second step, controllers' algorithms are investigated with mainly two generally known methods the PID and MPC method, and others methods such as H_∞ controller and LQR. Various modified algorithms are present in the literature and can be compared to one another. However, to account for the varying nominal operating points and the wide range of the operating map, varying controller parameters are used to account for the change of the dynamics of the system throughout the operating map.

A first paper [37] focuses on the development of control for an HGBP over a wide range of compressor capacities (10 to 80 tons). The control system consists of 3 valves in parallel instead of 1 valve

controlled using 3 PI controllers tuned with ZN. The choice of which valve to use is decided by a threshold value. The developed control is then tested using a 40-ton scroll compressor to validate the control scheme. During the testing with scroll compressor, instabilities are encountered and ways to deal with them are presented such as a reduction of the gains of PI gains for the suction temperature compared to gains from the suction pressure and a reduction of the mass flow in the condenser impacting the discharge pressure of the compressor. However, the report concludes with the fact that accurate steady-state data was unobtainable without further tuning of the controller showing the importance of a good controller for such a system.

Among them, the paper [5] presents a numerical Benchmark to the one-compression stage, one load-demand VCC using the software Thermosys, Matlab, and Simulink. It focuses on the control of the cooling power of the condenser and the degree of superheating at the outlet of the evaporator in a calorimeter testing method for a specific nominal operating point. A numerical model is first built with the software Thermosys directly linked with Simulink. Development of the model is based on the simplification of HX using a moving boundary approach which divides the heat exchanger into zones (superheated vapor, two-phase fluid and/or subcooled liquid. Afterward, a decentralized MIMO control without feedforward compensation is developed with the expansion valve opening and speed of the compressors. The control is able to withstand 7 different disturbances and is compared to a second controller using the IAE between the estimated outputs and the real output. However, it can be noticed that the paper focuses only on the control around the condenser on a single operating point for a calorimeter stand instead of a control on the compressor of a hot gas by-pass cycle with nominal point varying.

Another research [32] focuses on the dynamic modeling and advanced Control strategies of air conditioning and refrigeration systems. The stand consists of a classic VVC calorimeter applied to a transcritical system with R744. The dynamic modeling of the system framework is first presented using the first principles modeling approach and derived for each specific component for both non-linear and linearized cases using lumped parameters, discretized models, and moving boundary models. A first numerical model is then built on the Software Thermosys and Simulink with the use of a performance map of the compressor for calibration. However, for the system identification (p142), another numerical model is constructed based on data-driven approach to represent the VCC at different operating conditions. The individual input-output models are constructed offline using a 6 th order MIMO

model with a N4SID prediction algorithm based on state-space representation model structure. The newly built model is then validated with experimental data and the percentage of model fit based on RMS, the maximum and average residuals. As the model is highly non-linear, simple SISO controllers are judged not adapted (p143). Therefore, the choice of Gain Scheduling approach is chosen with controllers H_∞ of linear parameter varying (LPV) (p171). The 2 different local linear controls are designed by synthesis of linear matrix Inequality (LMI) at different nominal operating points. The stability is checked with the use of the Lyapunov constant quadratic function. In the end, the 2 local linear control models are then interpolated as Local Control Models (LCM) by the use of varying weights using fuzzy logic and applied to the stand. It is stated with results that the resulting controller can safely transition between design points, as well as off-design points. Even though the proposed algorithms are described and justified in terms of stability, high computational costs and uncertainties on the extended application on a whole compressor operation map can be noticed.

A third paper, the doctorate thesis [13] of V. Grelet focuses on the model control of a rankine cycle applied to heavy industry duty vehicles. Despite the application on a Rankine cycle, it presents a section in which a first-principles model approach is presented for a rankine cycle with linearization around nominal operating points to model the system with first order plus time delay (FOPTD) behaviors (p63 to p70). Therefore, the non-linear behavior of the system is split into several local operating regimes and a linear model can be built for each one. The resulting model is built by interpolation of the bank of linear models using a Bayesian estimator to calculate the weighting scheme based on recursive probability. Another simple weighting scheme using fewer tuning parameters developed in the thesis is compared to the Bayesian scheme. The resulting numerical models are validated for both weighting schemes with experimental data.
To control the numerical model, a gain scheduling method is applied with PID parameters calculated offline for nominal operating points using ZN, IMC, and more specific tuning correlations. A second method calculates the PID parameters online based on the global model estimation method. A third method with a non-linear controller using a moving boundary model as dynamic feedforward is also tested. A last method of Multi-model predictive control is also used with a modified numerical model built from SOPTD transfer functions. The different methods are then compared with the use of IAE and TV as criterion to determine the best controller. after analysis, online PID parameters estimation gives slightly higher performances compared to the MMPC. Experimental validation of both adaptive PID and MMPC controllers shows good performance with regard to disturbance rejection and set

point tracking. In the end, the introduction of observers is briefly described in the thesis and was not implemented. However, the use of a new observer structure for a time delay system could be introduced avoiding the finite approximation of the delay and making the control strategy more robust. In summary, the paper shows an implementation method for non-linear system with approximations of FOPTD or SOPTD transfer function interpolated by the use of a weighting scheme. The different controllers presented show that an online variable PID shows the best results. However depending on the application, the use of Multi-model predictive control could yield better results.

The article [10] studies a predictive functional control in a VCC to control the evaporator superheat with an electronic expansion valve instead of the traditional PID control to provide an accurate control of an evaporator superheat. The stand is numerically represented with a FOPTD transfer function with parameters. The transfer function for the dynamic representation of the model is obtained using a first principles modeling approach adapting the transfer function with information on geometrical data of HX and the fluids used. For the control algorithm, the predictive control can be assimilated to an MPC by the use of a coincidence horizon algorithm and a reference trajectory and is able to take into account variable parameters of the system and provide improved performance compared to the PID control. The control system is incorporated into an industrial programmable logic controller for a load stand consisting in a calorimeter testing type with one four-cylinder single-stage compressor able to vary in speed, 2 shell and tubes heat exchangers, and the refrigerant mixture R410A. The paper concludes that the controller implemented can offer high precision and robustness even when subjected to disturbances such as changes in flow rates at the condenser, change of cooling capacity, and on-off cycling.

Another example of a paper tackling the control of a hot gas bypass is the paper [18]. It presents the design and control development of Hot Gas By-pass chiller stand in a virtual manner only. It first models the system in steady-state in EES using correlations from Emerson-Copeland to cross-validate results. It switches then to the software Modelica with Dymola libraries in order to have a dynamic model. The control is then directly implemented in Matlab. The tuning method suggested by ZN is used to build a PI controller for both the superheat and the bypass valve. It evaluates the potential use of H_∞ controller (abandons due to the high mathematical knowledge required) and the LQG (Linear Quadratic Gaussian) controller which is an LQR combined with a kalman filter to account for white noise and uncertainty. It switches to a MIMO Linear Quadratic Regulator (LQR) controller as no white noise can be represented in Modelica (p32). The system identification is done through Matlab. The

system identification Toolbox in Matlab offers a function (ssest) that takes data from an Excel file and provides a best-fit state-space model or the user can specify the order of the system (typically 2 for a hot gas bypass). In the end, a comparison of the PI controller and the LQR controller is done through the Root Mean Square Error (RMSE) and stated that the MIMO LQR controller is far superior in controlling the HGPB. However, the control was developed in Modelica only and was not applied to a physical stand.

Conclusion. *From reviewing similar works in the domain of control systems, an apparent construction design can be remarked such that a first understanding of the process is done through scientific explanation or first principles modeling based on physical laws, then the construction of a dynamic numerical modeling of the system in terms of state-space representation or transfer function using calibration of first principles model or system identification, at last, the application of a controller algorithm on the dynamic model is done. Results are analyzed along the report to validate the model and characterize the performances of the controller algorithm.*

3.2 Dynamic modelization

To effectively apply a controller algorithm to a process it has been seen in the first part of the literature that a dynamic representation of the model is required. The dynamic model can be built on first-principles model based of physical laws to data-driven model using experimental data. In this part of the literature review, more specific papers on the modelization of an HGBP cycle are presented first to present ways to build a first-principles model then switching to the construction of a data-driven model. a Vapour compression cycle is essentially composed of a compressor, a condenser, a liquid receiver, an evaporator and of expansion valves. The following papers' main focus is applied to the description of components for a first principles approach before switching to a data-driven model with system identification.

To represent a heat exchanger, a first example can be obtained from paper [15] presenting an offset-free MPC based on MISO ARX models to represent a transfer function. The control is afterward tuned for a specific nominal operating point using the SIMC tuning rules for a PID and an offset-free MPC control is applied as well. As no constraints on the manipulated variable are present, the MPC presented is equivalent to a finite horizon LQG. The paper applied the process to the Newell and Lee forced circulation evaporator model [30]. It divides the model of the evaporator into four parts among

which the evaporator and condenser are particularly interesting. Looking on a bigger scale, the whole dynamic model of a VCC can be observed from paper [21]. It is focused on a moving boundary VCC model representing the transient conditions occurring in heat exchangers to represent the on-off cycling of a compressor. The model represents a traditional VCC with a numerical model based on Thermosys correlated with a physical stand. However, the dynamical model and experimental data do not match.

To represent a simple compressor, the first option is to use a linear regression such as the standard 10 coefficients correlation AHRI Standard 540 presented in paper[1]. However, the previous standard is only accurate for a fixed speed compressor. Therefore, for the case of a multivariable speed compressor, paper [34] which focuses on the modelisation of variable speed scroll compressors has been analyzed. It models 3 different compressors based on the map-based (empirical method) with the use of the 20 coefficients correlation AHRI-20 to represent an accurate variable speed scroll compressor. However, it required at least 20 to 21 tests to find the goodness of fit compared to 14-20 conditions for a fixed-speed compressor. The model of a compressor in general can be presented either in a detailed manner, in an efficiency-based manner, or map-based. This paper in particular uses the map-based empirical method with an expanded version of AHRI 10 coefficient correlations by adding 10 additional speed-dependant coefficients (20 coefficients correlation) and compares the proposed method to different compressor models such as W.Li[22] and Mendoza [27] which are not linear regression models. Manufacturers such as Emerson and Danfoss use the AHRI-20 correlation though. To validate the correlation, models are retrofitted on a test bench satisfying the Standard EN13771 for compressor ratings. The test bench is regulated by a set of PID controllers that can keep any operating condition stable within a range of 1 kPa and 0.1 ∘C from its reference without manual adjustments and charge regulation management seems to be regulated by a liquid receiver.

The last component of an HGBP that would need to be represented is the Electronic Expansion Valve which is used to control the amount of vapor bypassed and the pressure inlet. detailed theoretical paper [2] explains the different possibilities of flow equations for sizing control valves including turbulent and non-turbulent flow for compressible and incompressible fluids. In addition, Paper [23] presents a simplified model of EEV in which the fluid is considered compressible instead of the Bernouilli equation with incompressible fluid. It constructs the equation of mass flow through an EEV based on three regions: linear with flow proportional to the square root of the pressure difference; the non-linear, and choked where the flow remains constant. To clearly represent the throttling

mechanisms of EEV and take into account the two-phase downstream due to partial evaporation, the Bernoulli equation was improved by adding an expansion factor and the pressure differential ratio factor of a controlled valve. The choked condition is also accounted for with the maximal amount of flow rate through EEV when the inlet condition is kept constant and the outlet pressure is decreased.

The previous papers [10], [13] and [32] use the theoretical laws presented to represent the components of the system independently of one another. Another method based on inputs-outputs applicable to a physical stand or a numerical model based on first-principles can be used to build a representation of a model. The model based on experimental data is called data-driven and the relations between inputs and outputs of this type of model are found using system identification. The data-driven type of model is mainly used directly in industry as it fits the physical stand accurately without having the high computation time related to the construction of a numerical model to take into account. Research papers validate and calibrate the numerical model with the stand using experimental data.

To that extent, a state-of-the-art review of system identification can be read in paper [12]. The main idea of system identification consists of the study of the behavior of a physical system by recording the input-output relation in discrete time. The system is supposed a black box as the dynamics of the system are unknown and the dynamics are observed under a forced input variation test. Once tests are performed, a mathematical representation of the system can be generated under the form of transfer function, ARMAX model, or state-space model. In the end, the best model among the possible representations is chosen based on algorithms including error minimization such as Least-squares method, fuzzy system, or probability optimization. Once the mathematical representation is chosen, it needs to be validated through new experimental data to ensure a good model validation. Books written by L. Ljung [24] and by Isermann [16] can be read in further detail for more information on system identification.

Conclusion. *To sum up, to analyze a physical stand, system identification is a requirement to ensure a good representation of the stand. All of the papers mentioning a physical stand use a system identification method in order to apply control on the system afterward. As an example, papers [32] and [18] use a state-space representation, [13] and [10] a transfer function and [15] an ARMAX structure. To accurately represent a non-linear model such as the HGBP cycle, books [24] and [16] as well as papers [13] and [32] suggest the use of local linear dynamic models such as FOPTD to represent locally the different parts of the operation range of the model. This*

method is called Local Model Network (LMN). The different models are valid over a specified range of operations and a bank of those linear models can be created. The linear models can be interpolated together using a weighting scheme such as the Bayesian weighting scheme taking into account the error and the probability at a previous time. The nonlinear system is simply approximated by a multitude of local linear models which altogether can represent the non-linearities of the system.

3.3 Controller Algorithms

As can be seen in the similar work in literature, the first step was to represent the system accurately through system identification. The second step is according to the representation of the system, a controller algorithm can be implemented to control the system. Among the several methods of control existing in the literature, the control algorithms for PID and MPC are further investigated. In chapter 3 of the book [28], control algorithms of PID and MPC are presented briefly with the advantages related to the use of one over another.

The widely known PID controller is one of the oldest control methods existing and is used in various domains of the industry with refrigeration systems included due to their proven effectiveness and practicality. One of the oldest ways to tune a PID controller is presented by Ziegler-Nichols [42]. Other methods of tuning as often compared to the tuning of ZN as the tuning is very aggressive and often needs to be mitigated. Papers making use of ZN methods are various in this literature such as papers [37],[13], [18], [29],[25], and [38]. As presented in papers [29] and [42], Ziegler and Nichols presented two methods based on experiments to tune P, PI and PID parameters. The first method consists of using an open-loop response and based on the tangent of the flexion point of the curve, analyzes the slope, the apparent delay, and the gain. Using a table of correlation, the parameters of PID can then directly be found. However, the gains are generally too important and can be greatly reduced to obtain a satisfactory response. The second method consists of a closed loop using a P controller increasing until limit of stability are reached to determine the critical gain with the critical period associated. Based on the critical gain and period, the parameters of the PID controller can be calculated using the appropriate correlation. Paper [31] presents a general tuning correlation applied to a FOPTD transfer functions obtained in open-loop response.
The same paper [29] also presents the method of Astrom and Hagglund using a similar method to ZN apart from the fact that it uses a criterion of calibration in the maximum sensitivity function M_s with

$M_s = 1.4$ or $M_s = 2$ in relation to the Nyquist plot and an additional parameter which is the static gain of the process. The Astrom and Hagglund also determine gain and period then through a table of correlation, one can construct P, PI or PID controllers.

A third method called the Chien-Hrones-Reswick (CHR) method derived from the ZN open loop method is presented in paper [31]. the method's purpose is to give a quicker response without overshoot or with 20% overshoot. The correlations presented in the paper [31] can be applied to a FOPTD transfer function directly in a general manner.

A fourth method of tuning is presented in papers [28] at p124, the method is called Cohen-Cohen and is a modified version of ZN for systems with a large delay to overcome the slow steady-state response of ZN. This method of Cohen-cohen can be applied directly to FOPTD model using correlations from paper [31].

The paper [28] also presents the IMC tuning rules whose principle resides in the simplification of a model approximated by a FOPTD. This type of tuning has proved to be robust and yields acceptable performance resulting in an IMC-PID tuning rules that can be applied to the process. The IMC tuning method is also presented in more detail in paper [35].

Research has focused on the improvement of PID parameters over the years. As a result, paper [25] presents new PID tuning relations for transfer function FOPTD, SOPTD, and SOPTD adapted to unit step change and load step change separately with a derivative factor α set at 0.1. The tuning relations were derived with the objective function of minimization of IAE in a Matlab environment. A comparison with general tuning rules such as Ziegler-Nichols, Cohen-cohen and Lopez/ Rovera methods. The proposed tuning rules are developed based on the ratio of the dead time over the time constant ($\frac{\theta}{\tau_1}$ varying from 0.1 to 2 compared to conventional methods valid to 1. The proposed method's robustness, stability, and control effort were evaluated and deemed highly robust for simple, accurate, and efficient PID tuning rules for practitioners.

From the same point of view, another paper [38] presents as well an optimal tuning of proportional integral derivative (PID) parameters for different process systems: first order plus time delay (FOPTD), second order plus time delay (SOPTD), and second order plus time delay with lead (SOPTDLD). The developed PID control parameters are optimized to minimize integral absolute error (IAE) for stability, total variation (TV) for performance, and maximum sensitivity function M_s for robustness. The proposed method utilizes Ziegler–Nichols' initial guess and IMC tuning for optimization and yields generalized tuning rules based on process parameters. The proposed tuning rules offer simplicity, ac-

curacy, and efficiency for practitioners. At last, a discussion on tuning the controller for derivative action and integrating processes is presented.

The thesis [13] written by V. Grelet compares the different methods ZN, IMC, Skogestad method [38] and the new PID tuning from paper [25] and evaluates that the control suggested by Skogestad yields the best trade-off between error minimization of IAE and performance with TV while having a parameter to tune for faster convergence if required. It applied the following tuning method in an online PID controller which is based on a bank of linear FOPTD models and obtains good stability results. The online PID controller represents a gain scheduling approach. The gain scheduling approach takes into account the strong nonlinearities of a system by adapting the controller parameters to the operating conditions. The operating conditions are calculated by a dynamic model representing the system accurately by means of a Local Model Network (LMN) for example. As a gain scheduling approach can be implemented simply and has a low computational complexity is widely used in industry. However, it requires a certain number of variables representative of the operating points that catch the nonlinearities of the system to control. In summary, by the use of an algorithm based on the model representation, the PID parameters can be modified automatically and smoothly based on the model representation of the system. as presented in paper [13].

In case of large delays within the system, a Smith predictor presented in paper [39] can be introduced as the Smith predictor is the first time-delay compensation algorithm. The paper highlights the challenge of severe slugging in offshore oil production due to large stroke times of choke valves, causing variable input time delays. Traditionally, control methods struggle with variable delays, thus it proposes a solution through a modified Smith predictor using measurable valve positions and a linear model. Tested in simulation, it significantly improves slug control, enabling operation at larger valve openings. The case study illustrates its effectiveness in stabilizing systems with significant stroke time delays and leading to enhanced control performance. Overall, the Smith predictor proves advantageous in systems with large time delays. A description of the Smith predictor and the building process is presented in the paper. The paper [38] takes into account a Smith predictor in the proposed algorithm.

As the control algorithm known as the Smith Predictor contains a dynamic model of the time-delay process, it can be considered as the first model predictive algorithm. However, over the last decades, a model predictive control MPC has been developed and researched. Presented in book [11] and vari-

ous papers [10],[19],[9],[15],[36], and [13], the model predictive controller MPC is considered the most advanced controller structure used for industrial applications and has developed into a powerful solving method for multivariable control tasks with dead time handling, optimization costs function, and limitations on MV and CV. Compared to the traditional PID controllers, the MPC integrates a representation of the model and predicts the dynamic of the system in the future. Its algorithm consists of a prediction horizon that predicts future deviations from the set point, a cost function which is minimized by adjusting the MV over a control horizon. It uses the information of the prediction horizon to adjust the MV over the control horizon by minimizing a cost function and then measures the plant answer. The model is updated at each new measurement.

The book [11] written by Rainer Dittmar focuses exclusively on the implementation and design of Model predictive control with Matlab and Simulink and aims to be used for teaching and research. The book provides the basic ideas and application advantages of MPC, and shows examples of use of Simulink environment for the design of MPC. Moreover, the book presents a non-exhaustive list of MPC papers representing the research on the subject over the years. The book starts with an introduction to the field of model predictive control (MPC) and the algorithms described mathematically. The following chapter describes how to design a MPC controller for linear process models using the MPC designer app of Simulink. The rest of the chapters are dedicated to examples from the field of process control. In chapter 8, a gain scheduled MPC control is designed using a bank of linear models to represent a non-linear model for which a linear MPC is designed for each linear model. The last chapter presents the nonlinear MPC which is at the present time not handled by the designer app from Simulink but can be solved using Matlab line commands. In conclusion, the book [11] contributes to the general understanding of MPC and eases the application of a MPC controller to an industrial process.

As in the book [11], paper [36] presents the general concept of MPC associated with a focus on the effect of constraints in the system in a descriptive and mathematical way. The paper then pursues the analysis of constraints mitigation for the rate of change of control signal to reduce the crest factor in the response.

An example of the use of a MPC algorithm is the paper "Implementation of Model Predictive Control in Programmable Logic Controllers" [19] that presents the method of code generation tool for the

implementation of MPC based controllers in PLC software where the optimization problem is solved online. The controller architecture is composed of an SSTO (Steady-State Target Optimizer) to minimize the difference between the estimated output affected by disturbances and the reference, MPC algorithm, a predictor which is a discrete linear time invariant model linearized around the operating point, and a state-space estimator using an observer. The optimization problems of the SSTO and MPC are solved online through the use of FISTA algorithm (Fast Iterative Shrinking-Threshold Algorithm) which is an accelerated gradient method based on Nesterov's fast gradient method or ADMM algorithm (Alternating Direction Method of Multipliers). Without going into depth, these methods converge at most linearly thus within the purposes of the MPC optimization problem, it converges quickly to a value close to the optimal one. The code has been developed in Matlab and the controller is programmed as an FBD block that contains the controller's algorithm written in Structured Text according to the standard IEC 61131-3. The developed algorithm needs to receive the model matrices, systems bounds, and controller parameters to generate the code of the controller and the variable declaration that can be directly imported into the PLC software. The current tool is available for Schneider Electric PLCS and the PLC programming software CODESYS. At the end of the paper, an application of the method is applied to a case study of a non-linear system consisting of a double reactor and separator system composed of 12 states, 4 inputs, and 4 outputs. The non-linear system is simulated in real time using software QUARC in Simulink.

A first example is the paper [9] which presents the design of an MPC controller for time-delay processes. The case is applied to a numerical representation of a heat exchanger which is approximated by a SOPTD. The author uses the function idinput(N, type, band, levels) of Matlab with types such as sinus or Gaussian signal) to generate experimental data on the numerical model and the system identification is done through LSM or the fminsearch function of Matlab to approximate the model under the form of a SOPTD. Afterward, the model is then verified by the criterion of fitness LSM and a self-made criterion of estimate gain based on poles and zeros of the FOPTD. The model predictive control algorithm uses an estimation of the model over a prediction horizon, the Receding Horizon Control(RHC) to apply only a part of the estimate to control the future trajectory of the MV over the control horizon, and a Generalized Predictive Control (GPC) to minimize an objective function to determine the next control increments. The estimation part presented in the paper is based on the recursive computation of predictions by direct use of the CARIMA model. The paper concludes on a successful application of the MPC algorithm over the simulation model and also in real time laboratory conditions for control

of the heat exchanger.

Other examples of MPC control algorithms can be read in papers [15],[10], and [13]. The paper [15] illustrates the use of an unconstrained MPC based on MISO ARX-models in which the MPC is equivalent to an LQC optimization as the variables are unconstrained and no use of prediction and control horizon are present. Paper [10] presents the control algorithm as a predictive control that through the use of a coincidence horizon algorithm, an optimization cost function, and a reference trajectory is a variation of the traditional MPC algorithm with the estimate model made out of FOPTD transfer functions. The thesis [13] uses a Multi-MPC with a generalization of the algorithm with a control horizon fixed to 1, a variable prediction horizon, and an estimation of the mode by a bank of linear model FOPTD transfer functions. (Note: the weights of the Bayesian scheme are supposed constant over the prediction horizon)

Conclusion. *As can be read in the literature review, many different control algorithms exist and have been tested in the literature. Even within specified controller algorithm types such as MPC and PID, variation of the main algorithm can be observed with substantial results. However, it has been noticed that depending on the specific process, certain types of algorithms are preferred such as PID and MPC in industrial applications as they offer simplicity of tuning to avoid overfitting and understanding over their counterparts more mathematically oriented. For the case of vapor compression cycle (VCC), it can be noted that an approximation of the non-linear system by a bank of simple linear models of the form FOPTD coupled with an adequate weighting scheme seems promising. The resulting model of the stand can be fed to a general algorithm which will tune the parameters of the controllers online based on the approximate linear model at each time. The controller algorithm of the PID is the most renowned and offers a simplicity of use and tuning to the user. On the contrary, the MPC controller algorithm is harder to efficiently tune and relies more on the accuracy of the estimate model. However, with the model approximated by simple FOPTD, errors could give rise to a non-optimal controller performance due to overfitting or underfitting. As a result, the choice of a PID controller with parameters calculated online seems a good solution as the tuning of such a controller can be tuned in order to reduce the overfitting or underfitting of the model.*

3.4 Charge management

A part of the literature on the management of charge refrigerant in a refrigeration cycle is also searched in the literature. The method of charging and testing a compressor is also reviewed. One can notice that the management charge of refrigerant is usually handled by the use of a liquid receiver to ensure that liquid is not stacked in the condenser and some system adds an accumulator to prevent liquid from entering the compressor.

The company ASHRAE has developed a manual for refrigeration equipment and systems. In the specific chapter 8 [3], details on charging refrigerant, management of refrigerant, and methods of testing the compressor are available.

To start, charging refrigerant in the system depends on the size and application of the unit. The related accuracy can then be adapted to the specific applications. For standard charging, extreme accuracy is not necessary. On the opposite, fully automatic charging boards verify the vacuum in units, empty the charging line, and calculate the required amount of refrigerant for the system. Oil should be charged before refrigerant in order to avoid foaming, oil slugging, and improper oil distribution. When charging a system with refrigerant, the refrigerant is charged at the high-pressure side in order to avoid an accumulation of liquid in the compressor (flooded start) or a wet return at the suction side. In addition to that, the environment(pipes, gravity, and valves) should also be taken into account to prevent refrigerant migration during the charging process. As a side note, refrigerant lines have to be dry and clean, and charging lines kept away from moisture and noncondensable gases. Regular checks for moisture or contamination have also to be performed. When it comes to testing compressors, primary measurements consist usually of power and capacity, and second measurements of leakback rate, low voltage starting, noise, and vibration.

Testing compressors with refrigerant can be done in several ways. A testing part can be done without refrigerant, however, this part is not interesting for our case. A first example of a test to provide accurate measurement of the compressor's performance can be done via the use of a calorimeter and flow meter to evaluate performance testing, positive displacement compressors as described in ASHRAE standard 23.1. Another type of test for non-accurate determination of a unit's capacity and efficiency is the gas cycle (called 'vapor stand' in the book), The vapor stand consists of an expansion device (valve) and a heat exchanger (condenser) able to reject the equivalent of energy produced by the motor. The gas from the output of the compressor is cooled down in the condenser and then adiabatically ex-

panded back for the compressor inlet. The advantage of this method is that no evaporator is used and a smaller condenser is required. A third method of testing for small-capacity appliance compressors consists of a hot gas bypass cycle (called desuperheating stand). A small piece of tubing connects the discharge and the suction of the compressor using a hand-expansion valve. As a condenser is used, the discharge pressure is known, and water temperature and flow rate are used as capacity indicators. The working principle consists of the liquid refrigerant from the condenser output being mixed with the hot discharge gas to provide adequate suction pressure and temperature for the compressor. the hot gas by pass valve acts on the inlet pressure of the compressor and the valve situated after the condenser acts as a quench valve to control the temperature. It is also noted that higher range and stability are provided by the hot gas bypass cycle compared to the gas cycle.
If the system is charge sensitive meaning that predetermined discharge pressure, suction pressure, and temperatures have to be obtained, flow measurements can simply be installed in the system. However, if various sizes are to be tested or more than one point is tested, the introduction of a liquid receiver after the condenser can be used for full-liquid expansion.
Potential causes of malfunction in refrigeration systems are overcharging, undercharging, presence of non condensable gas, and blocked capillary tubes. To evaluate the allowed tolerances of a test, the unit is first tested within the known characteristics and then deviated from the test standard. As an example, assuming 30 g of refrigerant limits, the system is charged with 30 g more or less of refrigerant and if the unit performance is not satisfactory, the established charge limits need to be redefined.

In order to handle charge refrigerant, a thesis [6] of a comprehensive summary based on eight articles related to characteristics of the cooling system of a refrigeration cycle describes the working principle of a refrigeration system with a charge management-oriented approach. Additionally, the paper presents a simple experimental study of the refrigerant charge distribution which consists of trapping refrigerant of the desired component (compressor in our specific case) with the help of quick valves in order to weigh the refrigerant charge through the specific volume density and the volume at specific temperatures and pressures. Though briefly mentioned in the analysis of paper [8] and [7], an experimental method to find the optimum charge of refrigerant is described through the use of an external refrigerant bottle connected to the system with a valve while being weighted by a scale. The working principle consists of heating and cooling the bottle to vary the system charge. The refrigerant flow would typically flow the gradient of temperature. The refrigeration cycle from Paper [8] consisted of a condenser followed by a filter drier and a needle valve, an evaporator, and a pis-

ton compressor. In Paper [7] in addition to the previous system, a refrigerant tank sitting on a scale and a remotely controlled solenoid valve (Honeywell MC062) were added to the refrigeration system of paper [8] connected to the compressor service line in order to control the amount of refrigerant in the system. The compressor and the solenoid valve are controlled by software developed in HP-VEE which is a graphical dataflow programming software development environment from Keysight Technologies for automated test, measurement, data analysis, and reporting. However, no further data on the controlling environment of the compressor is described.

One method to assess the charge of refrigerant is presented in Paper [41]. It suggests a rationally based algorithm to assess the optimal refrigerant charge in a simple vapor compression cycle. The rationally based algorithm is an iterative process that uses the mass flow rate change to calculate the optimal charge of refrigerant in relation to the COP. The model developed takes into account a condenser, throttle/capillary tubes, and reciprocating compressor. As a result of the study, COP performances of the model have been observed in relation to the refrigerant mass to match the trends of the experimental data. However, the lack of consideration of an accumulator presence and the cooling effect of the capillary tube leads to a lower calculated refrigerant mass value for the optimal COP value.

On the other hand, Paper [14] proposed a consistent control strategy (CCS) independent of operations modes for CO_2 refrigeration systems in vapor compression cycles for a single, two-phase, and booster system. The study suggests the use of fixed refrigerant charges such as accumulators filled with superheated gas placed before the compressor inlet and a liquid receiver placed at the outlet of the condenser. The simple control strategy is applied to a single-stage system, a two-stage system, and a booster system of a load stand of 10 to 20 kW ambiance temperature ranging from -5 to 40 degrees Celsius. the system's main components consist of finned tube heat exchangers acting as evaporators and coolers, an electronic expansion valve, and a tube-in-tube heat exchanger sub-cooler for the two-stage and booster system. The systems are modeled with GREATLAB. In the end, results yield that by managing charge, CCS achieved comparable performance to the re-optimized multi-zone control strategy, with average COP losses below 0.5%. Notably, it simplifies control complexity significantly. However, a variation of the speed of the compressor was not taken into account in this study.

Conclusion. *The charge management of refrigerant in vapor compression cycles is handled by the use of liquid receivers or accumulators that automatically adapt the required amount of charge in the system. The*

other proposed methods of regulation based themselves on the calculation of optimal charge for specific nominal operating points. For the case of the gas cycle (with no liquid state), the introduction of a bottle connected to the system at the intermediate pressure can used, as mentioned by the paper [3], to vary the system charge through heating and cooling the bottle.

Chapter 4

Problem narrowing

In this chapter, the narrowing of the the thesis is done to focus the research on two specific controller algorithms for a specific stand with a chosen model representation.

4.1 Stand choice

Based on the problem formulation, the Sound Laboratory in Copeland consists of three different stands: two hot gas by-pass stands and one gas cycle stand. In addition, the controller algorithm is expected to vary from one stand to the others. With this in mind and the limited time allocated for this thesis, a focus on one specific stand is made.

The gas cycle stand is only used for compressors working with R744 and has a small range of power up to 10 kW of refrigerating power. Having only one refrigerant used and having a small refrigerating power makes the gas cycle stand a very specific stand which is why the methodology of the controller algorithm will not be applied to the gas cycle stand. Moreover, there are two HGBP stands on which the controller algorithm can be tested on directly to verify the performance of the general controller.

To choose which HGBP stands to apply tests on, the choice is not relevant to the user but is more dependent on the compressor being tested at the moment in the Sound room. Depending on the power of the compressor, the adapted stand power (either 15 T or 50T) is used. As explained in the following section, tests have to be performed on the stand to represent the system with a first compressor. The stand is then chosen based on the compressor tested in the sound room.

4.2 Modeling Approaches and software

In this part of the thesis, an explanation of the choice of the modeling approach to represent the load stand is presented. The model we want to represent is a non-linear model of a hot gas bypass cycle equipped with a multivariable size and speed compressor scroll. By definition, the model can be called a digital Twin as a Digital Twin is defined as an up-to-date representation/model of an actual physical asset by including relevant experimental data. A digital twin model is used in our case to refine the control and predict the future behavior of the model.

First, a model of a test bench of a compressor cycle involves mechanical and physical laws that need to be modelized either by linear regression of data or by physical law dynamics specifically for thermodynamic cycles. Moreover, the need to control the process requires a dynamic model to take into account the step responses of the manipulated outputs of the modeled process influenced by the possible implementation of controllers within the model.

There are essentially two main approaches to modeling a stand with a dynamic representation, a stand can either be modeled based on first-principles modeling using the physical laws between the components or data-driven modeling by using experimental data of the stand directly. The modeling can use a mix of both approaches as well to reach the desired modeling by using physical laws calibrated with experimental data. A presentation of both approaches is made and the resulting choice is explained.

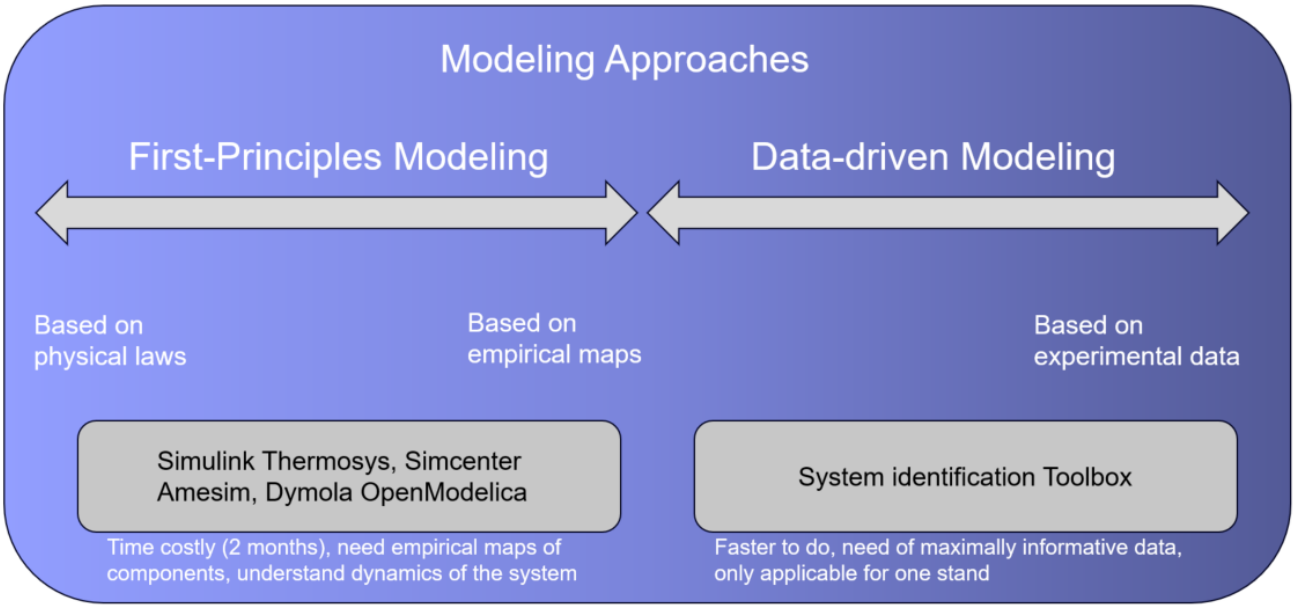

Figure 4.1: Modeling approaches

4.2.1 First-principles approach

From the point of view of first-principles modeling, several simulation environments offer the possibility of implementing such a model such as Modelica with Dymola, Thermosys, and Simcenter Amesim based on physical or empirical data. A non-exhaustive list of the different software can be found on the website: https://modelica.org/tools/. Through the use of adequate libraries, physical laws and empirical maps, software can model complex dynamic systems in steady-state or time-dependent with calibrations procedure.

For example, the Thermosys Toolbox for MATLAB® and Simulink® is a simulation tool for analyzing the behavior of air-conditioning and refrigeration systems (both steady-state and time-dependent) such as hot gas bypass cycle. In it, it is possible to define your own fluids by supplying *.mat files with a specific data structure. Empirical maps for expansion valves and compressors can be fed to the model as well.

On the other part, Amesim is a software for system simulation. It can accurately model fluid systems with the dynamic behavior of hydraulic and pneumatic components with the help of comprehensive component libraries. Simcenter Amesim provides a set of predefined functional components for heat exchangers, compressors, valves, actuators and a series of geometry-based components to study the evolution of pressures, flow rates, and temperatures in the complete system.

A third software, OpenModelica is an open source software in which you can define your own libraries to model your components or use already established libraries from commercial licenses such as Dymola. A library called 'Thermocycle' including thermodynamic components is also available through the University of Liège for thermodynamic components but the library needs to be actualized to the new software requirements of OpenModelica as it consists of an old library. The software can implement a large variety of dynamic systems which makes it a general tool used by many researchers in various applications. Models built in OpenModelica, Thermosys and Simcenter Amesim can all be transferred in Matlab Simulink in which it is possible to construct an efficient controller for the system.

However, first-principles modeling method has some drawbacks such as the complexity of the model to account for internal behavior. Moreover, the time required to construct and calibrate a first principles model is approximately two months (according to V. Lemort) which is very time-consuming. In the case of my Master's thesis, the main objective is to provide a faster convergence to reach nominal operating points of a compressor by improving the controller of the load stand. Therefore, as my

thesis is limited in time and not focused on modeling, the implementation of a first-principles model is not investigated any further. In addition, Thermosys and Simcenter Amesim are part of toolboxes in which resources were not accessible with access from the company or the university. Therefore, the use of OpenModelica would have been chosen otherwise. Even though the thermodynamics laboratory of University of Liège can provide a library 'Thermocycle' for the use of thermodynamic components, the library is not usable in the current state and needs to be actualized to the new OpenModelica configuration.

4.2.2 Data-driven approach

The other modeling approach called 'data-driven modeling' as its name suggests is based on the identification of the system through maximally informative experimental data and can be viewed as a black box model as no understanding of the thermodynamic principles of the system is required. The model is identified only from input-output behavior. The experimental data can be obtained through tests applied using the load stand by reaching reference points of the compressor and analyzing the system in open-loop with specific step input changes. The second step of the process is handled by the use of the system identification methodology. It can be done through the "System identification" Toolbox available in Simulink. The Toolbox provides several representation methods to create state-space representation and transfer functions from experimental data directly at specific nominal operating points of the stand. A model set is chosen and adjusted to specific ranges of the stand to construct a representation of the dynamic of the system. The resulting choice of model set is verified with an assessment of the fitness of the model based on the difference between estimated output and actual output. Once the model is verified, it can be validated using another set of experimental data to evaluate the fitness of the representation.

For the sake of simplicity and computational time reduction, the choice of using data-driven modeling based on analysis of experimental data obtained from the stand is chosen. The Data-driven model has several advantages over the simulation environments. First, the person assigned to the design does not need to understand the physical laws and the thermodynamics occurring in the system. Second, the time required to build the model is greatly reduced and mostly depends on the time required to perform step-change analysis on the load stand to gather useful experimental data. Third, fewer resources are required to provide a model of the load stand which is economically attractive. As a result,

most industries choose the option of a black box model to represent their stand. Nevertheless, a few drawbacks can also be noted. The model is only valid for the investigated system within the operating limits meaning that if the load stand's components change, the resulting model is not applicable anymore and the whole methodology needs to be applied once again. Moreover, useful information on the system dynamics for the company can be extracted from the modelization of components based on physical laws and thermodynamics as the model provides a simple way to model components and can be implemented with a large variety of components by changing the parameters of the components in the simulation software.

Another requirement to be added is that the software implementation needs to provide a way to use controllers inside of the model and to analyze the resulting dynamics of the system to changes while being able to generate a standard IEC 61131-3 structured text code that the controller m Tron T through the IDE CODESYS can read. To that extent, The *Simulink PLC coder* option offers the possibility to convert the controller algorithm from Simulink into Structured Text of standard IEC 61131-3 readable by the controller. Further details about the PLC coder Toolbox can be found in the following section. Another option would also be to directly implement the controller structure in CODESYS in Structured text once a suitable controller is found.

4.3 Controller Algorithms

In the literature review, several different types of controllers were presented from SISO to MIMO control, from complex matrix decomposition to more simple controllers for refrigeration systems. Despite the large choice of controllers in the domain, some algorithms are more widely used than others. For example, the two controllers PID and MPC are widely used in the industry as they can be implemented faster and require less computations.

In comparison, the $H\infty$ controller with LPV is not used in industry due to complex matrix decomposition and relatively low papers even mentioned its use. The linear quadratic controller (LQG) or other predictive algorithms generally include one or several features of the MPC controller and can then be considered as special MPC cases. The MPC controller includes optimization cost functions like LQC, constraints on the MV as well as prediction and control horizon. The extra features of the MPC make it the most advanced controller structure in the industry.

On the contrary, PID has proven its effectiveness and practicality for parameter tuning over the years. Several tuning methods can be used based on the methods of Ziegler-Nichols, Astrom and Hagglund, IMC tuning, Cohen-Cohen, and Lopez/ Rovera. New tuning correlations are also proposed and can be applied for any process through a general approach such as presented by papers [38] and [25]. In addition, the parameters of the correlations can be tuned to optimize the performance of the controller. Mitigation methods to improve the handling of dead time or of disturbances can also be implemented with the introduction of Smith predictor or feedforward action.

From another point of view, in the case of varying operating conditions of the stand, a method of gain scheduling can be applied easily to PID and MPC using an interpolated model of the system based on a bank of linear models to cover the range of operation of the stand.

As a result, the controller will first be implemented using a PID controller type due to the tuning possibilities proposed by such an algorithm. A MPC controller will also be discussed in a second time to compare the performances of controllers. In addition, uncertainties in the approximated model can be handled more efficiently with a PID controller compared to a MPC which relies more on the accuracy of the model.

Conclusion. *The problem narrowing section concludes with the stand choice, the modeling approach, and the control algorithms to focus on. The stand is chosen to be the HGBP stand of 15T based on tests and the model is identified through a data-driven modeling approach based on experimental data of input-output. The control algorithms of PID and MPC were chosen to be further investigated.*

Chapter 5

Research question

The research question presents the guiding thread of the report and drives the thesis toward a relevant conclusion. The investigation of the problem formulation sets the case study and the problem analysis. The section " Problem narrowing" helps us to reduce the scope of the project by excluding the use of first-principles modeling approach. Theory and Methods used in the "Analysis" section or necessary to the understanding of the project are also presented. The analysis explains and discusses the implementation of the solution to answer the research question. The last section "Discussion" concludes on the solution implemented and introduces some perspectives of analysis in the future to improve the solution.

The main research question presents the main study of the report.

> ***How can the controller of a load stand in a hot gas bypass configuration be improved to reach nominal operating points of the compressor faster?***

Some subquestions can be deducted from the main research question:

1. *Which numerical model can represent the dynamics of the system accurately enough?*
2. *How can the numerical model chosen be implemented and validated?*
3. *Using the numerical model, which controller algorithm provides the best performance on the model?*

A side research question is also briefly investigated.

> ***How can the refrigerant charge management be automatized in the stand for the case of hot gas bypass and gas cycle?***

The research questions are investigated and answered throughout the report.

Chapter 6

Theory

6.1 Control System

In this section, a non-exhaustive reminder of the control of linear systems is presented based on the book [33] including state-space representation, analysis of step response and frequency response, the robustness and stability of the controller and the tuning principle of PID controllers.

6.1.1 State-space representation

A representation of the general structure of a system and its controller can be seen in Figure 6.1.

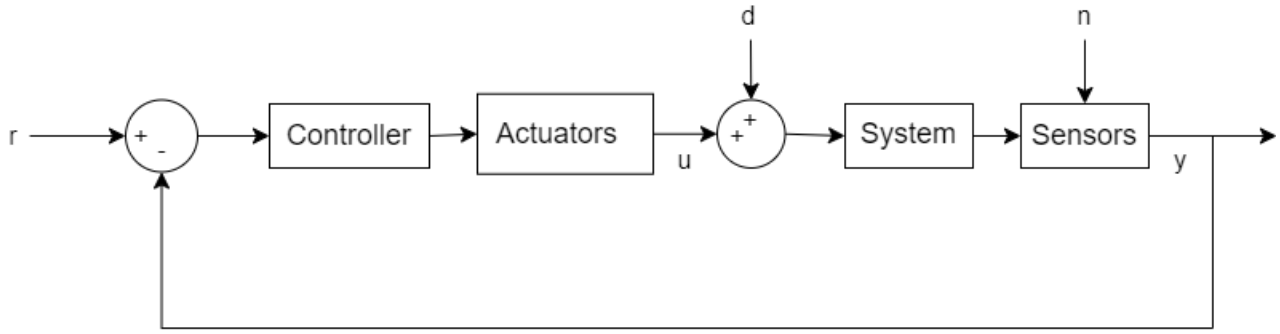

Figure 6.1: Representation of the general structure of a system with controller

The system is composed of a reference r or a setpoint SP fed to the controller which will act upon the actuators to approach the reference point. The actuators are the mechanisms able to vary the inputs u also called the Manipulated Variables (MV). There are also disturbances of the system that are not controlled but can still influence the system. The system is fed with the inputs u and the disturbances d. The response of the system is analyzed with sensors. However, errors of measurement called the noise measurement n are associated with the sensors. The output signal y also called the Controlled Variable (CV) is then obtained. If the output signal is fed back to a controller, the system is in a closed loop and the controller can act on the input signal in function of the output of the system.

A LTI system can be represented under the form of state-space representation as follows with x being the state vector of the system:

$$\begin{cases} \dot{x} = Ax + Bu \\ y = Cx + Du \end{cases} \tag{6.1}$$

Depending on the number of inputs y(t), outputs u(t), the dimension of the state space representation can take several forms. A SISO system is characterized by a system that can be described with a single input-single output relation. In most industrial applications, a system is usually described by several inputs and outputs resulting in a multiple inputs-multiple outputs (MIMO) system.

One can identify specific components of the above equation:

1. x defines the state vector corresponding to the dimension of the system
2. Matrix A corresponds to the dynamics of the system and its eigenvalues determine the dynamics and stability. The matrix A is not directly tunable and requires the introduction of a tunable matrix K representing the controller.
3. Matrix B represents the number and position of the actuators and is tunable.
   The concept of controllability is used to control the states of the system acting only on its inputs. The controllability matrix W_r is introduced and a system is controllable if the controllability matrix is full rank, i.e. its determinant $\neq 0$.

   $$W_r = \begin{pmatrix} B & AB & \cdots & A^{n-1}B \end{pmatrix}. \tag{6.2}$$

   The matrix B is constructed to be controllable.
4. Matrix C represents the number and position of the sensors and is tunable as well.
   The concept of observability is used to infer the values of the states from the measured output. The observability matrix W_o is introduced and a system is observable if the observability matrix is full rank, i.e. its determinant $\neq 0$.

   $$W_o = \begin{pmatrix} C & CA & \cdots & CA^{n-1} \end{pmatrix}. \tag{6.3}$$

   The matrix C is constructed to have an observable system with no hidden dynamics.

5. Matrix D represents the load disturbance affecting the system.

The introduction of a controller is made by assuming that all the states are directly measured. With the help of a simple controller with feedback gain represented by K and feedforward gain represented by k_r, the dynamics and stability of the system can be analyzed and modified. The output state signal of the controller feedback can therefore be used:

$$u = -Kx + k_r r \tag{6.4}$$

The system can then be represented by:

$$\dot{x} = (A - BK)x + Bk_r r \tag{6.5}$$

6.1.2 Time domain representation

In the time domain, the system has the dynamic of a pair input-output described by a step response representing the effects of the variation of an input on the corresponding output.

The relation between the pair input-output is described by the following equation in the time domain:

$$y(t) + a_1 y(t-1) + ... + a_n y(t-n) = b_0 u(t) + b_1 u(t-1) + ... + b_m u(t-m) \tag{6.6}$$

by isolating the output y(t), the step response can be represented in relation of the input u(t) variation:

$$y(t) = b_0 u(t) + b_1 u(t-1) + ... + b_m u(t-m) - (a_1 y(t-1) + ... + a_n y(t-n)) \tag{6.7}$$

Observing Figure 6.2, the dynamics of the system are represented graphically by a step response, and some parts can be easily identifiable:

1. The time delay: the delay time can be approximated with the time required for the response to reach half the final value

2. The rise time: the time for the response to pass from 10% to 90% of the desired response of the system.

3. The settling time: the time for the response to stay within the 5 % range of the desired response.

4. The overshoot: the maximum peak value of the response curve measured from the desired response of the system usually represented in percentages.

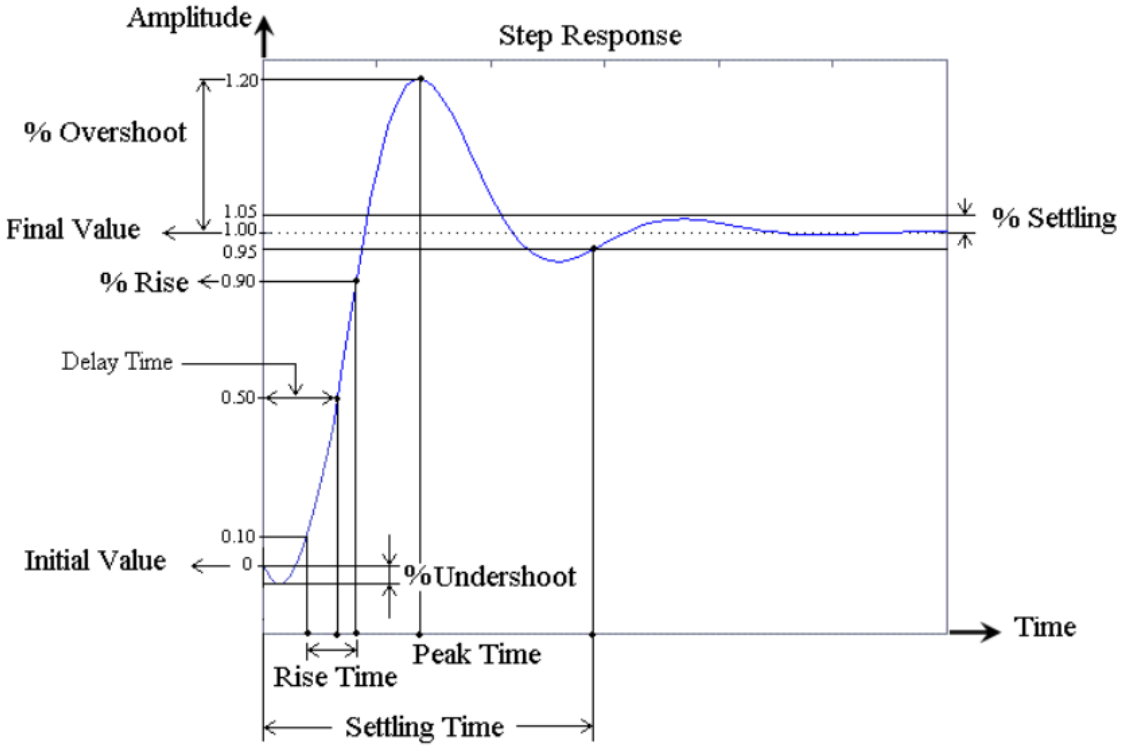

Figure 6.2: General step response of a system

6.1.3 Representation in the frequency domain

To perform an analysis of the response in terms of frequency, the system is transformed in the frequency domain through the Fourier transform. The resulting transfer function can describe the dynamics of the system in the frequency domain.

Starting from the difference equation in the time domain, the equation can be derived in the frequency domain using a sample time T_m and the Fourier transform:

$$y(t) + a_1 y(t-1) + \ldots + a_n y(t-n) = b_0 u(t) + b_1 u(t-1) + \ldots + b_m u(t-m) \tag{6.8}$$

$$y(s)\left(1 + a_1 s^{-1} + \ldots + a_n s^{-n}\right) = u(s)\left(b_0 + b_1 s^{-1} + \ldots + b_m s^{-m}\right), \tag{6.9}$$

Based on a general transfer function which is simply the Laplace transform input divided by the

Laplace transform output in the frequency domain with the complex frequency $s = \sigma + j\omega$ (i.e. mapping in the complex plane),

$$H(s) \equiv \frac{U(s)}{Y(s)} = |H(s)|e^{\angle H(s)} \tag{6.10}$$

With Y(s) the Laplace transform of y(t) and U(s) the Laplace transform of u(t).
The system is therefore represented by a transfer function in the frequency domain rather than a state-space representation from the time domain.
The response of the system can be represented in the frequency domain by the use of Bode plots representing the amplitude $|H(s)|$ and the phase $\angle H(s)$.

6.1.4 Robustness and Stability

The robustness and stability of a system can be evaluated in the frequency domain with the Bode and Nyquist plots as presented in the book [4].

The Nyquist approach was developed to look at the stability and robustness of a feedback system by looking at the properties of the loop transfer function $L(s) = P(s)C(s)$ made of the controller C(s) and the system considered P(s). The Nyquist plot is a plot of the loop transfer function for different values of the complex frequency s.

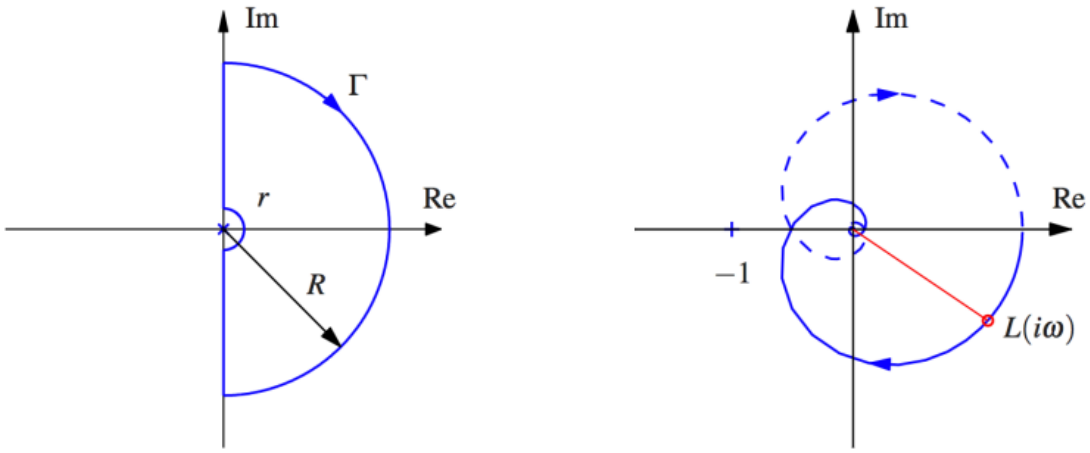

Figure 6.3: General Nyquist plot

Using the Nyquist plot with the Loop transfer function of the system, the stability of the system + controller can be justified. To explain the principle of stability of the simplified Nyquist criterion, an assumption on L(s) is made:

Let L(s) be the loop transfer function for a negative feedback system and assume that L(s) has no poles in the open right half-plane (except for single poles on the imaginary axis),
then the closed loop system is stable if and only if the closed contour given by equation 6.11 has no net encirclements of the critical point s = -1.

$$\Gamma = \{L(s) : -\infty < \omega < \infty\} \subset C \tag{6.11}$$

It means that the Nyquist criterion does not require that $|L(s)| < 1 \quad \forall\omega$.

The Nyquist plot/criterion shows how system stability is influenced by changes in the controller parameters when looking at stability margins.

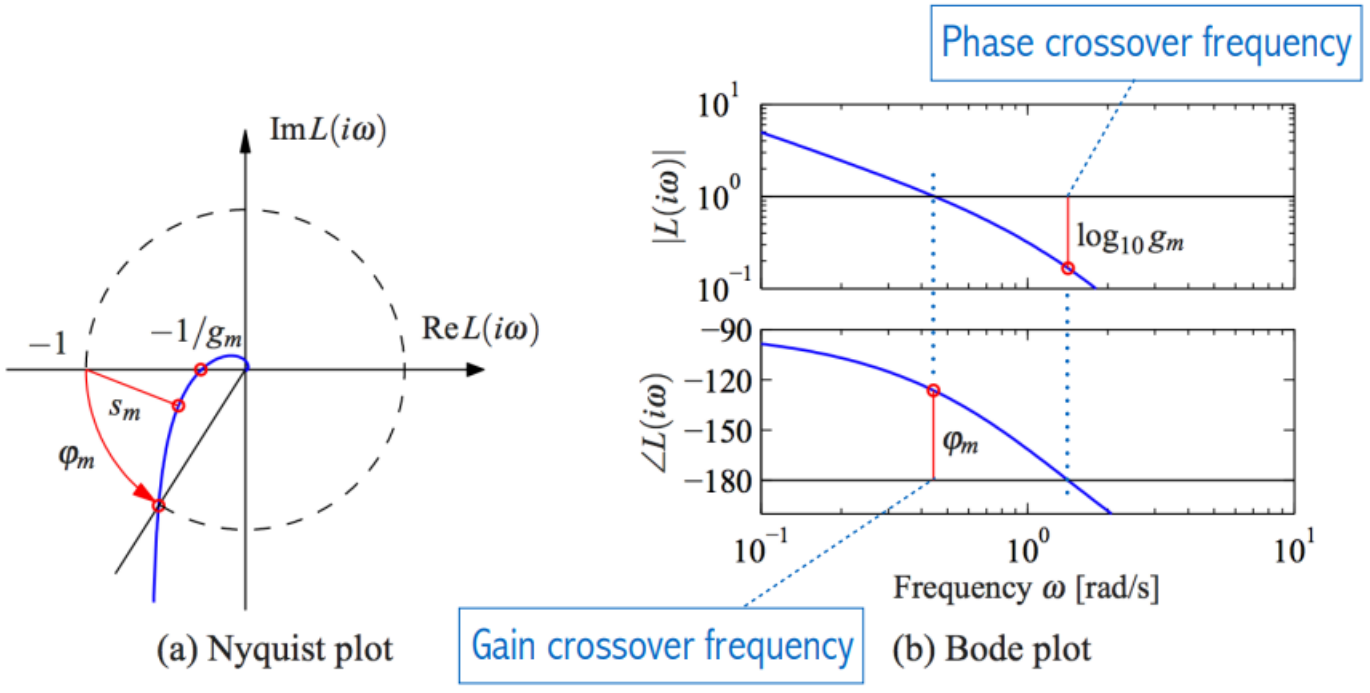

Figure 6.4: Representation of the stability margins

On a Nyquist plot, the frequency at which the Nyquist curve crosses the real axis at negative values corresponds to the frequency at which the phase crosses -180° in the corresponding Bode plot.

The stability margin can be defined as follows:

1. Gain margin (g_m): smallest increase of the open-loop gain at which the closed-loop system becomes unstable.

   Any gain increase leads to dilatation of the Nyquist curve potentially causing instability.

2. Phase margin (φ_m): 180° + phase at unit gain.

   Any time delay in the system rotates the Nyquist curve, hence reducing the phase margin.

3. Sensitivity margin (s_m): Shortest distance from the Nyquist curve to the critical point (-1).

Gang of four sensitivity function:

The pair system + controller can be evaluated in terms of noise rejection, disturbance attenuation, and reference tracking using four different sensitivity functions. The system is represented by P(s) and the controller is represented by C(s) both in the form of a transfer function in the frequency domain. As presented at the beginning of the Nyquist section, the loop transfer function L(s) is the combination of the controller C(s) and the system P(s).
To ensure stability, the four transfer sensitivity functions have to be stable

1. Sensitivity function

$$S(s) = \frac{1}{1+PC} \quad , n \to y \tag{6.12}$$

   It corresponds to the measurement noise rejection.

   At high frequencies (s very big), $S(s) \to 1$ and therefore $L(s) \to 0$

2. Load sensitivity function

$$PS(s) = \frac{P}{1+PC} \quad , d \to y \tag{6.13}$$

   It corresponds to the disturbance attenuation.

   At low frequencies (s very small), $PS(s) \to 0$ and therefore L(s) has to be big.

3. Complementary sensitivity function

$$T(s) = \frac{PC}{1+PC} \quad , r \to y \tag{6.14}$$

   To ensure a good tracking if the reference at frequency $\omega = 0$, $T(0) = 1$ and therefore $L(0) \to +\infty$

4. Noise sensitivity function

$$CS(s) = \frac{C}{1+PC} \quad , n \rightarrow u \quad \& \quad r \rightarrow u \tag{6.15}$$

It has the same purpose as the sensitivity function with the measurement of the noise rejection.

Papers [29] and [38] use the maximum of the sensitivity function to evaluate robustness based on the use of the sensitivity margin.
To evaluate the robustness of a controller applied to a specific system, one can use the maximum of the sensitivity function M_s defined as follows:

$$M_s = \max_{0<s<\infty} \left| \frac{1}{1+P(s)C(s)} \right| \tag{6.16}$$

M_s represents the largest amplification induced by the disturbances. In the Nyquist diagram, the inverse of M_s represents the sensitivity margin s_m. A typical value of M_s usually lies between 1.2 and 2. The lower M_s, the better the white noise robustness.

6.2 PID controller

A controller can be introduced to control a system and accurately follow the reference trajectory required. The most general controller known is the PID controller and is based on literature provided with the controller m Tron t from JUMO and paper [28] Most processes in the industry have been controlled using a PID controller.

A PID controller consists of three terms, namely proportional, integral, and derivative control. The combined operation of these three terms gives a control strategy for process control.

Proportional term :

The proportional constant or gain K_p is the basic action employed in a controller and corresponds to the constant magnitude of the change in the controller output to the change in error. In some control systems, the proportional term is sometimes represented in terms of percent proportional band X_p.

$$X_p = \frac{100}{K_p} \quad [\%] \tag{6.17}$$

Proportional control will result in deviations from setpoint except when the setpoint is at 50% of the span. When the gain k_P is increased, the error is reduced but not eliminated. As a reminder, the lower the proportional band, the more precise the control. However, if the proportional band is set too low (too high proportional constant K_p), the system becomes unstable and starts oscillating unless the time constant of the process is extremely high.

Integral term :

The integral term is defined by the integral time T_i for which the errors are accounted for. The integral term suppresses the static error by integrating previous errors to adapt the response in consequence and keeps the CV at the control point even as the process load changes

$$T_i = \frac{K_p}{K_i} \quad [s] \tag{6.18}$$

The integral action assures that there is no steady error but requires careful adjustment. An integral time set too fast (too low) will result in fast changes of MV while the process has not responded to the previous change. In the opposite, if set too slow (too high), the control will take a long time to integrate and reduce the error

Derivative term :

Proportional and integral control sometimes do not provide a fast enough correction. As a result, a derivative term is introduced to anticipate changes in process load. The derivative term is defined by the derivative time T_d representing the time over which it predicts future errors. It predicts the rate of change of the error to provide faster convergence and reduce overshoot.

$$T_d = \frac{K_d}{K_p} \quad [s] \tag{6.19}$$

If T_d is set too high, the system response is damped but amplifies high frequencies. As a result, derivative actions should be used with a filter (=lead compensator).

6.2.1 General form:

The PID controller can be represented by a general form called the ideal form. The PID controller directly links the output signal $u(t)$ to the error signal $e(t)$ and the algorithm can simultaneously handle the current error, eliminate the steady error, and anticipate future errors. PID optimization parameters studies have been conducted in research as can be read in the literature review.
The following equation represents the temporal form of the signal:

$$u(t) = K_p \left(e(t) + \frac{1}{T_i} \int_0^t e(\tau) d\tau + T_d \frac{de(t)}{dt} \right) \tag{6.20}$$

with error defined as follows:

$$e(t) = SP(t) - y(t) \tag{6.21}$$

with SP(t) as the setpoint or reference signal and y(t) as the output signal of the process.
The relative transfer function in the frequency domain is then written :

$$G_c(s) = \frac{U(s)}{E(s)} = K_p \left(1 + \frac{1}{sT_i} + sT_d \right) \tag{6.22}$$

A representation of a PID controller can be observed in Figure 6.5.

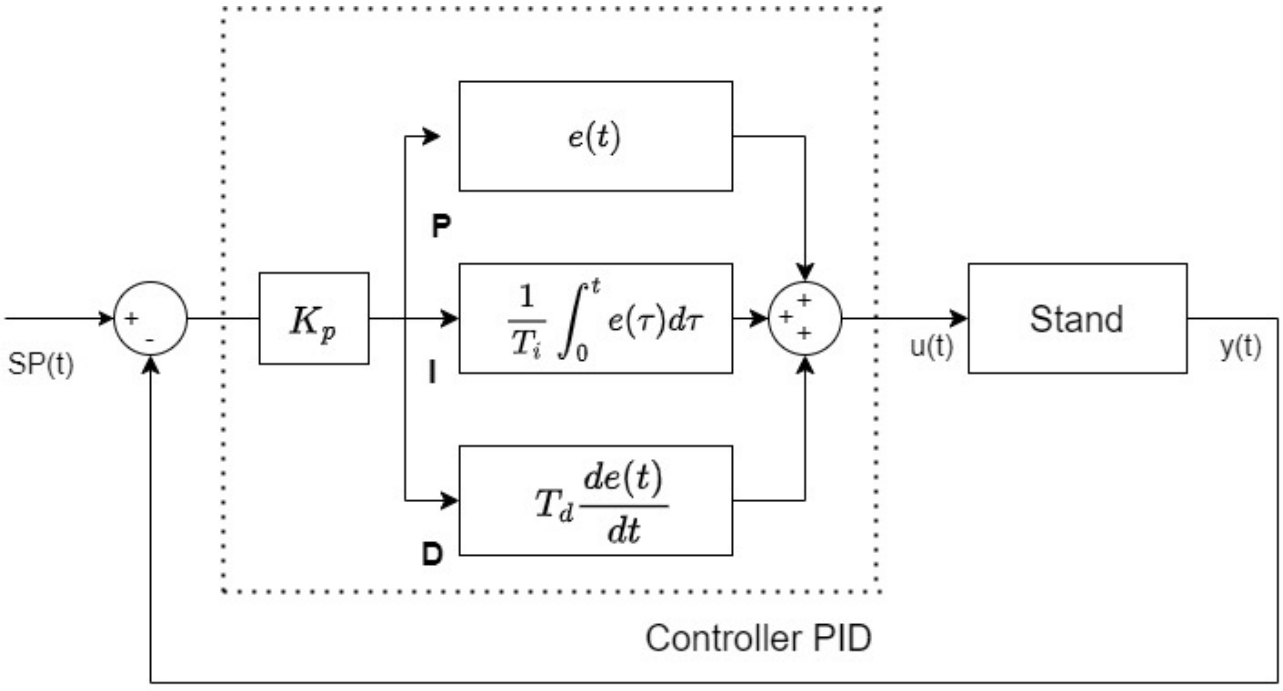

Figure 6.5: A representation of the ideal PID controller

Different types of controllers can be built from this general form. A P controller can be represented with only a proportional gain by setting the integral and derivative part to zero (this type of controller is not recommended). Another PI controller can also be presented which introduces the integral term to take into account the steady-state error by integrating previous errors. This controller is widely used in the industry. The derivative parameter can be added to the controller to form a PID controller. This derivative part as explained above is used to predict future errors and can provide faster convergence.

6.3 Model Predictive Control

Model predictive control also known as MPC is a powerful control system for optimizing complex systems in real-time taking into account the dynamics of the system. The control system is generally a MIMO system and the controller operates in a closed loop. A closed loop means that the controlled variables (CV) of the process are fed back to the MPC controller which is also provided with setpoints. In addition, the MPC controller can be made aware of measured disturbance variables that can be used for feedforward compensation. An observer can also be introduced to estimate and control the unmeasured variables.
However, the effectiveness of MPC heavily relies on the accuracy of the model representation as it determines the optimal inputs based on an optimization function of future outputs. The model can either be represented by transfer functions or state-space models.
Moreover, the optimization for each time step needs to be solved faster than the sampling time of the system.
In the following, The MPC algorithm is presented in the form of a SISO control with state-space representation to simplify the notation.

Regardless of the model representation used, all MPC control algorithms have the following common elements:

1. a model prediction of the future course of the controlled variables
2. an optimum function to control future manipulated output changes
3. an application of the principle of receding horizon control (RHC)

The basic concept of MPC can be described using Figure 6.6 applied for a SISO model. The left side of the figure shows the past development of the controlled variable and the manipulated variable while

the right side shows the future development of the MV and CV. The MPC main purpose consists of optimizing the future control inputs to reach the setpoint target in the best way possible. To that extent, the MPC is composed of a prediction horizon M and a control horizon P. The control horizon is defined by the finite future time over which the future control variables are calculated by optimization of a control function based on the future estimated outputs and the prediction horizon is the finite time over which the future estimated outputs are calculated to reach the set point in an optimal way. As a result, the control horizon P is always lower or equal to the prediction horizon M as the control horizon is based on the prediction horizon results: $0 < P \leq M$.

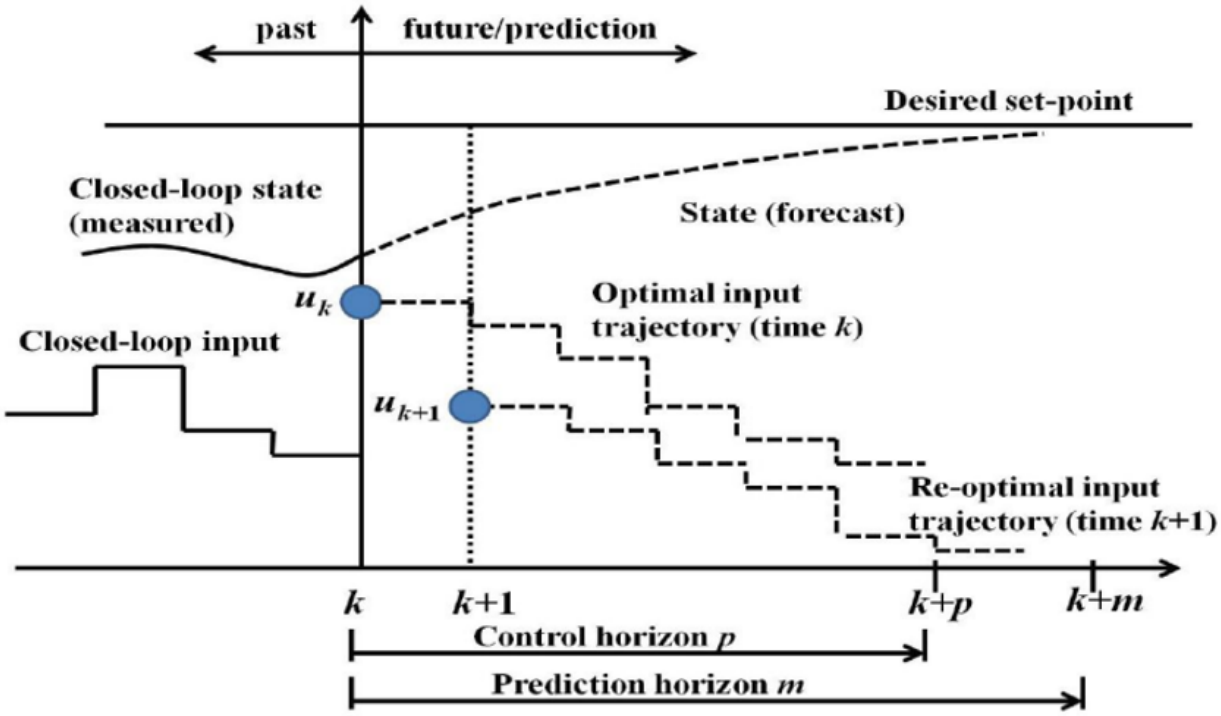

Figure 6.6: Basic concept of MPC

6.3.1 Forecast

MPC controls uses the dynamic model not only in the design phase as a PID controller would but also in the operating phase of control. At the current time t, the future behavior of the controlled variable is predicted using the mathematical model and the current data.

Based on a future setpoint, the future behavior $y(\hat{k})$ can be estimated by the use of two parts: the "free" and the "forced" movement of the system. The free movement describes the future course of the

controlled variable under the assumption that the manipulated variable does not change in the future. The forced movement results from the consideration of the future course of the manipulated variables over the control horizon M. The future behavior is represented by the dashed line in Figure 6.6.
Using the estimation of the future behavior, the future control variable curve can also be calculated by iteratively solving an optimization function. At each optimization step, a new set of future MV changes is created and is then used by the forced movement to recalculate the future behavior of the system again.

6.3.2 optimum function to control future manipulated output changes

The third essential element of the MPC algorithm is the determination of an optimal sequence of future manipulated variable changes $\Delta u(k)$= [$\Delta u_1(k), \Delta u_2(k), \cdots, \Delta u_P(k)$] over a specified control horizon P which is in practice much sorter than the prediction horizon M. The optimal sequence of future CV is determined by solving a quadratic optimization problem. The quadratic function denoted J minimizes the future output differences while keeping the changes in the MV as small as possible. The ideal optimal solution leads to $J(u_k^*) = 0$ with a perfect tracking ($\hat{y}(k) = SP(t) \ \ \forall t$) and a steady-state control ($\Delta u_k = 0 \ \ \forall t$).

6.3.3 Application of Receding Horizon Control

Although an entire sequence of future manipulated variable changes was calculated in the previous optimization step, only the first element of the future manipulated variable changes is applied to the process. This also means that the whole estimation, prediction, and optimization is repeated in each sampling interval rather than waiting for M sampling intervals until the next optimization is performed.

6.3.4 Constraints handling

Constraints can also be implemented in the MPC controller. The constraints are the boundaries in which the system operates and the introduction of constraint handling helps to prevent material destruction and dangerous conditions. Constraints can be applied to the amplitude of the control input u(k), rate of change of control input $\Delta u(k)$, and amplitude of the output y(k) to stay within an opera-

tional range using an upper and lower input limit.

$$\begin{cases} u_{min} \leq u(k) \leq u_{max} \\ \Delta u_{min} \leq \Delta u(k) \leq \Delta u_{max} \\ y_{min} \leq y(k) \leq y_{max} \end{cases} \tag{6.23}$$

6.3.5 Mathematical representation

Taking the example of a state-space representation of a SISO model as presented in the state-space representation in the section Control System with no disturbance matrix, the control algorithm can be mathematically described.

$$\begin{cases} x(k+1) = Ax(k) + Bu(k) \\ \hat{y}(k) = Cx(k) \end{cases} \tag{6.24}$$

Using the first equation of the state-space representation representing the future state vector x(k+1) based on the previous input u(k) and the previous state vector x(k), the future output y(k+1) can be predicted.

$$\hat{y}(k+1) = Cx(k+1) = CAx(k) + CBu(k) \tag{6.25}$$

Solving the quadratic optimization function, the future control input can be calculated. The quadratic optimization function is based on the minimization of the difference between the setpoint SP and the predicted output y(t) while keeping the change of MV Δu_k as small as possible.

$$\min J(u_k) = \int_{t_k}^{t_k+1} (\hat{y}(t) - SP(t))^2 + w_u \Delta u_k^2 dt \tag{6.26}$$

where w_u is a scaling factor and a penalty weight for the control move.

Once the future control input u(k+1) is determined, the estimated output y(k+2) can be determined.

Recursively, the following sample points of the prediction horizon are calculated based on the previously calculated input change and state estimation.

$$\begin{cases} x(k+i) = Ax(k+i-1) + Bu(k+i-1) \quad \text{with } i = 1, ..., M \\ \hat{y}(k+i) = Cx(k+i) \end{cases} \tag{6.27}$$

The optimization function is solved along the estimate to optimize the future control input until the end of the control horizon P is reached

$$\min J(u_k) = \int_{t_k}^{t_k+t_p} (\hat{y}(t) - SP(t))^2 + w_u \Delta u_k^2 dt \tag{6.28}$$

where $\Delta u_k = u_k - u_{k-1}$ and t_p increases by one at each recursion until $t_p = P$.

The optimization function is performed until the end of the control horizon and once it is reached, the input change does not change and is fixed for the next estimate output.

At each sampling rate, the MPC computes a set of P projected outputs

$$\hat{y}(k+i); i = 1, 2, ..., P \tag{6.29}$$

and a set of M future controlled inputs

$$u(k+i-1); i = 1, 2, ..., M \tag{6.30}$$

at the current sampling time k to efficiently reach the setpoint SP.

A Receding Horizon Control (RHC) is then used to apply only the first moves of the control horizon M calculated at each sampling rate to the current system of control. At the next sampling, a new set of M controlled inputs is calculated and only the first control input move is applied once again.

Chapter 7

Methods

7.1 Testing methods of a compressor

Different methods to test a compressor with refrigerant are explained. The content of this section presents in more detail three different testing methods. The three different testing methods presented are implemented at Copeland Welkenraedt. In addition, the manual [3] for refrigeration equipment and systems written by the company ASHRAE explains the available testing methods of the compressor.

7.1.1 Calorimeter

A first method is the calorimeter and can be applied to provide accurate measurements of the performance of the compressor. The method is used to gather experimental data. It consists of using an electrical heating source instead of an evaporator. A representation of the model can be observed in Figure 7.1.

The mass flow in the second cycle of the condenser is controlled using a gate valve. Opening the gate valve leads to an increase in flow rate and enables to decrease the pressure P_2. Inversely, closing the valve leads to a lower heat exchange resulting in an increasing pressure P_2 and the compressor will no longer provide any work.
In addition, the amount of heating furnished to the refrigerant in the heater enables to control the inlet temperature of the compressor T_1.
The expansion valve is on the other side used to vary the inlet pressure of the compressor P_1.

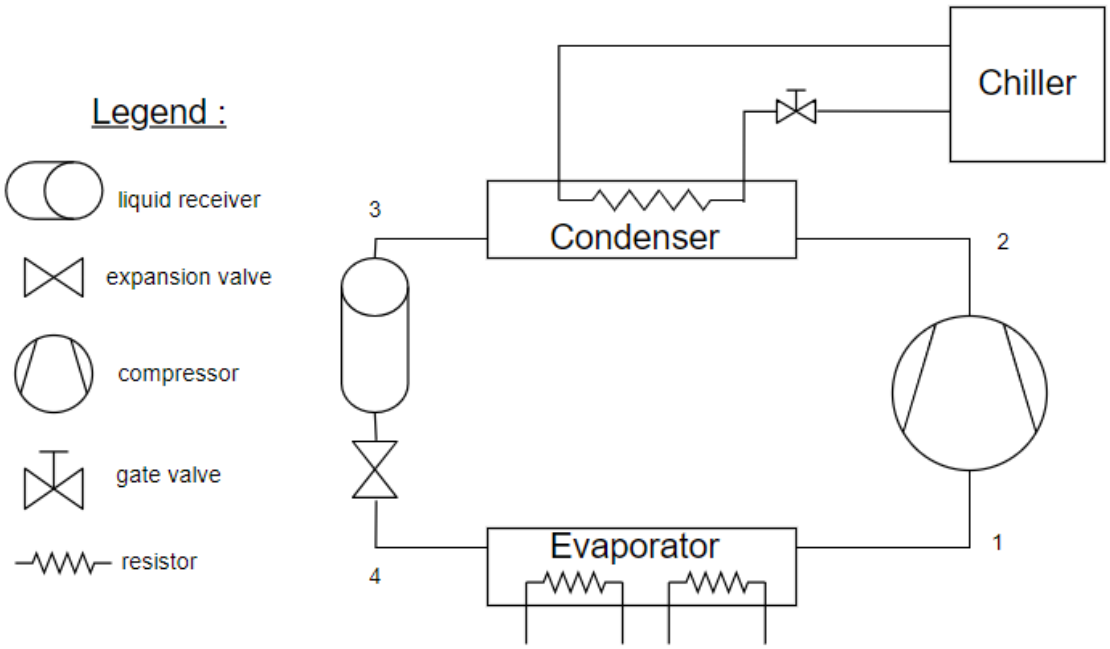

Figure 7.1: Model of the calorimeter

The model can be represented with a P-h diagram to observe the refrigeration cycle and the corresponding P-h diagram is equivalent to the diagram of the basic compressor cycle in Figure 2.2 presented in the problem formulation.

Energy balance

However, the use of another heating source independent from the basic system requires a high amount of energy as can be seen in the total energy balance of equation 7.4.

Let's suppose that the heat required from the heater is $Q_{heater} = 100kW$ and assuming that a good $COP = 3$, one can evaluate the energy required in the cycle. The power supplied to the compressor is found using the definition of COP.

$$P_{mot} = \frac{Q_{heater}}{COP} = 33[kW] \tag{7.1}$$

Using the total energy balance,

$$Q_{chiller} = P_{mot} + Q_{heater} = 133[kW] \tag{7.2}$$

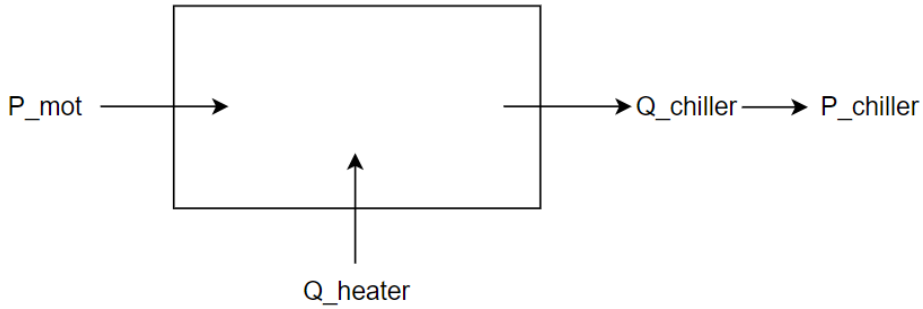

Figure 7.2: Energy balance on the calorimeter

Considering again a COP of 3, the circuit relative to the chiller requires :

$$P_{chiller} = \frac{Q_{chiller}}{COP} \approx 45[kW] \tag{7.3}$$

As a result, the total energy required by the cycle with a calorimeter is humongous compared to other methods presented in the following.

$$\text{Total energy required} = P_{mot} + Q_{heater} + P_{chiller} \approx 188[kW] \tag{7.4}$$

7.1.2 Hot Gas Bypass cycle

Another method implemented At Emerson/Copeland laboratory is the Hot Gas Bypass cycle which consists of replacing the previous heater in the calorimeter with a bypass of hot gas. This method uses the discharge gas to heat up expanded gas instead of using electric resistance resulting in an economy of energy.

The valve of the bypass controls the quantity of hot gas bypassing and therefore controls the inlet temperature of the compressor T_1.
As the mix of vapor and liquid is not perfectly homogeneous, a mixing chamber ensures an ideal mix to avoid liquid particles from entering the compressor. The valve from the chiller circuit still controls the outlet pressure of the compressor P_2 and the valve following the condenser still controls the inlet pressure of the compressor P_1. A representation of the model can be observed in Figure 7.3.

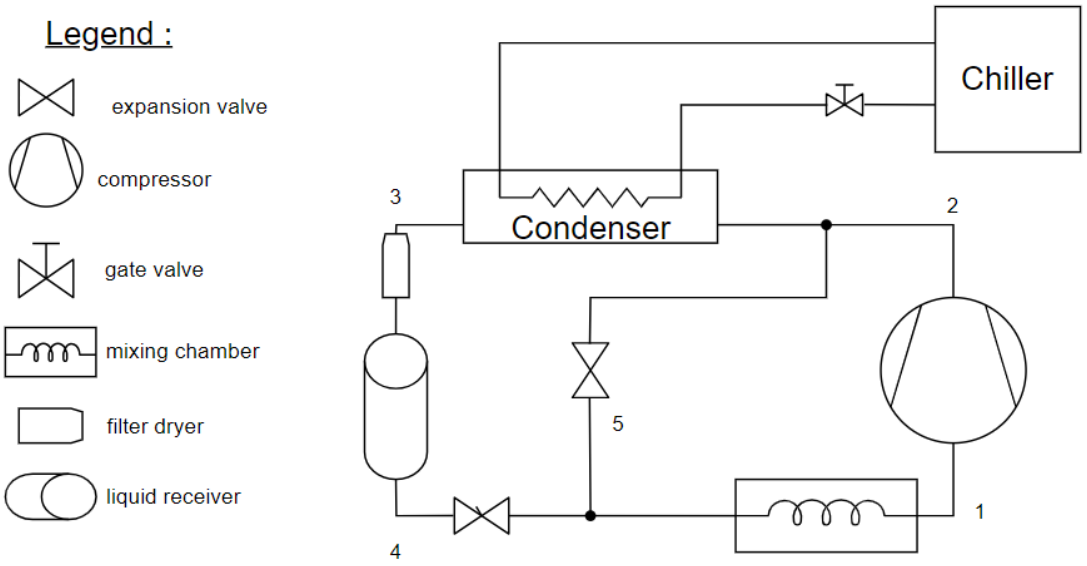

Figure 7.3: Model of the Hot Gas By-Pass

The P-h diagram of a hot gas bypass cycle is represented in Figure 7.4. The figure represents the compressor YHV0461U-9X9 working between between 17 and 32 bar with R744 based on the catalog of Copeland for R744 compressors.

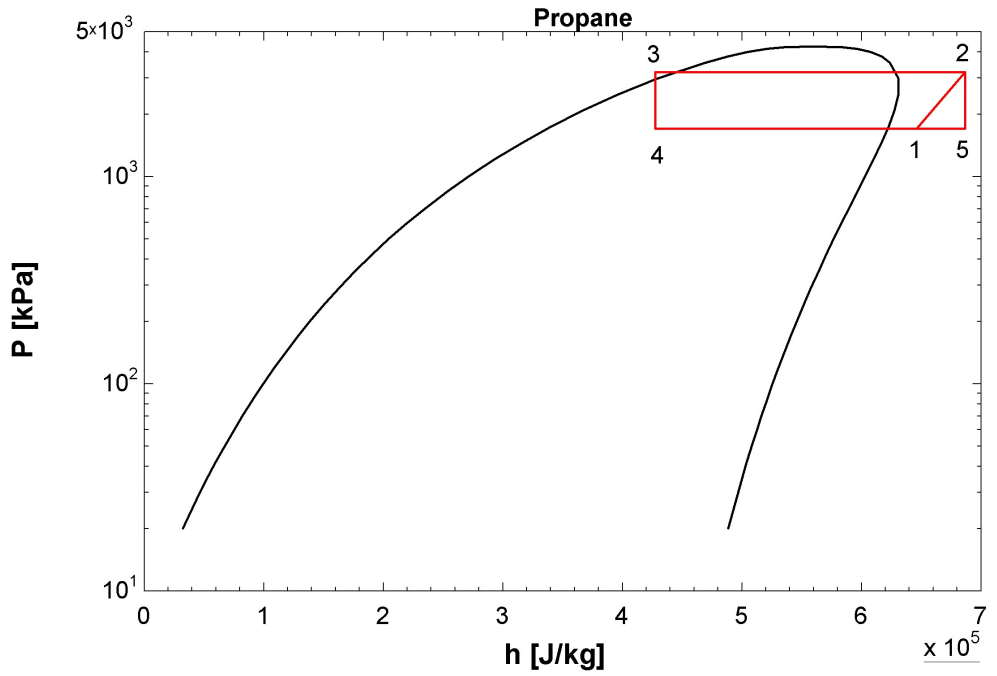

Figure 7.4: P-h diagram of the Hot Gas By-Pass of compressor YHV0461U-9X9

Energy balance

The main advantage of this method results in the economy of energy as no evaporator or heater is needed. The evaporation process is ensured by the mixing of hot gas and sub-cooled liquid. A simple look at the energy balance of the system gives an idea of the energy saved.

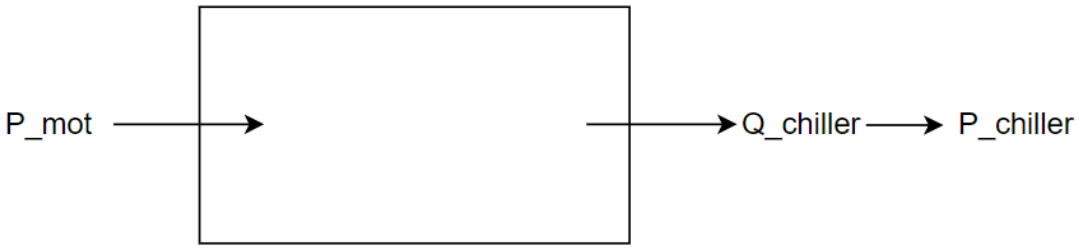

Figure 7.5: Energy balance on the Hot Gas By-Pass

Supposing the same assumptions as in section 7.1.1 ($COP = 3$ and $Q_{heater} = 100[kW]$) and the energy balance in Figure 7.5,

$$P_{mot} = \frac{Q_{heater}}{COP} = 33[kW] \text{ and } Q_{chiller} = P_{mot} = 33[kW] \tag{7.5}$$

Considering again a COP of 3, the compressor relative to the chiller circuit requires :

$$P_{chiller} = \frac{Q_{chiller}}{COP} \approx 11[kW] \tag{7.6}$$

As a result, the total energy required by the cycle with a hot gas bypass is ridiculously low compared to the method of the calorimeter (4 times less).

$$\text{Total energy required} = P_{mot} + P_{chiller} \approx 44[kW] \tag{7.7}$$

7.1.3 Gas Cycle

The last method used is called Gas Cycle. The working principle can be understood through two major aspects:

- the implementation of an intermediary pressure P_{int} for which in all cases, $P_1 < P_{int} < P_2$
- the refrigerant is permanently in a vapor state above the saturation curve

To respect the two points above, an additional valve is introduced in replacement of the evaporator in the basic compressor cycle. The following model can be observed in Figure 7.6.

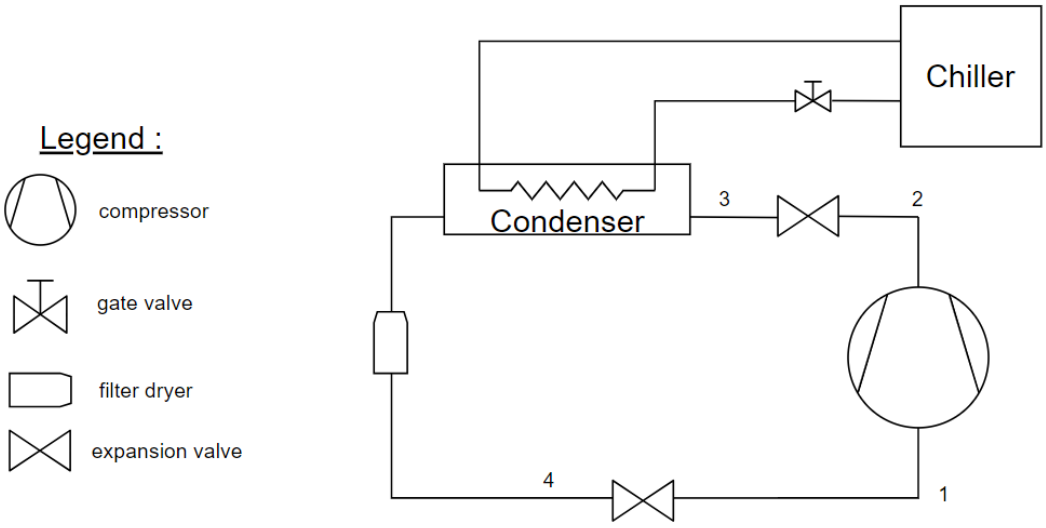

Figure 7.6: Model of the Gas cycle

The outlet pressure of the compressor can be controlled by the first expansion valve at the outlet of the compressor. The second expansion valve of the refrigerant circuit controls the inlet pressure of the compressor P_1. Additionally, the valve from the chiller's circuit influences the intermediate pressure P_{int} and the inlet temperature of the compressor T_1. Note that the intermediate pressure has to be chosen optimally to always stay in a vapor state and to be smaller than the high pressure P_2 and greater than the low pressure P_1.

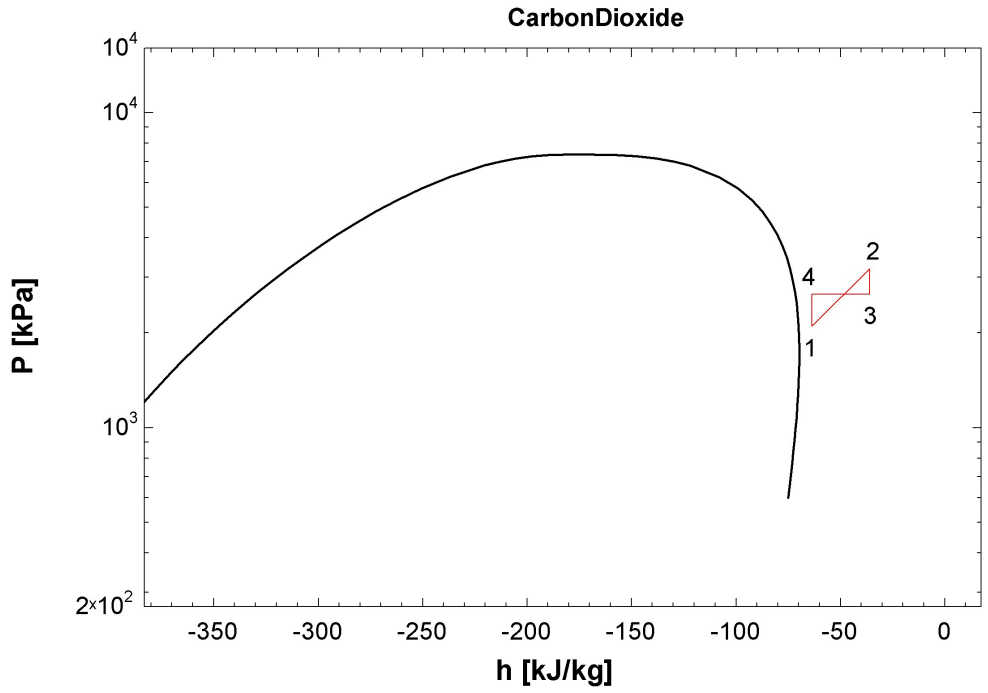

Figure 7.7: P-h diagram of the gas cycle of the compressor ZB15KCE

The P-h diagram corresponding to the model can be seen in Figure 7.7. The figure represents the compressor ZB15KCE working between 21 and 32 bar with R744 based on the catalog of Copeland for R744 compressors.

Concerning the energy balance of the gas cycle, section 7.1.2 explains the principle of the energy balance. The methodology is the same as in hot gas bypass because of the absence of the evaporator. However, the heat exchange in the condenser is smaller for the gas cycle as it works only in a vapor state, and as a matter of fact, the refrigerant does not exit the condenser in a liquid state.
As a result, the overall energy needed in the gas cycle is the lowest of the three methods presented.

7.2 System identification

System identification is a methodology to construct a dynamic model from experiments in the form of a mathematical and graphical model following a natural logical path based on experimentation and usually consists of an iterative process that needs to be reevaluated several times to yield acceptable results. Further information on the method can be read in books [24], [16], and [20].

The system identification loop procedure is a general method that uses the data set, a set of candidate models, and a rule such as the least squares to assess the fitness of the model. A representation of the loop can be seen in Figure 7.8. The collection of experimental data is the first step followed by the

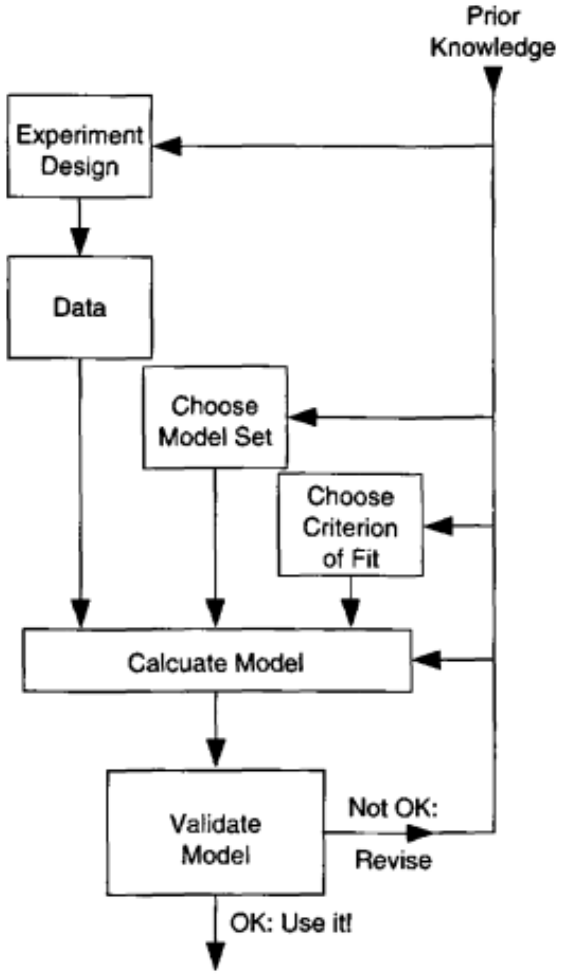

Figure 7.8: system identification loop

choice of the model set to represent the model and the third step is to choose a criterion of fit adapted to the problem. Once those 3 steps have been done, one can calculate the model. For the validation

part, the model parameters calculated are analyzed by using a different set of data to see if the estimated output fits the actual output meaning that the chosen model set correctly represents the system. However, if the method is not accurate enough, a need to revise the various steps of the procedure is required. Several reasons can be the cause of an invalidation of the model such as a non-optimal criterion, a deficient model set or a lack of informative enough data to provide guidance.

To resume, the identification process is an iterative process influenced by previous attempts and prior information to identify a good model set.

7.2.1 Data set

To construct a dynamic model based on experimental data, the first step is to correctly evaluate the model with the relative input-output and the disturbances affecting the model. This step consists of identifying the manipulated variables (MV) which are the inputs and the control variable of the system. The outputs known as the controlled variables (CV) are the variables that in fine, need to be controlled through the inputs. The disturbances are more complicated to assess as the user needs to understand which undesired variables vary over time and can have an effect on the system.

A data set can be constructed using excitation signals that need to be simple and reproducible, applicable to the process in relation to actuators, and provide a good excitation not affected too much by noise to provide interesting system dynamics. An excitation signal can be a simple step response or more complex with a sine wave as seen in Figure 7.9.

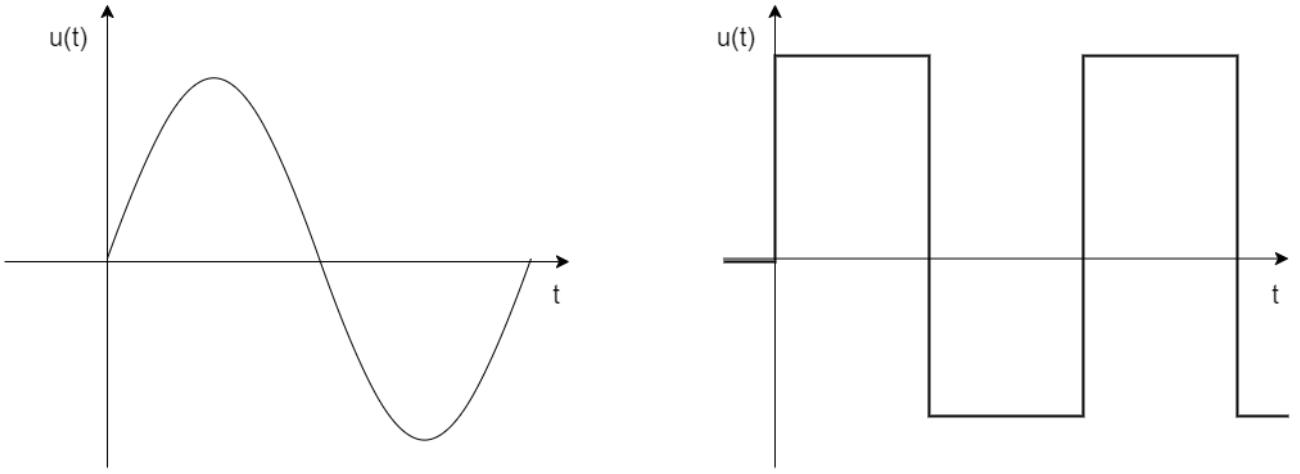

Figure 7.9: Excitation signal

7.2.2 A set of candidate models

Using a data set, the mathematical representation of the model of a single-input single-output (SISO) at time t by the input u(t) and the estimated output $\hat{y}(t)$ can be represented easily under a linear difference equation:

$$\hat{y}(t) + a_1 y(t-1) + \cdots + a_n y(t-n) = b_0 u(t) + b_1 u(t-1) + \cdots + b_m u(t-m) \tag{7.8}$$

The system is represented in discrete time. The discrete time is obtained from data by sampling. The sampling interval is a fixed time for which a value from data is taken every sampling time to represent that time t in the discrete time.

The first equation can be written in a more compact way by introducing two vectors:

$$\gamma = [a_1, \cdots, a_n, b_0, b_1, \cdots, b_m]^T \tag{7.9}$$

$$\varphi(t) = [-y(t-1), \cdots, -y(t-n), u(t-1), \cdots, u(t-m)]^T \tag{7.10}$$

The vector φ(t) is called the regression vector and the vector γ contains the linear parameters to estimate the output the MV and CV of the system. The estimation mostly lies in good parameters of γ and a good enough sampling time representing the system.
A new equation can therefore represent the output at time t using the previous observations and vectors

introduced:

$$\hat{y}(t) = \varphi^T(t)\gamma \tag{7.11}$$

The model can either be represented under a state-space form or a transfer function form P(s) of the stand with Laplace transform of the input and the output with a sample time T_m applied to the linear difference equation following the general form:

$$P(s) = \frac{Y(s)}{U(s)} = \frac{b_0 + b_1 s + \cdots + b_m s^m}{a_1 s + \cdots + a_n s^n} \tag{7.12}$$

With Y(s) the Laplace transform of y(t) and U(s) the Laplace transform of u(t).

7.2.3 Validation and fitness of model

As one can see, the representation of the model depends on the previous inputs and outputs of the system forming the data set and a set of models represented by $\varphi^T(t)$ composed of the parameters to approximate the current output. A last part required is the validation of the model representation by evaluating the fitness of the model with another set of data.

The residual ε(t) is introduced as follows $\varepsilon(t) = y(t) - \hat{y}(t)$ with $\hat{y}$ as the predicted output of the simulation model and y as the measured output of the physical stand. To determine which set of models represents the stand better, a rule to validate the fitness of a model is used.

A first generally well-known validation criterion is presented in the book [24] at p204: the Least squares method. An assumption is made that for a given system the values of the inputs and outputs are measured over a time interval $1 \leq t \leq N$. The least-square V_N is denoted by the following equation with y(t) the output and $\hat{y}(t)$ the estimated output:

$$V_N(\varphi) = \frac{1}{N}\sum_{t=1}^{N}(y(t) - \hat{y}(t))^2 = \frac{1}{N}\sum_{t=1}^{N}(\varepsilon(t))^2 \tag{7.13}$$

The method of the least squares helps to analyze the different vectors $\varphi^T(t)$ to determine the parameters that best approximate the model. The lower the number of the least square method, the more the model is correctly approximated by the parameters.

The fitness of the model can be evaluated with equation 7.14.

$$Fit = 1 - V_N(\varphi) \cdot 100\% \tag{7.14}$$

There is a wide range of validation rules to evaluate if a simulation model correctly fits the physical stand. For example, three other validation rules using the model residuals can be performed based on p144 of book [32]. The maximal residual, the average residual and the relative error measure are calculated using respectively equation 7.15, equation 7.16, and equation 7.17 with N being the number of measurements and $\bar{y}$, the mean value of y:

$$S_1(\varphi) = max|\varepsilon(t)| \tag{7.15}$$

$$S_2(\varphi) = \sqrt{\frac{1}{N}\left(\sum_{t=1}^{N} \varepsilon^2(t)\right)} \tag{7.16}$$

$$S_3(\varphi) = \frac{\left(\sqrt{\sum_{t=1}^{N} \varepsilon^2(t)}\right)}{\left(\sqrt{\sum_{t=1}^{N} (y(t) - \bar{y})^2}\right)} \tag{7.17}$$

Using these criteria, the percentage of model fit can then be calculated as $Fit = 100\% \cdot (1 - S_r)$ with $r \in [1, 2, 3]$.

7.3 Controller performance

Controller performance corresponds to the accuracy of adjustment of controller parameters to match the dynamic characteristics of the system.

Despite its great importance, the improvement of controller performance is generally the least understood concept of control system.

As a result, "trial and error" method is usually applied to obtain satisfactory tuning parameters for the case study. Tuning a controller consists of adjusting the parameters of the controller to have a desired control response.

The assessment of a tuning method can be done using several error performance criteria to observe and analyze controller performance.

Papers [38] and [25] mention the use of an Integrated Absolute Error to evaluate the output performance. The IAE can be used to evaluate if the controlled variable follows accurately the reference (setpoint) over time.

$$IAE = \int_0^\infty |\varepsilon(t)|dt \tag{7.18}$$

With the error defined as $\varepsilon(t) = SP(t) - y(t)$.

Using a sampling value T_m appropriate, it can be reduced to a discrete number of measurements N and analyzed with less computation time.

$$IAE = \sum_{t=1}^{N} |\varepsilon(t)| \tag{7.19}$$

The resulting IAEs can be analyzed when controller tuning methods are compared to one another. The best model is identified as it minimizes the IAE.

Another performance factor can also be used to evaluate the manipulated input change. The Total Variation (TV) of an input u(t) is the sum of all the variations of the input. A representation in the time domain can be seen in the following:

$$TV = \int_0^\infty |u(t+1) - u(t)|dt \tag{7.20}$$

Using a sampling value T_m appropriate, it can be reduced to a discrete number of measurements N and analyzed with less computation time.

$$TV = \sum_{t=1}^{N} |u(t+1) - u(t)| \tag{7.21}$$

The smoothness of variation of the input signal is sought and can be identified with a low value of TV.

Chapter 8

Analysis

8.1 System identification

The first part of the analysis starts with the construction of a dynamic model to perform improvement tests of the controller applied to the system. Two books [24] and [16] introduce system identification and describe the methodology for various systems and applications as well as the construction of linear and non-linear systems. Two main approaches for the dynamical modeling of stand can be used: first-principles model and data-driven model. The first is based on physical laws and empirical relations and needs to be calibrated for each specific model. To that extent, numerical software can be used such as Amesim, Thermosys from Mathworks, Modelica with Dymola license. The second approach consists of using experimental data through system identification to build the numerical model with the use of the system identification Toolbox from Simulink.

Most of the research is based on the construction of a numerical model with the first-principles approach. The research aims to first construct a numerical model of a process as it involves fewer resources and is more versatile to validate or change the parameters of the research. The papers [13],[14],[19] derives their model from physical laws, thermodynamics, and prebuilt libraries to build a dynamic model. Several other papers [5] [32],[21] use the software Thermosys. Another paper[18] opts for the option of Modelica and its open source.
However as mentioned in the problem narrowing, constructing a numerical model to represent accurately the load stand from first principle modeling is time-consuming and often very complex. The numerical model from such software is based on physical laws adapted to the specific components. In addition, the model needs to be calibrated to ensure a good representation of the actual stand which can be very sensitive to data. Data can be generated either by performing tests on the stand to determine the different parameters or by being directly given by manufacturers in the form of performance maps on which linear regression can be performed.

In general, a good numerical model can be achieved through the use of appropriate libraries and with full data in approximately two months. Dedicating two months to the modeling of the load stand would result in a lack of time to investigate and apply the improvement of the controller which is the main scope of this Master's thesis. The advantage of a numerical model from first-principles lies behind the fact that the model can be adapted to several similar load stands by varying specific parts of the model in case of partial replacement of components. Another big advantage is that tests can be performed directly on the numerical model at a faster rate without risking any material destruction. Nonetheless, the main drawback is the time required to build the model which would be the subject of a thesis in itself.

Another option chosen in this project called system identification consists of obtaining a model of the load stand without modeling the complex dynamics and physical relations between components of the stand as it has been reviewed in a state-of-the-art [12] and paper [15]. More specifically, papers [10],[37],[9] apply the methodology of system identification to a compression-vapor cycle. To obtain the dynamic model, Simulink is used to identify the system for each pair of input-output to form a MIMO model. This method is usually used in the domain of control and automation as it does not require catching the essential dynamics of the system to tune the controller.
The basic idea is to use an appropriate excitation signal on an input and observe the effects in the output responses while the actual controller is turned off. This modeling approach heavily relies on experimental data obtained from the stand. Therefore, the accuracy of the model representation is a crucial part of the modeling. In the case of the system studied, the experimental data can accurately represent the model in the form of a state-space representation or a transfer function only for a specific operating point at which data tests are performed. As a result, in the case of a replacement of components of the stand or to represent the whole operating conditions of the stand, the methodology of system identification of a black box model would need to be applied several times to construct a bank of linear models representing the nonlinearity of the system.
Generally in the case of industrial applications, despite the adaptability and the information gained, a first-principles model is too resource and time-consuming compared to a black box system identification model for a specific stand. Moreover, a toolbox in Simulink called 'System Identification' can help construct the representation of the model using data obtained from experiments.

Using system identification, the papers [13] and books [24], [16] mention the representation of a

nonlinear model with the linearization around nominal operating points by a bank of linear models each valid over a specific range. Each linear part is represented by a transfer function FOPDT (First Order Plus Dead Time) relative to each pair of input-output calculated with the use of the 'System Identification' Simulink toolbox for a precise nominal operating point. The interpolation of linear models can correctly represent a non-linear system such as the vapor compression cycle.
If the representation through FOPTD is not adequate, the paper [32] suggests the use of a MIMO 6th order model with a N4SID algorithm to take into account the relative effects of different inputs together for a specified range as well. Another paper [15] suggests the use of linear regression tools such as an ARMAX structure to represent the local linear models as well. Linear regression tools have a wide variety of structures and further information can be read in the books [24] and [16].

In our specific case, the stand first studied is the HGBP stand of the SoundRoom as mentioned in the problem narrowing. To represent the system dynamically, the use of a black box identification model to represent the model in a transfer function form is chosen mainly due to time constraints as the company objective is the improvement of a controller and not the modeling of the load stand. The identification method can effectively catch the dynamics between input-output and the delay of the system induced by the length of pipes between sensor T1 and the regulation valve of the condenser. As our system is non-linear, the developed model should be linearized around specific nominal operating points in order to fit the whole range of the non-linear stand. In industry, the number of operating points used for the bank of linear model usually ranges between 10-20 points depending on the specific applications. The main methodology applied for system identification is described in Methods 7.2.

8.1.1 Black box model

The first step to system identification is to identify the parameters that are to be manipulated also called the manipulated variables MV or inputs and the outputs that are observed and controlled called the controlled variable CV.

The stand as explained in the problem formulation section can be controlled mainly by three valves to cover the operating map of the compressor. The valve from the waterside A_v of the condenser would mainly control the outlet pressure of the compressor P_2 by adapting the volume flow rate of water in the condenser impacting the refrigeration power and thus, the pressure. The electronic expansion

valve of the bypass EEV_{bp} principally controls the inlet pressure of the compressor P_1 by the opening of the valve. The last manipulated variable is the electronic expansion valve after the condenser EEV_{cd} controlling the inlet temperature of the compressor T_1 by adjusting the amount of cooled refrigerant flowing to the inlet of the compressor.

The basic system of the stand is disturbed by parameters of the system that need to be taken into account to develop robust and efficient control. The system is influenced by the speed rotation of the compressor N varying the refrigerating power of the compressor and the refrigerant amount m_{ref}. The displacement volume of the compressor V_{displ} and the amount of refrigerant m_{ref} can also be changed by using bigger compressors acting on the refrigerating power. The temperature of the waterside of the condenser T_{cd}, subcooling ΔT_{sub}, and superheating ΔT_{sr} do not vary under normal conditions and are fixed at the beginning of the stand test. However, the type of refrigerant ref and amount of refrigerant m_{ref} represent disturbances that are likely to induce problems in the construction of the model as they can greatly influence the dynamics of the stand. A representation of the black box model can be seen in Figure 8.1.

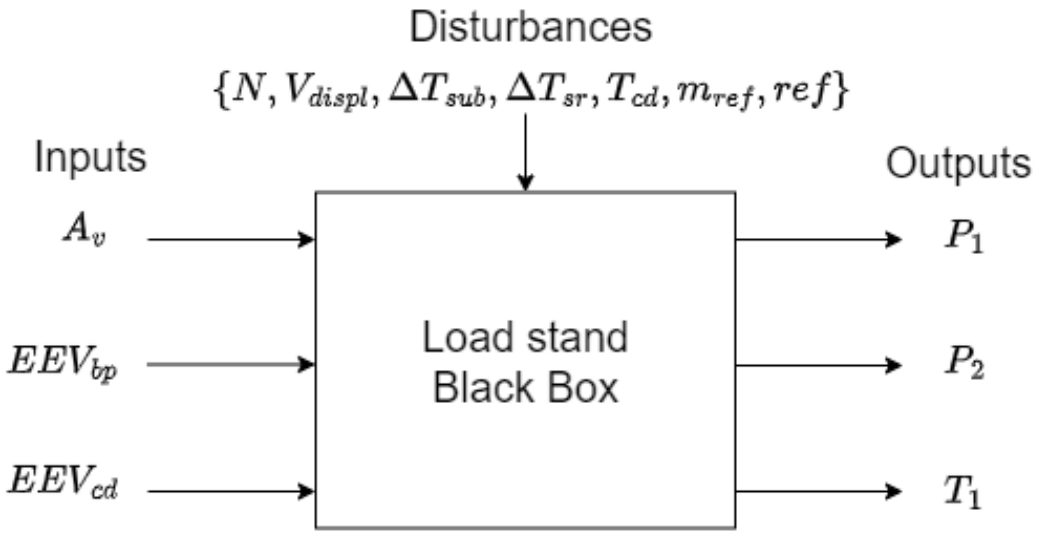

Figure 8.1: Black box model Inputs-Outputs

8.1.2 Data set

As mentionned in theory, the construction of a model from data involves a good choice of maximally informative data. The data of each pair of input-output is recorded for specific experiments in which the user determines which signals to measure, when to measure them, and the variation of MV for each of the experiments. The objective in mind is that the experiment design is to make the data maximally informative (even if the model can be subject to the constraints of the system). The more informative the data, the better the representation of the system.

To record data, the first step is to reach a nominal operating point with stabilized conditions. The second step is to turn off the controller relative to the manipulated variable which is varied while the other controllers of the system are still active. It means that the test is applied in a partial open-loop without a retro-action of the controller on the manipulated variable studied. It is partially in an open loop as the other controllers use a feedback loop and are therefore in a closed loop. Using an identification in an open loop helps to understand the fundamental dynamics of the system by removing feedback from the controller which tends to linearize the response. After the variation of a first MV, the stabilized point needs to be reached once again in order to vary the next MV of the system until all inputs of the system have been varied. To vary the next MV of the system, the controller of the previous MV is turned on and the controller of the next MV is turned off to be in an open loop. This test is done for every MV of the system.
Other testing methods in a fully open loop or in a fully closed loop are also possible. However, the fully open loop method requires turning off all the controllers which can lead to material destruction and consequently is rarely used in industry. The closed loop method on the other side is safer to perform but bigger changes in setpoint are required to observe the dynamics of the system and the resulting data need to be removed from the transfer functions of the controllers.

The variation of MV also called the excitation signal needs to be simple, reproducible, and provide good excitation to catch the dynamics of the system as mentioned in Methods 7.2. The ideal excitation signal is a PRBS signal with fast and versatile variations of the MV and can be observed in Figure 8.2.

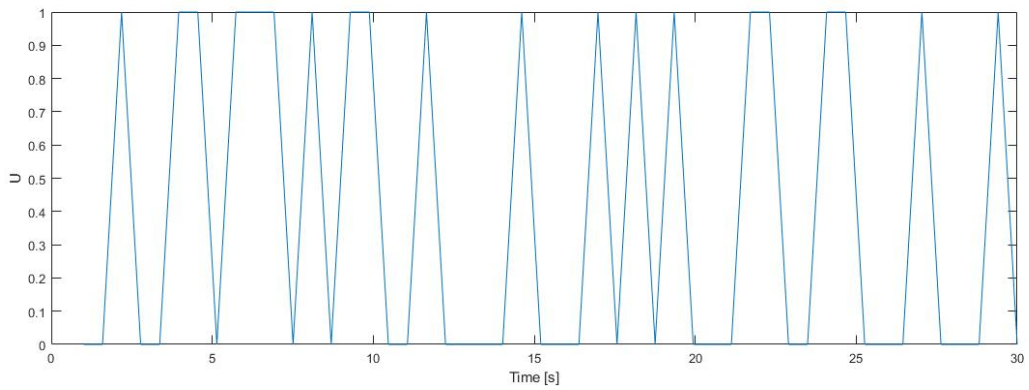

Figure 8.2: PRBS signal

However, the use of a two-step signal is also a good enough excitation signal in order to maximize the information with a short experimentation time. The two-step signal is not fixed and may vary according to each specific input at each specific nominal operating point based on the maximum allowable amplitude and speed of the change of the input signal u(t) and the maximum allowable amplitude of the output signal y(t). However, a general test form can be seen in Figure 8.3. The two-step signal is chosen as a trade-off between time requirements for tests and accuracy of determination of the frequency response at low, medium, and high frequencies. The system identification book [16] p 118 recommended the use of a few step responses to determine the frequency response at low frequencies and a sequence of rectangular pulses to determine the response at medium and high response. In addition, the response should be evaluated in both ascending and descending values to correctly represent certain dynamics.

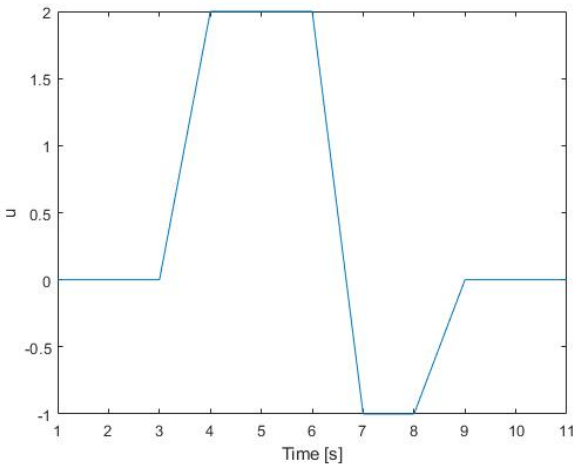

Figure 8.3: Two-step general form

A good two-step signal is represented by a clear variation in the output signal response of the CV which can be differentiated from the noise induced by disturbances. The noise can induce an error in the state-space representation which is why the step response needs to be able to be differentiated from the noise. To that extent, filtering can be applied to the data to remove a part of the minor disturbances in the system. In order to correctly choose the step change in the inputs, prior information provided by the technicians of the SoundRoom will provide insights into the potential variation occurring in the system when a set of inputs is changed.

8.1.3 Sampling time

In order to build a MIMO model, the use of a sample time is useful to reduce the amount of data to process and maximize the information.

The sampling time T_m can be approximated to build the transfer function in the frequency domain (s). A good approximation of the sampling time can be found by looking at the responses of the MV to specific input changes more precisely the different rise times of the system or settling time defined in Theory 6.1.2. The rise time or settling time of the system can be manually seen in the output response. The rise time corresponds to the time required by the output to pass from 10% to 90 % of the desired response output and the settling time corresponds to the time for which 95 % of the desired response output is reached.
As a reference value the book [16] suggests that for PID control algorithms, one can select:

$$T_m = \left\{ \frac{T_{95}}{5}, \cdots, \frac{T_{95}}{15} \right\} \tag{8.1}$$

with T_{95} the settling time of the system.

The Ph.D. Hernandez Andres specialized in control systems suggested the use of the time for a step response to reach 63% of the reference value, T_{63}. The sampling time can then be calculated from:

$$T_m = \left\{ \frac{T_{63}}{5}, \cdots, \frac{T_{63}}{10} \right\} \tag{8.2}$$

Different sampling times are to be obtained for each specific input-output and can be compared. However, taking the fastest time divided by 10 is a good approximation $T_m = \frac{T_{63}}{10}$ to have sufficient accuracy over the step responses of the system. However, if the time constants differ too much from one another,

non-useful data are expected to be captured and the sampling time can be reduced to $T_m = \frac{T_{63}}{5}$ to avoid non-useful data.

8.1.4 Choice of model structure

In system identification, one of the main steps consists in the search of a suitable model to provide an accurate description of the system. The set of candidate models has to be chosen depending on prior knowledge or engineering intuition. The prior knowledge is provided by research papers or books focusing on the representation of a non-linear model such as the HGBP cycle. The books [24] and [16] as well as papers [13] and [32] suggest the use of FOPTD dynamic models. The FOPTD model type that is used in the analysis is a standard transfer function of a linear model without reference to the physical background. This type of model is viewed as a black box as it fits the model to the set of data and specifically for the stand evaluated.

By feeding the input-output data to the 'System Identification' toolbox, Simulink can produce a state space representation and/or the relative transfer function of the model that can be used to represent a range of the non-linear model by a linear approximation model.

The general form of a transfer function is then introduced,

$$H(s) \equiv \frac{Y(s)}{U(s)} = |H(s)|e^{\angle H(s)} \tag{8.3}$$

In our case, the First Order Plus Time Delay (FOPTD) transfer function is chosen as it requires less computation time and is a commonly adopted linear model in the industry. Moreover, combined with the use of a PID that rectifies the measurement error, the lower accuracy of the FOPTD model is, therefore, an advantage as even if simulated results are slightly different from the results of the stand, the PID controller chosen would remain efficient over a wide range of the stand. The local linear model can be represented in the frequency domain by the use of a sampling time and a first-order plus time delay (FOPTD) transfer function of the form:

$$H(s) = \frac{K \cdot e^{-s\theta}}{(s\tau + 1)} \text{ with } \gamma = [K, \theta, \tau]^T \tag{8.4}$$

With K the static gain of the system, θ the delay of the system, and τ the time constant.

Several clarification points have to be further developed.

First, the FOPTD transfer function only represents a pair of input-output. To represent the stand, a MIMO model taking into account all MV and CV is introduced using the FOPTD as building bricks. Secondly, the FOPTD is expected to capture a part only of the dynamics of the non-linear system valid over a specified range and not the whole dynamics of the non-linear system. A suitable linear representation of the stand can be obtained in terms of time constant, delay, and gain for a definite range with the FOPTD MIMO model. Using several of those linear models, a piecewise linear approach is able to produce a representation of the nonlinear system using a bank of linear models.

Representation of the MIMO model

Based on all the different SISO FOPTD, a relation between each output and input can be built to have a multiple input Single output (MISO) with m being the number of manipulated variables (MV) and y_i the i^{th} output of the model:

$$y_i = \sum_{j=1}^{m} H_{i,j} u_j \tag{8.5}$$

The MIMO structure can be formed with a vector **y** of n outputs or controlled variables (CV), a vector **u** of m inputs, and a matrix **H** of rank n x m :

$$\underbrace{\begin{pmatrix} y_1 \\ y_2 \\ \vdots \\ y_n \end{pmatrix}}_{\mathbf{y}(s)} = \underbrace{\begin{pmatrix} H_{11} & H_{12} & \dots & H_{1m} \\ H_{21} & H_{22} & \dots & H_{2m} \\ \vdots & \vdots & & \vdots \\ H_{n1} & H_{n2} & \dots & H_{nm} \end{pmatrix}}_{\mathbf{H}(s)} \underbrace{\begin{pmatrix} u_1 \\ u_2 \\ \vdots \\ u_m \end{pmatrix}}_{\mathbf{u}(s)} \tag{8.6}$$

In the case of the hot gas bypass system, there are 3 CV (P_1, P_2, T_1) so n = 3 and there is 3 MV (EEV_{bp}, A_v, EEV_{cd}) resulting in m = 3. The rank of the matrix **H** is 3 x 3 which means it is composed of 9 terms.

Other state-space representations or transfer functions can be used and compared with the FOPTD such as the second-order plus time delay (SOPTD) transfer function and a state-space representation with subspace N4SID prediction algorithm. Nevertheless, it is not done in this work as the FOPTD transfer function is supposed enough to represent a part of the non-linear system over a specified range and the following section can use those local linear FOPTD to represent the dynamic of the whole sys-

tem.

The MIMO model is to be constructed with the system identification Toolbox from Matlab with FOPTD transfer functions relative to each pair of input-output and can be fed with a quick estimation of the delay of the system to respond to an input change.

The piecewise linear approach

To model the complete behavior of a non-linear model, the system can be split up into a range of local operating point points for which a linear MIMO model based of FOPTD can be built. A series of L matrixes $\mathbf{H}(\mathbf{s})$ of FOPTD MIMO models can be constructed for the L nominal operating points. The series of FOPTD models can be identified with the subscript $r \in [1L]$ and the input-output pair can be identified with the subscript $k = i, j \in [19]$ with the respective gain vector $K_{r,k}$, the time constant vector $\tau_{r,k}$, and the delay vector of the system $\theta_{r,k}$ contained in the matrix of $\gamma_{r,k}$:

$$H(s, r, k) = \frac{K_{r,k} \cdot e^{-s\theta_{r,k}}}{(s\tau_{r,k} + 1)} \text{ with } \gamma_{r,k} = [K_{r,k}, \theta_{r,k}, \tau_{r,k}]^T \tag{8.7}$$

The non-linear system is then represented by a series of L matrix transfer functions $\mathbf{H}(r)$. A matrix $\mathbf{H}(r)$ is composed of 9 elements represented by k which consists of FOPTD transfer function as defined in equation 8.4.

The series of L matrix of transfer function forms a bank of local models. The bank of L local models is created to combine the different linear parts valid over a specific range of the operation map of the compressor into a whole model able to describe the behavior of a non-linear system entirely. The combination can be done using an interpolation scheme based on weight or probability.

In the paper [13], two different approaches are mentioned:

1. The first approach uses interpolation between the models by the use of time-varying weights identified online to best approximate the output of the process with the model.

2. A second approach calculates the probability of the different models among the bank of models to correspond to the measurements of the stand. A difference between the measured outputs of the stand and the estimated outputs of each local model helps to approximate an optimal model from the bank.

The model error ϵ_r can be represented by the difference between the real measurement of the outputs y_{k,t_k} and the r^{th} model estimated output $\hat{y}_{r,k,t_k}$ at a current time t_k.

$$\epsilon_{r,k,t_k} = y_{k,t_k} - \hat{y}_{r,k,t_k} \tag{8.8}$$

Based on the probability function chosen and the different model errors ϵ_{r,k,t_k}, a weighting scheme attributes a specific weight $w_{r,k}$ to each linear model at each time t_k. As a result, the more accurate estimation model would be associated with a greater weight.

In the case of the work, the second approach with the probability weighting scheme is preferred as it can be applied to a wider variety of systems and can compensate efficiently with an estimated model in case of a lack of linear models in the bank.
A presentation of the general Bayesian estimator as a weighting scheme is presented. The Bayesian estimation takes into account the previous probability at the time $t_k - 1$ to have a recursive probability.

Bayesian estimator:

The Bayesian estimators have demonstrated their potential to select the best model at each time step from a bank of models. The Bayesian estimation method uses a probability $p_{i,k}$ calculated at each time t_k for each linear model of the bank using the model error ϵ_{r,k,t_k}, a convergence vector M, the previous probability calculated at the previous step, and a cut-off probability $\delta_{cut\ \ off}$. The cut-off probability has a purpose of excluding the influence of models with high model error ϵ_{r,k,t_k}. Nevertheless, the cut-off probability is kept very low to ensure that hardly any model has a weight of zero (no influence over the global model).

$$\begin{aligned} p_{r,k,t_k} &= \frac{\exp\left(-\frac{1}{2}\epsilon_{r,k,t_k} M_r \epsilon_{r,k,t_k} p_{r,k,t_k-1}\right)}{\sum_{m=1}^{L}\left(\exp\left(-\frac{1}{2}\epsilon_{m,k,t_k} M_m \epsilon_{m,k,t_k} p_{m,k,t_k-1}\right)\right.}. \\ w_{r,k,t_k} &= \begin{cases} \frac{p_{r,k,t_k}}{\sum_{m=1}^{L} p_{m,k,t_k}} & \text{for } p_{r,k,t_k} > \delta_{cut\ \text{off}} \\ 0 & \text{for } p_{r,k,t_k} < \delta_{cut\ \text{off}} \end{cases} \end{aligned} \tag{8.9}$$

The convergence vector M is tuned to amplify the impact of some models compared to others. The values inside the vector can be tuned to the same value if no particular model represents the dynamics of the model more accurately than another. The vector M is often composed of the same value in order to decrease complexity in calibration. In the same order of idea, the value $\delta_{\text{cut off}}$ can be set arbitrarily

low to ensure that a large variety of models have an impact over the whole range of operations of the stand. Nonetheless, a fine-tuning of the cut-off frequency and the convergence matrix M can improve the estimator performance.

Using the estimation of the Bayesian scheme, one can identify that the methods require the tuning of L parameters of the vector M, the number of models used L, and the cut-off value $\delta_{\text{cut off}}$. In total, L+2 parameters are to be tuned.

At each time t_k, the weighting scheme assigns a value between 0 and 1 to each specific linear model and the sum of the weighting scheme parameters tends to 1 to ensure a correct representation of the global model.

$$\sum_{r=1}^{L} w_{r,k} \longrightarrow 1 \quad \forall k \tag{8.10}$$

The resulting model output can be defined for each time t_k for each particular input-output part to form the MIMO model and their resulting transfer function can be built at each time t_k.

$$\begin{aligned} y_{k,t_k} &= \sum_{r=1}^{L} w_{r,k,t_k} y_{r,k,t_k} \\ H_{k,t_k}(s) &= \frac{K_{k,t_k} \cdot e^{-s\theta_{k,t_k}}}{(s\tau_{k,t_k}+1)} \end{aligned} \tag{8.11}$$

The number of models L stored in the bank is an important tuning parameter as the calibration of the numerical model is directly linked to the number of linear FOPTD models used to represent the system. Having more models to represent the system means more accuracy but increases the difficulty in calibrating the parameters of the Bayesian scheme.

8.1.5 Model validation

In this part, the validation of a model is discussed and presented. To validate a model, a chosen validation criterion or rule of fitness is used to evaluate the accuracy of the model, guided by the data. The model validation has to be performed for each of the linear models based on a nominal operating point of the stand and for the global model based on the bank of linear models.

The particular model has been developed according to experimental data and a chosen criterion of fitness if required to validate the accuracy of the model. However, the data used to validate the model

cannot be the same data used for building the model representation. Usually, one-third of the experimental data is used to validate the model representation constructed from the other two-thirds.

Moreover, an assessment needs to be performed to evaluate if the model is "good enough" for other independent data. A large enough model can reproduce a measured output arbitrarily well for a specific set of data, but it does not mean that all data would fit correctly into the specified model.
The specific range is determined by an error between estimate and measured output of 20 % according to a validation criterion chosen to ensure a good fit.

The validation of the model is done to observe how the model behaves compared to observed data, prior knowledge, and intended use. If the model does not correspond, it will be rejected while a good performance asserts our confidence in the model. The assessment of a model's quality is typically based on how well the model performs when it attempts to reproduce the measured data.

Validation criterion:

To define if the linear representation correctly fits the experimental stand, a criterion using the model residuals ϵ(t) can be used with the residuals defined in equation 8.8.

The estimated output of the system $\hat{Y}(s)$ in the frequency domain can be represented.

$$\hat{Y}(s) = U(s) \cdot H(s) \tag{8.12}$$

where $\hat{Y}(s)$ is theestimated output of the system in the frequency domain, U(s) is the MV (input) in the frequency domain, and H(s) is the transfer function defined in equation 8.4.

The predicted output $\hat{Y}(s)$ can be transformed in the time domain using the Laplace Transform to correspond to measurements of the stand in the time domain.

As presented in 7.2, the most general criterion to validate the fitness of a model is the Least-squares criterion. Other criteria of fitness that can be used are presented in Methods 7.2. Among them, the relative error measure criterion denoted S_3 from equation 7.17 is chosen to be applied in the case of this

work as it is directly available in the Toolbox System Identification to validate the model by measuring the fitness of a model.

To assess the fitness of the model, the criterion assumes that the outputs and inputs of the system are measured over a time interval of N measurements.
The relative error measure criterion is a quadratic criterion function presented on page 144 of the paper [32] defined by the following using the residual, model error $\epsilon(t) = y(t) - \hat{y}(t)$ and the mean output value $\bar{y}$:

$$S_3 = \frac{\left(\sqrt{\sum_{t=1}^{N} \varepsilon^2(t)}\right)}{\left(\sqrt{\sum_{t=1}^{N} (y(t) - \bar{y})^2}\right)} \tag{8.13}$$

The criterion is optimized by choosing the model giving the lower value of S_3 or calculating the fitness of the model.

To validate the linear model, the goodness of fit can be used and calculated as follows:

$$Fit = (1 - S_3) \cdot 100\% \tag{8.14}$$

A rule of thumb given by the PhD researcher Hernandez Naranjo Jairo Andres from the University of Liège is that a goodness of fit over 80% is required to approximate the system accurately enough. Therefore, the criterion rule is to have an error inferior to 20 % to validate the model representation :

$$\frac{\left(\sqrt{\sum_{t=1}^{N} (y(t) - \hat{y}(t))^2}\right)}{\left(\sqrt{\sum_{t=1}^{N} (y(t) - \bar{y})^2}\right)} \leq 20\% \tag{8.15}$$

with $\hat{y}(t)$ the estimated output of the stand at a specific nominal operating point and $y(t)$ the real measured output.

In the case of the thesis, an extended use of that method can be applied to determine the range over which the system can be approximated by the linear model representation of the transfer function. Different sets of validation data are provided with different ranges around the nominal operating point over which the linear model is built. By trial and error, once the criterion of fitness is below 80%, a new

linear model has to be built at both extremum of the non-validated range, therefore defining the next operating points required to construct the bank of linear models of the system.
If the estimation differs more than 20% from the measured output, the model representation does not represent the system accurately enough for the range and a new nominal operating point has to be used to build a new linear model representation covering a new range.

By adding linear systems constructed around different operating points of the stand to form a bank of linear models, a non-linear model such as the HGBP stand can be approximated over the entire operating range of its system as can be observed from Figure 8.4. The method to assemble the different linear models has been explained under the piecewise linear model approach with the Bayesian estimator.

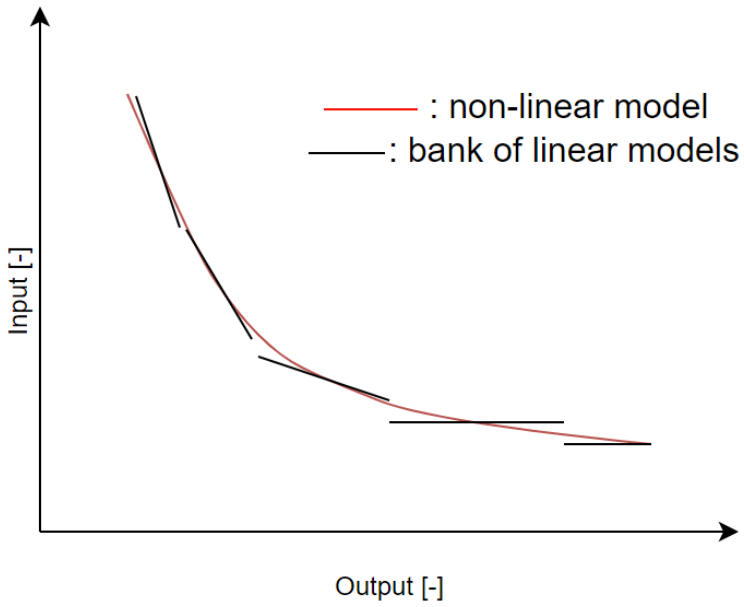

Figure 8.4: Approximation of a non-linear model with a bank of linear models

To represent a non-linear model, a bank of linear models is generally composed of 10-20 linear models to cover the entire range of a non-linear model. However, the number L of specific models is expected to vary from one application to another depending on the operating range.

In the end, the fitness can be used to describe the quality of the linear models, to evaluate the next operating point on which to build a linear model, and to validate the global model built from the piece-

wise linear approach.

Conclusion. *In the section 'Black box model', the different MV and CV have been defined for the case of the HGBP stand along with the disturbances that can impact the dynamics of the stand.*
Using the section 'Data set', an explanation of how to perform tests in a fast and efficient way to obtain maximally informative experimental data can be read using a two-step input change and by turning off the controller relative to the input.
The section 'Sampling time' provides a sampling time adapted to the experimental data to reduce the amount of data into more useful data or to transform data in the frequency domain.
The section 'Choice of model structure' focused on the presentation of the transfer function FOPTD to represent each pair of input-output in a simple and efficient manner. To that extent, a representation of the MIMO model is made out of FOPTD functions to construct a local linear model around a nominal operating point of the stand. Moreover, a piecewise linear approach is then developed to form a global model made from a bank of MIMO linear models through the use of a Bayesian estimator algorithm.
The last section 'Model validation' explains how to validate a model representation for a local model over their defined operating range and for the global model over the entire operating range of the stand. To validate a model, the validation criterion rule of the relative error measure is used to assess the fitness of the representation model and is further used with an extended application to determine the next operating point of the stand from which a local linear model is to be built. The local linear model newly built will be part of the bank of linear models from which the global model is constructed. The global model once constructed has to be validated to ensure an accurate representation of the stand.

8.2 Experimental model

In this section, the methodology of system identification presented in the previous section is applied to the HGBP stand to obtain a MIMO FOPTD model representation of the stand for one nominal operating point of a compressor. Due to a lack of time and availability of resources to test different nominal operating points of a compressor, only one set of data was gathered. After observing and analyzing the data set, the experimental data were not representative enough of the system dynamics. As a result, no linear model using FOPTD is presented. Furthermore, the piecewise linear approach presented theoretically is not implemented in the following as no bank of linear models is currently available. Instead, insights on how to improve the experimental tests to gather a more maximally informative data set are discussed.

8.2.1 Experimental data

To obtain a data set for the construction of one linear model, tests were applied to the stand.In order to do the tests, the controller of the valve tested is turned off and the opening of the valve is manually fixed. Nevertheless, the controllers of the other valves are still active to ensure the safety of the stand and try to stay at the setpoint fixed.

The tests were applied on the HGBP 15 T stand in which clear variations of valve openings (MV) can be observed. The system is characterized by the variable speed compressor **YHV-029** working with R290 and a volume displacement of 29 cc for a nominal operating point at $P1 = 3.8$ bar; $P2 = 17.1$ bar; $T_1 = 3.3$ °C; $T_2 = 85.5$ °C.
The red dotted lines in the following figures represent the time of change of valve opening and the data were recorded every second.

A first manipulation of variable is applied on the opening of the valve EEV_{bp} which controls the pressure P_1 principally. The valve opening was first stable at 6.6 % then increased to 8% before being decreased to 5 %. After a certain amount of time, the controller of the valve is reactivated. The resulting responses of the different CVs of the stand to the variation of valve opening can be observed in Figure 8.5.

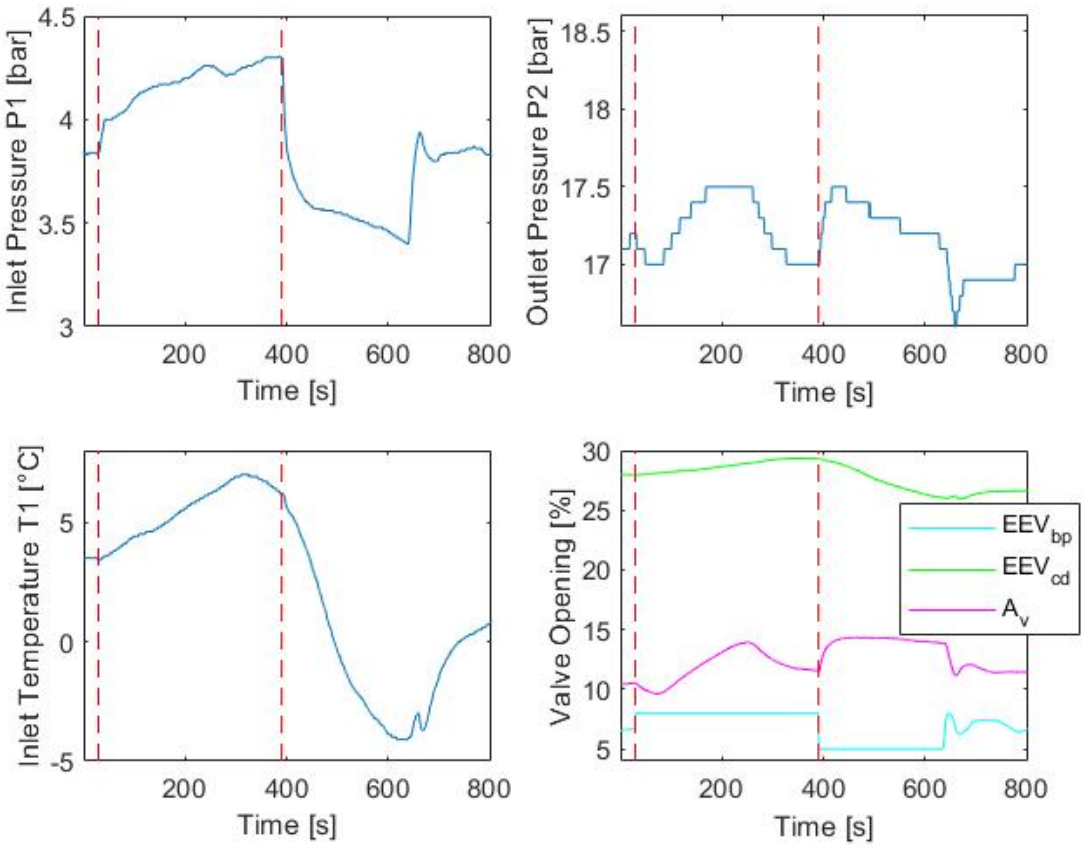

Figure 8.5: Influence of the variation of the valve opening EEV_{bp} on the CVs over time

As can be observed from Figure 8.5, the controlled variable P_1 seems to be influenced by the opening of the valve EEV_{bp}. However, the openings of A_v and EEV_{cd} also vary a lot due to the action of the active controllers that tends to limit the "disturbance" induced by the variation of EEV_{bp} in order to stay at the setpoint. As a result, no real dynamics of the system can be extracted as the influence of the controllers through the feedback loop has too much impact.

The second variation applied is the change of the opening of the electronic expansion valve EEV_{cd} which controls the inlet temperature of the compressor T_1. The valve opening is stable at 25.8% and is increased to 28% then decreased to 24.5% before turning the controller on again. The responses of the CV to the change of the manipulated variable EEV_{cd} can be observed in Figure 8.6.

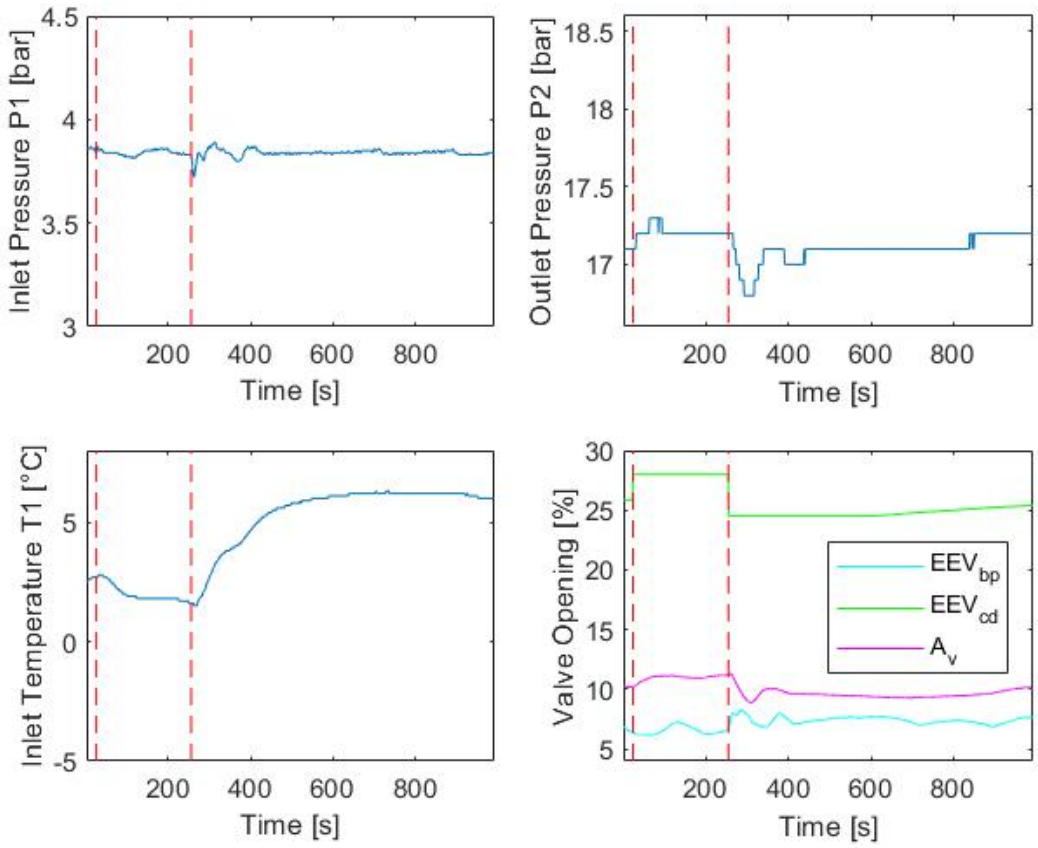

Figure 8.6: Influence of the variation of the valve opening EEV_{cd} on the CVs over time

When observing Figure 8.6, T_1 the inlet temperature seems to inversely proportionally react to the change of valve opening EEV_{cd} within a certain time delay. However, as for the previous test, the controllers have too much impact on their respective MV to clearly identify the dynamics of the system using the 'System Identification' Toolbox.

A last manipulation consisting of the change of opening of the valve from the water side of the condenser A_v is done. The valve A_v is mainly controlling the pressure P_2. The valve opening is at a stable condition at 17% determined by the controller. The opening is then changed from 17% to 19%. As no clear variation was observed the opening is increased once again to 22%. After approximately 100 sec, the opening is decreased to 10% opening and the controller is turned on after approximately 300 sec. Figure 8.7 represents the responses to the variation of the valve opening A_v over time.

As one can observe in Figure 8.7, the same problem as for the two previous tests occurs once again

with the influence of the other controllers on the system dynamics. Even though, the effects of the variation of valve A_v induce a weaker response from the controllers as the two other valve openings are less modified by the controllers.

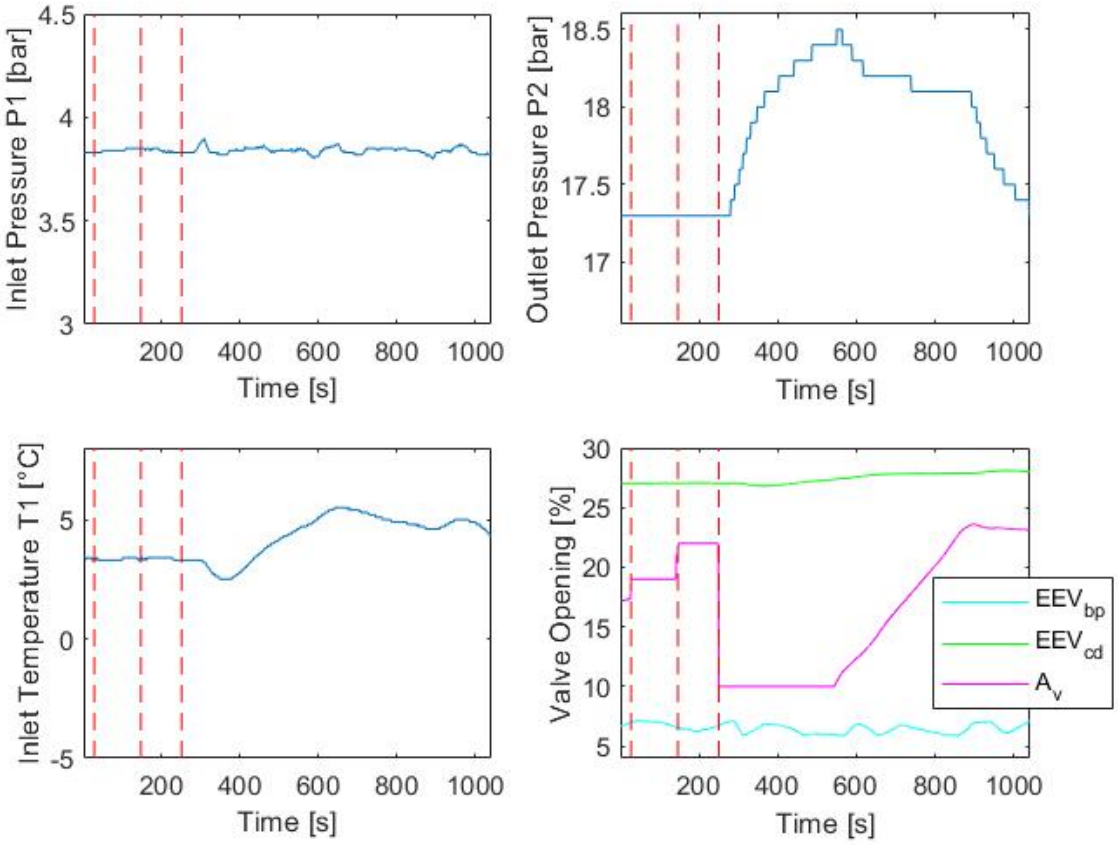

Figure 8.7: Influence of the variation of the valve opening AV_v on the CVs over time

By observing the step responses, one can conclude that the data are not representative enough of the system dynamics. The data is considered not representative enough due to the influence of controllers affecting the dynamics of the system. In fact, the controllers tend to linearize the system through the feedback loop modifying the real dynamics of the system. Moreover, interactions between the different variables and loops make it hard to observe the real effect of the change of valve opening applied as the two active controllers are inducing changes in the other valves opening at the same time. The controllers are trying to counteract the change of valve opening tested. To sum up, using the experimental data gathered in this first test does not result in a suitable model representation of the system with a good enough fitness model.

However, insight on how to perform the test can be deducted. Observing Figure 8.5, Figure 8.6, and

Figure 8.7, one can notice that a variation of 5% in the opening of the valve for each MV provides a visible response and clue on the dynamics of the system while being unaffected by noise. On the other hand, one can see that each MV has an influence over all the CV (outputs) which comforts the idea of using a MIMO representation to model the system instead of simple SISO for each main pair of input-output.

An example of sampling time calculation is applied to the first data set gathered. The different times T_{95} and T_{63} relative to each main SISO pair (P_1 with EEV_{bp}, P_2 with A_v, and T_1 with EEV_{cd}) can be observed in Table8.1. The different times were graphically calculated on Figures 8.5, 8.6, and 8.7.

Table 8.1: Table of different times T_{95} and T_{63} for each main SISO pair

	T_{63} [s]	T_{95} [s]	Based on Figure
P_1 - EEV_{bp}	68	186	8.5
T_1 - EEV_{cd}	133	259	8.6
P_2 - A_v	42	81	8.7

To ensure that all the useful data are taken into account, the choice of the shortest time divided by 10 is chosen meaning that equation 8.2 is used with the time T_{63} of the SISO pair P_2 - A_v. The sample time is graphically calculated and equals 4.2 sec.
As the experimental data were monitored and registered every 1 sec, the resulting time sample is therefore approximated to the unit.

$$T_m = 4 \quad [s] \tag{8.16}$$

The time sample T_m is used to reduce the amount of data to process while catching all the dynamics of the system. It is used for the construction of the linear model according to the model structure relative to the nominal operating point studied.

As the first data set gathered is not representative enough of the dynamics of the stand, a new experiment procedure has to be planned to ensure that the next set of data accurately catches the dynamics of the system.

With the problem of the controllers' influence in mind, two different possibilities of new tests are possible to obtain more informative data.

The first is to operate the test in a fully open-loop environment. This can be done by turning off all three controllers and setting fixed values of valve openings. The openings of the valves are then changed by two step changes with small amplitudes for each valve. The test in a fully open loop is the ideal scenario as it can give better insight into the real dynamics and interactions of the different loops. However, there is a higher risk of material destruction with this method. Therefore, careful manipulations are required and the output values have to be checked consistently to ensure the safety of operation.
A second option is to gather data in closed loop and knowing the parameters of the controllers, it is possible to remove the transfer functions of the controllers from the experimental data to obtain the true dynamics of the system. The test can be done by doing two to three large changes in the setpoint for each parameter and recording the data influenced by the controllers. The advantage of the closed-loop test is that it is easier to obtain two different sets of data for identification and validation. In addition, doing tests in closed loop is normally faster, more secure, and bigger changes in the setpoint are possible.

To obtain maximally informative data, the choice of doing a test in a fully open loop is preferred to identify the model representation. A sufficient amplitude of variations of the valve openings is 5% as deduced from the previous data set. Once the tests in open loop are performed, the activation of the controllers to reach the nominal operating point tested will give us a response in the closed loop that can be used to validate the model. Therefore, the identification data would be obtained from the open loop and validation data from the closed loop.

Conclusion. *In this section, the tests to obtain data for system identification resulted in a problem of data not representing the dynamics of the system due to a too important influence of the controllers over the system dynamics. An explanation of a pathway to improve information obtained from future tests is presented using a fully open loop for identification data and a closed loop test for validation data.*

8.3 Controller of the system

In this section, different solutions to improve the performance of the controller of the stands are evaluated and discussed to find the most suitable one. It is assumed that a FOPTD MIMO global model made from the bank of linear models is valid and accurate over the range of operation of the stand.

The actual hot gas by-pass stand is at the moment controlled by three PID controllers acting on the main input-output pairs (EEV_{bp}- P_1, A_v-P_2, EEV_{cd}-T_1) provided by the m Tron T basic parameters from Table 2.3 as mentioned in the problem formulation.
The working principle of the PID controller is explained in Theory 6.2 and can be represented under the ideal form in the frequency domain:

$$G_c(s) = K_p \left(1 + \frac{1}{sT_i} + sT_d\right) \tag{8.17}$$

Even though technicians modify the controller parameters, it is beyond doubt that the controller architecture is not optimal to control the stand. The principal doubt comes from the observation of large oscillations around the reference value of the inlet temperature T_1 of the compressor which takes long periods to disappear due to the delay caused by the distance between the control of the expansion valve after the condenser EEV_{bp} and the sensor of temperature T_1.
This observation leads to the assumption that the controller does not correctly take into account the delays of the system and rectifies the error faster than the system can react.
Moreover, the slow dynamics of the system are further enhanced at low refrigerant volume as the refrigerant flows slower in the pipes. The main focus of this thesis is to implement a controller algorithm to reach in a fast and efficient way the nominal operating point of the compressor in HGBP stands. To solve the problem of slow setpoint convergence, several solutions are presented from the most simple to more complex solutions.

A first basic solution to envisage is the simple use of an improved PID controller. However, a fixed parameters PID controller is highly improbable to solve our problem as the dynamics of the system vary with the operating conditions of the stand.
The controller algorithm has to take into account the change of dynamics of the system throughout the

whole operating map of the compressor while being simple enough for the technicians to understand the working principle of the algorithm.
As a result, several PIDS optimized offline for different nominal operating points, a gain scheduling approach with online PID parameters calculations. The PID controller is theoretically explained in Theory 6.2.

8.3.1 Offline PID tuning optimized for different nominal operating points

In this part, two simple PID solutions are presented and then rejected as even if implemented, they would not provide a satisfactory response to our problem. However, the information gained from the applications of the two solutions can help decide on the implementation of the final solution.

A first idea rather simple that could provide helpful data about the current system consists of using the self-optimization function of the m Tron T controller.
The first way to use the self-optimization function consists of reaching one stable operating point of the compressor. Once the setpoint value equals the measured output value (signal stabilized) with an error inferior to 5% referring to the definition of settling time, the use of the auto-tune function provided by the m Tron T is done to evaluate the response of the system and the optimized parameters determined by the auto-tune function are directly saved in the controller. By application of the modulation rate change close to the reference value, there is no risk of material destruction of the sensors.
If the experiment is repeated for various sets of nominal operating points, data on optimal operating conditions of the controller in relation to the system can be collected. However, the reaction of the controller to setpoint change is not handled by the self-optimization function which will result in non-optimal PID parameters between setpoints.

In the end, this method could provide the technicians with data on the best PID parameters for each nominal operating point in a steady state. Nevertheless, conducting those tests would be time-consuming and the system delay and dynamics for setpoint change would not be taken into account resulting in a general non-optimized controller. Moreover, the controller has to respond fast and accurately to set point change while ensuring good stability in steady state.
Therefore, this self-optimization function was not applied to the stand. Moreover, the controller has to respond fast and accurately to set point change while ensuring good stability in steady state.

A second idea is an offline PID tuning for different nominal operating points using tuning methods identified in the literature. The tuning methods are used to improve the trade-off between fast convergence to the setpoint while controlling the overshoot amplitude to avoid material destruction.
The tuning of PID can directly be done in Simulink with the *Control system Tuner* Toolbox. The different PID tuning can then be compared in terms of stability and robustness with the maximum sensitivity function M_s in theory 6.1.4 and in terms of controller performance with the IAE and TV presented in Methods 7.3.

Comparing the performance of the different tuning algorithms for different nominal operating points of the compressor can help us to identify the best PID algorithm corresponding to the case study. Doing this comparison asserts our trust in the improved performance of the controller.
The PID algorithm chosen by analyzing the system should provide a good enough and well-established response by taking into account disturbance rejection, reference tracking, and overshoot limitations for the specific case of the hot gas by-pass stand.
This improved PID algorithm could then be applied to the final solution of Gain scheduling with online PID parameters which is elaborated in the next section.

The methods identified in the literature and to be compared are the methods of Ziegler-Nichols [42], CHR [31], Cohen-Cohen [31], IMC-PID tuning by Rivera et al [35], Madhuranthakam [25], and SIMC-PID tuning from Skogestad [38]. These methods provide correlations based on characteristics of the response output or transfer function either in open-loop or closed-loop. All the methods listed above can be derived from the original correlations to improve the response of the system. Among them, the method suggested by Skogestad [38] has a tuning parameter a_c which can act on the handling of the delay. General tuning correlations relative to each of those methods are presented hereafter.

Ziegler- Nichols Tuning :

The classical Ziegler-Nichols [42] tuning can be presented first as it is one of the oldest tuning methods for PID even though the controller obtained often leads to an aggressive tuning. The method consists of identifying the ultimate gain K_∞ and the corresponding period P_∞ using a first-step response that generates constant oscillations at the limit of stability. The ultimate gain and ultimate period can be found using a proportional controller P and increasing the proportional gain until the limit of stability

is reached. Using these two values, one can build a controller P, PI, or PID.

$$\begin{aligned} \text{P controller: } & K_p = 0.5 \cdot K_\infty \\ \text{PI controller: } & K_p = 0.45 \cdot K_\infty; \quad T_i = \frac{P_\infty}{1.2} \\ \text{PID controller: } & K_p = 0.6 \cdot K_\infty; \quad T_i = \frac{P_\infty}{2}; \quad T_d = \frac{P_\infty}{8} \text{ from paper [29] and [42]} \end{aligned} \tag{8.18}$$

However as mentioned in papers [29] and [38], Ziegler-Nichols has aggressive tuning that does not necessarily provide a fast response and for most control applications, oscillations and overshoot have to be limited. As done in paper [38], the parameters of ZN method can easily be divided by two to improve the performance of the controller and reduce the aggressive settings proposed in theory.

$$\text{PID controller: } K_p = 0.3 \cdot K_\infty; \quad T_i = \frac{P_\infty}{4}; \quad T_d = \frac{P_\infty}{4} \text{ from paper [38]} \tag{8.19}$$

As one can notice, the method of ZN is not directly applicable to FOPTD models defined in the previous section of system identification. To solve that problem, paper [31] suggests equivalent correlations using parameters of the FOPTD which are the gain K, the delay, θ, and the dead time τ of the approximated model. According to paper [31], the PID parameters are then obtained from the FOPTD parameters using the following correlations:

$$K_p = 1.2 \cdot \frac{\tau}{K\theta}; \quad T_i = 2 \cdot \theta; \quad T_d = \frac{\theta}{2} \tag{8.20}$$

Chien-Hrones- Reswick Tuning:

As presented in the literature review, there are variations of the ZN tuning methods with different improvements.
A first variation method presented in paper [31]is the method of Chien-Hrones-Reswick (CHR) renowned for giving quick responses for systems without overshoot or with overshoot limited to 20 %. The correlations relative to the PID tuning under the CHR method result in the following.

$$\begin{aligned} \text{With 0\% overshoot: } & K_p = 0.6 \cdot \frac{\tau}{K\theta}; \quad T_i = \tau; \quad T_d = \frac{\theta}{2} \\ \text{With 20\% overshoot: } & K_p = 0.95 \cdot \frac{\tau}{K\theta}; \quad T_i = 1.4 \cdot \tau; \quad T_d = 0.47 \cdot \theta \end{aligned} \tag{8.21}$$

Cohen-Cohen Tuning:

A second extension method of ZN method is called the Cohen-Cohen (CC) method and can be used in a system for which the ZN tuning gives a slow steady-state response. The method of CC gives better responses to systems with large delays which accounts for not only the dynamics of the the main process but also the effect of the measuring sensor. General correlations for the method of CC applied to FOPTD models are also obtained from paper [31].

$$K_p = 0.135 \cdot \frac{\tau}{K\theta} \cdot \left(1 + \frac{0.18\tau}{1-\tau}\right); \quad T_i = \frac{2.5 - 2 \cdot \tau}{1 - 0.39 \cdot \tau}; \quad T_d = \frac{0.037 - 0.37 \cdot \tau}{1 - 0.81 \cdot \tau}\theta \tag{8.22}$$

As seen just before, the general Z-N tuning is known to have rather aggressive settings that give poor performance for processes including time delay but have a good disturbance response. On the other hand, the IMC method is robust and gives a good response to setpoint changes but has a poor disturbance response.

IMC-PID Tuning:

The IMC PID tuning suggested by Rivera et al [35] can be applied to various processes including refrigeration cycles. The IMC tuning is known to be robust and generally gives very good responses for setpoint changes but results in poor disturbance handling. In the case of this thesis, a general tuning method can be applied using the general first order plus time delay (FOPTD) transfer function to identify the PID parameters.
The method suggests the use of a PI setting under normal conditions:

$$K_p = \frac{0.588}{K}\frac{\left(\tau + \frac{\theta}{2}\right)}{\theta}; \quad T_i = \tau + \frac{\theta}{2} \tag{8.23}$$

In the case of large delays, a PID setting can still be integrated for cascade PID in series:

$$K_p = \frac{0.769}{K}\frac{\tau}{\theta}; \quad T_i = \tau; \quad T_d = \frac{\theta}{2} \tag{8.24}$$

The use of a derivative term does not affect the error of estimation under normal circumstances but it may improve robustness and reference tracking.

Madhuranthakam Tuning:

The fifth method listed is the method proposed by Madhuranthakam [25] that can be applied to a wide range of delayed systems. The general tuning parameters of the controller can be calculated using the tuning principle presented in paper [25]. The proposed tuning can be applied to systems with a dead time over the time constant ($\frac{\theta}{\tau}$) varying from 0.1 to 2 compared to conventional methods valid until 1.

$$\begin{aligned} K_p &= \frac{0.4967}{K}\left(\frac{\theta}{\theta+\tau^2}\right)^{-1.2299} \\ T_i &= 0.6739\cdot\frac{\theta}{\tau}\left(\frac{\theta}{\theta+\tau^2}\right)^{-1.317} \\ T_d &= \tau\left(1.138\left(\frac{\theta}{\theta+\tau^2}\right)^2+0.1992\left(\frac{\theta}{\theta+\tau^2}\right)\right) \end{aligned} \tag{8.25}$$

As the method proposed by Madhuranthakam [25] is based on minimization of IAE, it would normally give the best tracking performance but is very aggressive which can cause some robustness issues if the model is not accurate enough.

SIMC-PID Tuning:

A last method called SIMC-PID tuning rules presented in paper [38] is used in the thesis [13] to tune PID parameters based on FOPTd models. The method differs from the IMC-PID tuning by the introduction of a parameter a_c and a modification of the integral time. The tuning method can also be extended to SOPTD models if required.

$$\begin{aligned} K_p &= \frac{1}{K}\frac{\tau}{\cdot(1+a_c)\cdot\theta} \\ T_i &= \min\left\{\tau, 4\cdot(1+a_c)\cdot\theta\right\} \\ T_d &= 0 \end{aligned} \tag{8.26}$$

The parameter a_c can act on the delay of the system to provide either faster speed and good disturbance rejection with a low value assigned or either good stability and small input variation with a large value assigned. The parameter can be tuned according to the specific experiments but a good trade-off is obtained by setting $a_c = \theta$, the dead time of the system to provide fast response with good robustness. More information on tuning the parameter can be read in the discussion part of paper[38].

If the delay is not well handled by the controller, a derivative term $T_d = \frac{\theta}{2}$ can be introduced increasing the gain at high frequencies. Nevertheless, the impact of noise measurement occurring at high frequencies should still be well handled by the good robustness of the controller.

Using the 6 different tuning methods presented, the different PID parameters can then be analyzed and compared in the frequency domain using the maximum sensitivity function M_s to observe stability and in the time domain using the minimization of IAE to check the reference tracking and TV to observe the amount of input changes. The comparison can determine the best controller parameters to apply to the process of the hot gas by-pass.

As presented in Theory 6.1.4, the maximum sensitivity function can be calculated with the formula:

$$M_s = \max_{0<s<\infty} \left| \frac{1}{1 + P(s)C(s)} \right| \tag{8.27}$$

The maximum sensitivity function represents the sensitive margin and thus the robustness of a model. In general, a robust model has an M_s value ranging from 1.2 to 2 with in mind that the lower the value, the better the robustness.
The performance of the controller can also be evaluated using the IAE and TV as presented in Methods 7.3 defined with:

$$IAE = \sum_{t=1}^{N} |\varepsilon(t)| \tag{8.28}$$

$$TV = \sum_{t=1}^{N} |u(t+1) - u(t)| \tag{8.29}$$

The minimization of IAE optimizes the tracking of the reference and in the same way, a low TV value means that the controllers efficiently change the MV to give a better control.

Nonetheless, as no accurate model of the stand was available, the comparison of the different tuning methods was not possible to determine the optimal tuning methods relative to the system of the HGBP stand. The comparison is to be applied to several specific nominal operating points to ensure that it stays the optimal PID tuning methods over the whole operation map of the compressor.

However, the idea of using offline PID parameters for different nominal operating points is still

far from optimal as the technician or the algorithm would have to modify the PID parameters of the controller when a different nominal operating point is reached or when the model representation is modified. In addition, the PID tuning methods would be optimized for specific nominal operating points and not all the operating points of the stand. Furthermore, the implementation of an offline method would be time-consuming as well due to the manual tuning of all nominal operating points separately.
Taking into account the different issues, the use of the gain scheduling with online PID parameters is introduced to automatically adapt the PID parameters according to the model representation. In the following, only the optimal tuning method is to be used in the gain scheduling with online PID parameters controller.

8.3.2 Gain scheduling with online PID parameters

The method presented in this part consists of a strategy based on a multi-model gain scheduling approach in order to construct a Multi PID controller. The gain scheduling approach consists of an online adapting PID parameters that will calculate the parameters of the PID controller based on the estimated model FOPTD given by the piecewise linear approach and using the general optimal tuning method. The optimal tuning method was determined by the analysis of robustness, stability, and controller performance at different nominal operating points for the different tuning methods presented in the previous section.

As the piecewise FOPTD model representation of the stand varies, the resulting PID parameters will vary accordingly using correlations of the tuning method. The FOPTD model at a specific operating point is defined by the global model presented in section 8.11. Using the characteristics (delay, time constant, and gain) of a FOPTD model, varying PID parameters can be implemented to form a Multi-PID controllers.
The varying parameters of the PID controller can be calculated at each time t_k through a Matlab function using the chosen general tuning method and the FOPTD characteristics. The function can be applied in a general manner for each main pair of input-output.
A general representation of the Multi PID controller is represented in Figure 8.8.

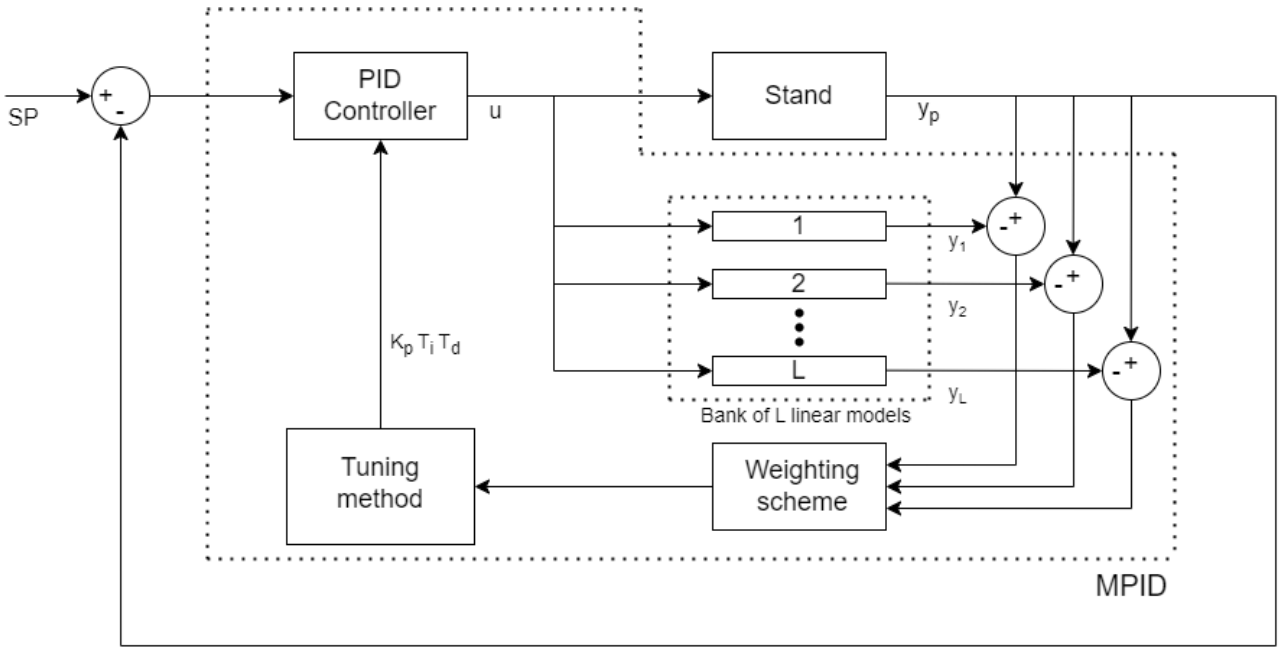

Figure 8.8: MPID block diagram

Based on the assumption that an accurate FOPTD representation of the stand, the suggested method ensures optimized and variable PID parameters throughout the operation map of the compressor to provide fast transitions between operating points of the stand.

Conclusion. *In this chapter, different PID tuning methods are presented and investigated such as Ziegler-Nichols, Chien-Hrones-Reswick, Cohen-Cohen, IMC-PID, Madhuranthakam, and SIMC-PID. A comparison of the different methods is proposed to choose the optimal tuning method relative to the HGBP stand based on the different operating points of the system. The comparison is made in terms of robustness using the maximum sensitivity function, of reference tracking using IAE, and of the amount of input changes using TV. A gain scheduling with online PID parameters is then presented to apply the optimal tuning method to the global model representation of the stand. The control algorithm at the end forms a MPID control of the stand using the piecewise linear approach for the global model and the gain scheduling approach for variable PID controllers*

8.4 charge management of refrigerant

In this part of the analysis, improvements in the charge management of refrigerant are discussed for the case of the HGBP and the gas cycle stand. These improvements can be implemented in the system for better regulation of the refrigerant charge in the system.

A general step to improve the management of charge refrigerant in the system is to install a sensor in the tank or liquid receiver to measure the amount of charge refrigerant. This information can then be used to estimate when refills or withdrawals are needed. When the sensor detects a low amount of refrigerant, the technician can check and refill the liquid receiver/ tank if needed. In the same manner, the sensor can also send a signal when the liquid receiver is almost full in order to withdraw refrigerant from the liquid receiver/tank.

8.4.1 Hot Gas By Pass stand

In the case of a hot gas bypass, the management of charge refrigerant in a system is done by a liquid receiver. Therefore, the only thing to take into consideration is that the liquid receiver capacity is large enough to cover the whole operation of the map. The volume required of the liquid receiver can therefore be calculated in relation to different refrigerants (R410a, R290,...). If the already implemented capacity of the liquid receiver (3.9 L at 45 bar) is sufficient, there is no need to add a regulation of charge refrigerant.

As mentioned in the problem formulation 2.3.1, The testing order of the different compressors starts with the compressor working at low-speed rotation to high-speed rotation. Taking the case of the compressor with the highest volume (or refrigerating power), the maximal amount of charge in terms of mass in the system can be calculated by accounting for all the refrigerant inputs/outputs occurring in the system over the testing operation of the compressor.

A second essential information is the density of the refrigerant in the liquid receiver. The density of the refrigerant at the pressure of the liquid receiver (45 bar) can be obtained by assuming that the temperature at the outlet of the condenser is the same as the liquid receiver. Using the density and the volume of the liquid receiver (3.9 L), the mass of refrigerant that the liquid receiver can manage is known. The highest temperature at the outlet of the condenser for the compressor with the larger refrigerant power is chosen as it represents the lowest density because the density is inversely propor-

tional to the temperature for the propane.
An example with a condenser outlet temperature Tcd = 35 °C, with density = 493.2 kg/cubic meters results in a variation of mass of 1.924 kg that can be managed by the actual liquid receiver.

Using the previous information with the mass difference between the higher refrigerating power and the lowest refrigerating power of the biggest compressor, one can evaluate if the liquid receiver is dimensioned correctly or was under-dimensioned. From there, the decision-making of Copeland can take the decision to replace the previous liquid receiver with a more adapted one or determine when it is needed to add refrigerant to the system before having non-optimal operating conditions characterized by a lack or surplus of refrigerant.

A suggestion on the implementation of a method to add refrigerant to the system is presented. To help assess the lack of refrigerant quantity, a sensor in the liquid receiver sending a signal when the refrigerant content is low and high would be useful and very valuable. The sensor in the liquid receiver would send a signal when the refrigerant level is lower than a pre-determined level enabling the refrigerant to flow in the system by the use of an actuator or a technician opening a valve. In the same way, another sensor in the liquid receiver would signal to withdraw refrigerant from the system. Using the already built configuration of charge and discharge of charge refrigerant, the simple mechanism can be applied fairly easily.

8.4.2 Gas cycle stand

In the case of a gas cycle stand, the refrigerant does not return to a liquid state as can be seen in Figure 7.7 in Methods when the gas cycle method is presented. Hence, the liquid receiver cannot be used to automate the charge of refrigerant and another option has to be sought.

A more practical way to regulate the charge of refrigerant is to use a refrigerant storage tank equipped with a cooling and heating system through a coiled tube where hot or cold water flows inside depending on the amount of pressure to reach. The tank is to be maintained at intermediate pressure, the pressure of the condenser. The refrigerant recovery and injection principle is to alter the storage tank temperature and by doing so, refrigerant would flow following the opposite direction of the temperature gradient. When increasing the temperature of the tank, the refrigerant will flow from

the tank into the cycle. On the other hand, cooling the tank would result in refrigerant filling the storage tank.
The physical explanation lies behind the general known formula of ideal gas:

$$\begin{aligned} P \cdot V = n_{ref} \cdot R \cdot T &= \frac{R}{MM_{ref}} \cdot m_{ref} \cdot T \\ \iff V \cdot \frac{MM_{ref}}{R} &= \frac{1}{P} m_{ref} \cdot T \\ \iff Constant &= \frac{1}{P} \cdot m_{ref} \cdot T \end{aligned}$$

Where P is the pressure in bar at the inlet of the compressor, V the volume in m^3, n_{ref} the number of moles in mol, R = 8.314 in [J/K mol] gas constant, T temperature in K, MM_{ref} molecular mass in g/mol, and m_{ref} the mass in g.

The pressure P of the tank should vary according to the intermediate pressure of the system corresponding to the pressure of the condenser. The pressure in the tank can be increased by increasing the temperature of the refrigerant in the tank. When the pressure inside the tank is higher than the intermediate pressure, a valve can be opened for example and refrigerant will flow from the tank to the system until the pressure reaches an equal pressure. It can be done either by functioning in an open regime or with a valve opening when the pressure is reached and through heating or cooling refrigerant will flow into or out of the tank.

The formula of an ideal gas is indeed false as no gas in reality is an ideal gas. However, even though ideal gas conception is strictly theoretical, certain conditions provide a possibility to estimate real gases as "ideal". For example, a system characterized by very low pressures or high temperatures enables the use of the assumption of an ideal gas. This is justified as fewer intermolecular forces are present in low pressure or/and high temperature. Therefore for calculation purposes, real gases can be considered “ideal” in either low pressure or high-temperature systems.

A model of the new stand charge regulation system can be observed in Figure 8.9.

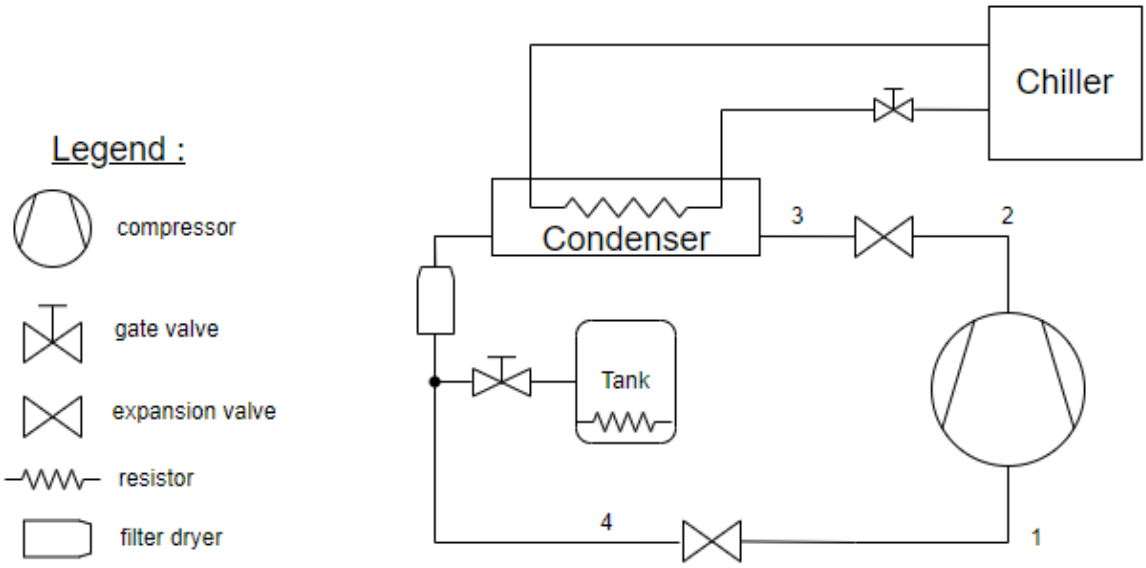

Figure 8.9: Model of the suggested charge regulation in the gas cycle

To implement the idea suggested, the maximal amount of refrigerant required in the operation map of the compressor with the highest volume displacement is required. One can measure the amount by knowing the amount of refrigerant put in the stand for the working point of the compressor with the most refrigerating power or the highest rotation speed. An evaluation of refrigerant to be added to the system is also required for every nominal operating point to tune the regulation mechanism.
A second step is to search for a tank yielding a volume capacity to cover the maximal amount of refrigerant required with adequate pressure requirements (up to 130 bar). The tank is to be installed with a coiled tube heat exchanger inside in order to provide the cooling or heating needed in the system.
At last, a control algorithm has to be implemented to control the temperature of the tank to act on the pressure in the tank and on the opening of the valve in order to provide more or less refrigerant to the system. As presented in the method testing of a gas cycle, the pressure of the condenser has to stay at an intermediate pressure in between the high pressure and low pressure. The condition of staying at the intermediate pressure can be used as the main condition to fill or withdraw the system with refrigerant. An efficient management of the refrigerant is required in the system as if too much refrigerant is in the system, the condenser area of cooling will be reduced as a lot of refrigerant in a liquid state will saturate the condenser. On the other way around, a lack of refrigerant leads to a compressor working with an unstable amount of refrigerant at the inlet and thus providing compression to an incomplete volume of refrigerant.

Conclusion. *In this part of the analysis, improvements for the management of refrigerant in the HGBP and gas cycle stand are presented. A general improvement is the installation of level sensors in the liquid receiver. The actual liquid receiver at 45 bar can manage a variation of 1.924 kg of refrigerant of R290 at a condensing temperature of 35 °C adequate. A method to calculate the adequate size of the liquid receiver using the maximal difference in the amount of refrigerant between compressors tested at the HBP stand is presented. In case the current liquid receiver is not adequate, a solution using level sensors can be used to provide indications on when to add or withdraw refrigerant from the liquid receiver. Concerning the gas cycle, charge management is suggested from the law of ideal gas applied to a tank at intermediate pressure equipped with a coiled tube heat exchanger to heat or cool down the tank to respectively add or withdraw refrigerant from the system.*

Chapter 9

Discussion

In this chapter, the current advancement of the model identification is explained and improvements or mitigation solutions are introduced to improve even further the solution suggested. The discussion presents the results of the first and second tests performed, the possible use of a new model structure, the concept of the Smith predictor, a feedforward action, or the use of an MPC algorithm of control. There is no discussion concerning the management of refrigerant in the system.

Due to a lack of time and availability of resources, only two tests to identify the system of the stand were performed. The first test was performed with data compromised by the influence of the controllers which resulted in a biased identification of the dynamics of the system as explained in analysis 8.2. The test consisted of turning off one controller out of the three and varying the opening of the valve previously controlled by the controller. The three controllers were turned off each at a time.
As explained at the end of section 8.2, a solution to maximize the information provided by the data consists of applying tests in a full open loop meaning that the three controllers are turned off. The responses obtained in a full open loop test represent the true dynamics of the system. To experiment, the openings of the three valves controlling the system have to be set to fixed values corresponding to the stable operating point and one valve at a time, the opening is varied with a two-step signal as presented in Figure 8.3 with an opening amplitude of 5% assumed sufficient from the first test performed. The data recorded will act as identification data. Afterward, the controllers are to be activated again and a closed-loop test is to be performed by varying the setpoints of the system one at a time with three different setpoints variation each. The experimental data obtained will act as our validation data to validate the model identified in the open-loop.

The improved test explained above to improve the system identification procedure was applied to the stand in a second test and can be seen in Annex 11.1 for open loop and Annex 11.2 for closed loop. The experiment resulted in problems in the identification of a MIMO model of the stand. There-

fore, a SISO identification for each pair of input-output was still performed to identify a model set by comparing FOPTD and SOPTD. The SISO identification resulted at best with a FOPTD model of 70% of fitness using the open loop data for identification and the closed loop data for validation as can be seen in Annex 11.3 for the main pair of input-output. The identification of a good representation of the system can also be improved by selecting a better range of input-output data which requires time and experience. Nevertheless, insights can be acquired from the second experiment to improve future tests. First, the performance of the controllers is poorer than expected and therefore closed loop identification is not possible for the system unless the controllers' parameters are slightly improved. Tests are then to be carried out in an open loop as it holds the benefit of observing the true dynamics of the stand without the controllers' influence.
Secondly, the amplitude of valve openings was too important (5%) which led to reaching limit authorized values of T_1 to avoid material destruction while the full dynamics of response were not observable. Therefore, the amplitude of valve opening variation needs to be lowered to 3% instead of 5% for the three valves.
Thirdly, the valve opening change was varied while the full dynamics of the output were not observed, especially in the case of temperature T_1. As a result, a longer period of time for the system to respond is required and is set to 10 minutes after each valve opening variation to observe the full dynamics of the response.
Furthermore, more steps variation of inputs (valve openings) are required to approach a PRBS signal input as shown in Figure 8.2 to identify the system fully. A good guess is to have 5 variations of valve opening for each input in an open loop test.
At last, the identified models follow the dynamics of the validation data of the closed loop but with different gains sometimes which probably shows the range of a model at an operating point. It might also be impacted by inputs changing at the same time as all the controllers are active. As a result, validation data in open loop instead of closed loop is required to validate the model obtained from identification. The open loop data obtained from the future tests will then be split into 2/3 of the data for identification and 1/3 for the validation of the model.

Another choice of model representation could also be compared with the FOPTD model in the case the system is not well approximated with a narrow range of validity. The comparison can be made over the range of representation of one linear model which influences the total number of model representations needed in the bank to represent the whole system. The other models that can be tested are the

second order plus time delay (SOPTD) and the N4SID prediction subspace model presented in paper [32]. As the FOPTD model is a simple representation of the model compared to more complex models, it usually represents less accurately the system and over a reduced range. As a result, a more complex model which could considerably reduce the total number of models required could be worth considering. Nevertheless, the presented methodology is only applicable with the use of a FOPTD model, therefore the complexity of the new model structure can pose a problem in defining a gain scheduling tuning method. In the case of an SOPTD model, it can be easily reduced to an FOPTD model based on the SOPTD parameters.

After the implementation of the global model and the gain scheduling approach with online PID parameters with the optimal tuning method relative to the HGBP stand, the control of the stand could still have some improvements needed in case of bad handling of the delay, disturbances or insufficient performances of the algorithm.

A first improvement could be the implementation of the Smith predictor to more effectively handle the delay of the system. The Smith predictor presented in paper [39] consists of adding to the primary structure, a predictor structure. The predictor is composed of a model representation without delay and a delay block to be compared with the measured outputs of the system. In case the prediction outputs are equal to the measured outputs of the stand, the signal of the prediction model without delay can be used for control improving therefore the response time of the controller.

A second improvement to mitigate the impact of high disturbances is the implementation of a feedforward action. In the case study, many disturbances can impact the performance of the system as presented in section Black box model 8.1 and the use of an adapted feedforward action could extend the application of the global model determined by the piecewise linear approach. The feedforward control can be defined as a control strategy to anticipate disturbances and take corrective measures to prevent the impact of disturbances in the system. It relies on an accurate estimation of the impact of disturbances on the model to adjust the MV of the system accordingly.

A last improvement that is discussed is the use of a Multi-Model Predictive Control (MMPC) which would be based on the global model constructed by the piecewise linear approach. The theory explaining the working principle of a MPC controller can be read in Theory 6.3. The use of the MPC algorithm

holds many benefits such as handling complex non-linear systems, constraints, and interactions between different process variables.
Concerning performance, MPC optimizes control actions based on a defined objective function and constraints by considering the future behavior of the controlled system over a specified prediction horizon. This optimization allows MPC to make control decisions that optimize performance, minimize errors, and achieve desired setpoint tracking while considering constraints on process variables, control signals, and equipment limitations.
By taking into account the constraints during the optimization process, it ensures that the control actions remain within safe and feasible operating ranges of the system. In an industrial environment where safety is crucial, the ability to handle constraints is particularly beneficial.
Adaptability is another key aspect as MPC can easily adapt to changes in process conditions and setpoints. As it predicts future behavior and optimizes control actions, it can adjust its response to changing operating conditions and disturbances. This adaptability allows MPC to provide robust control even in the presence of varying process dynamics or setpoint changes.
Moreover, the user can prioritize specific objectives by defining a different objective function for energy efficiency, setpoint tracking, or control stability.
Even though, implementing and tuning MPC is more complex compared to traditional PID control as it requires a thorough understanding of the process dynamics and an accurate process model. In fine, MPC provides a superior optimized control performance when properly implemented and tuned to offer solutions to complex industrial systems.

In the case of this work, the MPC controller can replace the PID controller using the gain scheduling approach to form a Multi-Model Predictive Control (MMPC). To help tune the complex controller, one can use the "MPC Design" Toolbox from Mathworks and the book [11] which is a specialized book explaining how to properly tune a MPC controller. The following block diagram of the MMPC is represented in Figure 9.1.

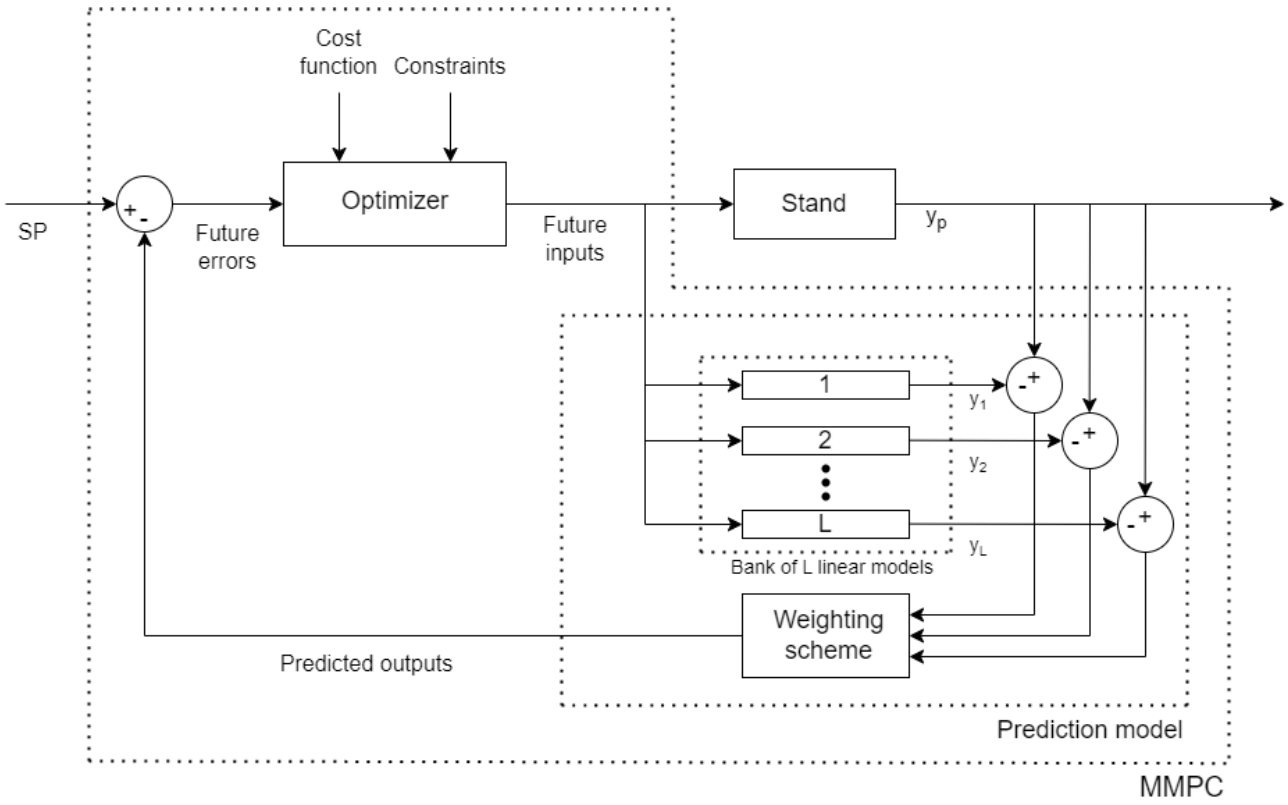

Figure 9.1: MMPC block diagram

Future research in the domain of system identification can be investigated for the case of HGBP stand to give the improved technical and implementable controller algorithm for the Sound room of Copeland Welkenraedt. To that extent, tests in open loop on different operating points of one compressor can be done following the different directives given such as the amplitude of valve opening variation, number of input changes, and time required between input changes. The construction of a bank of linear models for the HGBP stand would require a huge amount of time to correctly identify the models at each operating point. Once the bank of linear models is identified and the Bayesian estimator is implemented, the improvement suggested with the use of gain scheduling with online PID and the comparison between the different PID tuning methods can be compared easily using Simulink. To implement the improved algorithm in the m Tron T controller, a *Simulink PLC coder* Toolbox can be used to generate hardware-independent IEC 61131-3 Structured text and Ladder Diagrams from Simulink models and Matlab functions. Structured Text can be implemented in the IDE of the m Tron T controller called CODESYS. If the results of the controller are not satisfying, the implementation of a Smith predictor, feedforward action, or MMPC can be investigated.

Concerning the charge management part, a thesis on his own would be required to test the idea of charge management of the gas cycle presented in the analysis as it involves analyses on the size of the tank required, cooling and heating necessary, and experiments to determine the flow of refrigerant depending on the pressure difference between the tank and the gas cycle stand.

Chapter 10

Conclusion

The improvement of the controllers' performance to reach nominal operating points of the compressor faster requires an investigation of system identification to represent numerically the stands followed by an investigation of different control algorithms mainly PID to control the stand in an efficient manner. A second part of the thesis investigated the management of charge refrigerant in the stands. Three stands are present at Copeland Welkenraedt among them, two are HGBP with respectively 15 T and 50 T and one is a gas cycle with 10 kW. The stands are controlled with the help of three SISO PID controllers with non-optimized parameters resulting in slow convergence to steady-state when the set-point is changed. Concerning the management of charge refrigerant, the HGBP stands are managed by a liquid receiver and no charge management is present for the gas cycle.

To model the HGBP stand with a data-driven modeling approach, a black box model representing the different MV and CV is identified. Afterward, the data set for system identification is suggested to be obtained with a two-step variation of a MV while the connected controller was turned off. A method to estimate sampling time to reduce the amount of data to process while capturing the dynamics is presented using the settling time or 63 % of the rise time. Then, the model structure of a FOPTD transfer function is chosen to represent the system for each pair of MV-CV to form a MIMO model of the stand. The resulting MIMO model is a linear model at one nominal operating point of the compressor valid over a certain range of the compressor map. To represent the whole non-linear stand dynamics, a piecewise linear model algorithm using a Bayesian estimator algorithm estimates a global linear model based on a bank of MIMO linear models constructed at different nominal operating points of the stand. To validate the given model, experimental data different from the identification data are used to validate the model representation using the validation criterion of the relative error measure. An extended use of the validation criterion is suggested to determine the next operating point on which to build the next MIMO linear model of the stand.
A first experimental test using data set recommendations resulted in a bad identification of a MIMO

model due to the influence of controllers over the dynamics, Therefore, a second test in open loop and closed loop was then applied. The closed loop data obtained resulted in an impossibility of identifying the system based on the closed loop due to poor controllers' performance. Tests in open loop resulted in a low fitness of model due to too-important MV changes, insufficient time to observe the full dynamics between input changes, a too-low number of input changes, and non-optimal validation data. The second test resulted in the choice to use open loop data to identify and validate the system and insights on how to improve tests in the future are given in the discussion.
To choose which controller algorithm to apply to the global model, general PID tuning methods such as Ziegler-Nichols, Chien-Hrones-Reswick, Cohen-Cohen, IMC-PID, Madhuranthakam, and SIMC-PID are investigated in the literature to apply to FOPTD models. The tuning methods are to be compared to one another for different linear models of stand in terms of stability and robustness using the maximum sensitivity function M_s and in terms of controller performance with the Integrated Absolute Error IAE and the Total Variation TV. The optimal PID tuning method for the stand is then to be implemented in a gain scheduling approach to calculate PID parameters online using the global model of the stand. The total control of the stand is then suggested to be achieved with a MPID control but the discussion introduces the possibility to use a MMPC control if a highly accurate model of the stand is obtained.

Concerning the management of charge refrigerant, an improvement to be made for the HBGB is the installation of level sensors to send a signal when the amount of refrigerant in the liquid receiver reaches a high or low value to know when to add or withdraw refrigerant. To automatically manage the refrigerant in the system, a method to calculate the adequate size of a liquid receiver is presented using the maximal difference in the amount of refrigerant between the compressors tested for the specific HGBP stand. Another method using the level sensors could be achieved by implementing a mechanism to add or withdraw refrigerant from the liquid receiver based on the signal. As information, the actual liquid receiver can efficiently manage the variation of 1.924 kg of R290 refrigerant in the system at a condensing temperature of 35°C.
The gas cycle stand cannot use a liquid receiver as the refrigerant does not enter a liquid phase after the condenser. Therefore, a new method to manage refrigerant using a tank at intermediate pressure equipped with a coiling tube inside is presented. Based on the ideal gas formula and using the coiling tube, the tank pressure can be varied by heating or cooling the tank to respectively add or withdraw refrigerant in the gas cycle.

Bibliography

[1] AHRI, *Standard for Performance Rating of Positive Displacement Refrigerant Compressors*, Air Conditioning, Heating, and Refrigeration Institute, 2020.

[2] American National Standard, *Flow Equations for Sizing Control Valves* , 2002, IEC 60534-2-1.

[3] American Society of Heating, Refrigerating and Air-Conditioning Engineers, Inc. *2022 ASHRAE Handbook - Refrigeration*, Chapter 8, 2022.

[4] Åström K. J., *Control System Design Lecture Notes for ME 155A: Chapter 5 Feedback fundamentals*, Department of Mechanical and Environmental Engineering, University of California, Santa Barbara, Pages 177-215, 2002.

[5] Bejarano G., Alfaya J. A., Rodríguez David, Morilla F., Ortega M. G., *Benchmark for PID control of Refrigeration Systems based on Vapour Compression*, Volume 51, Issue 4, 2018, Pages 497-502, ISSN 2405-8963.

[6] Björk E., *Energy Efficiency Improvements in Household Refrigeration Cooling Systems*, KTH Royal Institute of Technology, 2012.

[7] Björk E., Palm B., *Performance of a domestic refrigerator under influence of varied expansion device capacity, refrigerant charge, and ambient temperature*, International Journal of Refrigeration 29, Pages 789-798, 2006

[8] Björk E., Palm B., *Refrigerant mass charge distribution in a domestic refrigerator: Part II- Steady-state conditions*, Applied Thermal Engineering 26, Pages 866-871, 2006.

[9] Bobal V., Kubalcik M., Dostal P., Matejice J., *Adaptive predictive control of time-delay systems*, Computers and Mathematics with Applications, volume 66, 2013, Pages 165-176, https://www.sciencedirect.com/science/article/pii/S0898122113000655.

[10] Changenet C., Charvet J., Géhin D., Sicard, Frederic, Charmel B., *Study on predictive functional control of an expansion valve for controlling the evaporator superheat*, Proceedings of The Institution of Mechanical Engineers Part I-journal of Systems and Control Engineering, 2008, PROC INST MECH ENG I-J SYST C. 222.571-582. 10.1243/09596518JSCE566.

[11] Dittmar R., *Model Predictive Control with MATLAB and Simulink*, IntechOpen, 2019.

[12] Ghafooripour A., Aghakoochak A.A., Kiamehr H., *An overview of system identification methods and applications Part II: Theory, Type of tested structures, history and prospective of system identification*, 2000.

[13] Grelet V., *Rankine cycle based waste heat recovery system applied to heavy duty vehicles: topological optimization and model based control*, Unpublished doctoral thesis, University of Liège, 2016.

[14] He Y. , Tai Y., Zhao X., Zhang C., *Consistent control strategy for CO2 refrigeration systems based on refrigerant charge management*, International Journal of Refrigeration, Volume 145, 2023, Pages 19-29, ISSN 0140-7007. https://doi.org/10.1016/j.ijrefrig.2022.09.009.

[15] Huusom J. K., Jørgensen J. B., *A Realistic Process Example for MIMO MPC based on Autoregressive Models*, IFAC Proceedings Volumes, Volume 47, Issue 3, 2014, Pages 3086-3091, https://doi.org/10.3182/20140824-6-ZA-1003.00461.

[16] Isermann R., Münchhof M., *Identification of Dynamic Systems: An Introduction with Applications*, Advanced Textbooks in Control and Signal Processing Series, Springer Berlin Heidelberg, 2010.

[17] JUMO GmbH & Co. KG, *JUMO mTRON T Measuring, Control, and Automation System: Setup Program Manual*.

[18] Khurram K. Makhani, *Design, Simulation, and Construction of a Hot-Gas Bypass Chiller for a Commercial Scale Psychrometric Coil Testing Facility* , Oklahoma State University, 2020.

[19] Krupa P., Limon D., Alamo T., *Implementation of Model Predictive Control in Programmable Logic Controllers*, in IEEE Transactions on Control Systems Technology, vol. 29, no. 3, Pages 1117-1130, May 2021, http://dx.doi.org/10.1109/TCST.2020.2992959.

[20] Landau I. D., Zito G., *DIGITAL CONTROL SYSTEMS: Design, Identification and Implementation*, 2020, http://dx.doi.org/10.13140/RG.2.2.19321.49764.

[21] Li B., Alleyne A. G., *A dynamic model of a vapor compression cycle with shut-down and start-up operations*, International Journal of Refrigeration, 33(3), 538-552.(2010). https://doi.org/10.1016/j.ijrefrig.2009.09.011.

[22] Li W., *Simplified steady-state modeling for variable speed compressor* Appl. Therm. Eng., Pages 318-326, 2013, https://pdf.sciencedirectassets.com/271641/1-s2.

[23] Li W., *Simplified modeling analysis of mass flow characteristics in electronic expansion valve*, Applied Thermal Engineering, 53, Pages 8-12, 2013, https://doi.org/10.1016/j.applthermaleng.2012.12.035.

[24] Ljung L., *System Identification: Theory for the User*, 2nd edition, Englewood Cliffs: Prentice Hall, 1999.

[25] Madhuranthakam C.R., Elkamel A., Budman H., *Optimal tuning of PID controllers for FOPTD, SOPTD and SOPTD with lead processes*, Chemical Engineering and Processing: Process Intensification, Volume 47, Issue 2, 2008, Pages 251-264, ISSN 0255-2701.

[26] Marlin T., *Process Control*, Mc Graw-Hill, NY, 1995.

[27] Mendoza-Miranda J.M., Mota-Babiloni a., Ramírez-Minguela J. J., Muñoz-Carpio V.D.,Carrera-Rodríguez M., Navarro-Esbrí J., Salazar-Hernández C., *Comparative evaluation of R1234yf, R1234ze(E) and R450A as alternatives to R134a in a variable speed reciprocating compressor*, Energy, 114, pages 753-766, 2016.

[28] Mokhatab S., Poe W. A., *Chapter 14 - Process Control Fundamentals*, Handbook of Natural Gas Transmission and Processing (Second Edition), Gulf Professional Publishing, 2012, Pages 473-509, ISBN 9780123869142, https://doi.org/10.1016/B978-0-12-386914-2.00014-5.

[29] Mudry F., *Ajustage des Paramètres des Régulateurs PID*, Institu, d'automatisation industrielle, 2006, https://forums.futura-sciences.com/reglage-regulateur-pid-regulateurspid.pdf.

[30] Newell R. B., Lee P. L., *Applied Process Control - A Case study*, Prentice Hall, 1989.

[31] Rajat S., Chinmoy P., Samik D., Ranjan S., *Comparison Between Three Tuning Methods of PID Control for High Precision Positioning Stage*, MAPAN. 30., Pages 65-70, 2014.

[32] Rasmussen B. P., Alleyne A. G.,*Dynamic Modeling and Advanced Control of Air Conditioning and Refrigeration Systems*, University of Illinois at Urbana-Champaign, June 2006.

[33] Ogata K., *Modern Control Engineering*,3rd edition, University of Minnesota, Tom Robbins, 1997.

[34] Ossorio R., Navarro-Peris E., *Testing of Variable-Speed Scroll Compressors and their inverters for the evaluation of compact energy consumption models*, Applied Thermal Engineering, Volume 230, Part B, 2023, https://doi.org/10.1016/j.applthermaleng.2023.120725.

[35] Rivera D.E. , Morari M., Skogestad S., *Internal model control*, 4, PID controller design, Ind. Eng. Chem. Res., Pages 252–265, 1986.

[36] Sarker T., Ramasamy G., *Optimal Signal Design in System Identification for Model Predictive Control (MPC)*, 2023 , https://www.researchgate.net/Optimal_Signal_Design.

[37] Singleton J., Schmidt D., Bradshaw C. R., *Control and commissioning of a hot-gas bypass compressor load stand for testing light-commercial compressors on low-GWP refrigerants*, International Journal of Refrigeration, Volume 112, 2020, Pages 82-89, ISSN 0140-7007, https://doi.org/10.1016/j.ijrefrig.2019.12.031.

[38] Skogestad S., *Simple analytic rules for model reduction and PID controller tuning*, Journal of Process Control, Volume 13, Issue 4, 2003, Pages 291-309, ISSN 0959-1524, https://doi.org/10.1016/S0959-1524(02)00062-8.

[39] Tandoh H., Cao Y., Awoyomi A., *Smith predictor for slug control with large valve stroke time*, Computer Aided Chemical Engineering, Elsevier, Volume 40, 2017, Pages 1531-1536, ISSN 1570-7946, ISBN 9780444639653.

[40] Tyreus B.D., Luyben W.L., *Tuning PI controllers for integrator/ dead time processes*, Ind. Eng. Chem. Res., Pages 2628–2631, 1992.

[41] Vjacheslav N., Rozhentsev A., Wang C., *Rationally based model for evaluating the optimal refrigerant mass charge in refrigerating machines*, Energy Conversion and Management, Volume 42, Issue 18, 2001, Pages 2083-2095, ISSN 0196-8904, https://doi.org/10.1016/S0196-8904(00)00164-3.

[42] Ziegler J.G., Nichols N.B., *Optimum settings for automatic controllers*, Trans. A.S.M.E. 64, 1942.

Chapter 11

External appendices

11.1 Appendix 1

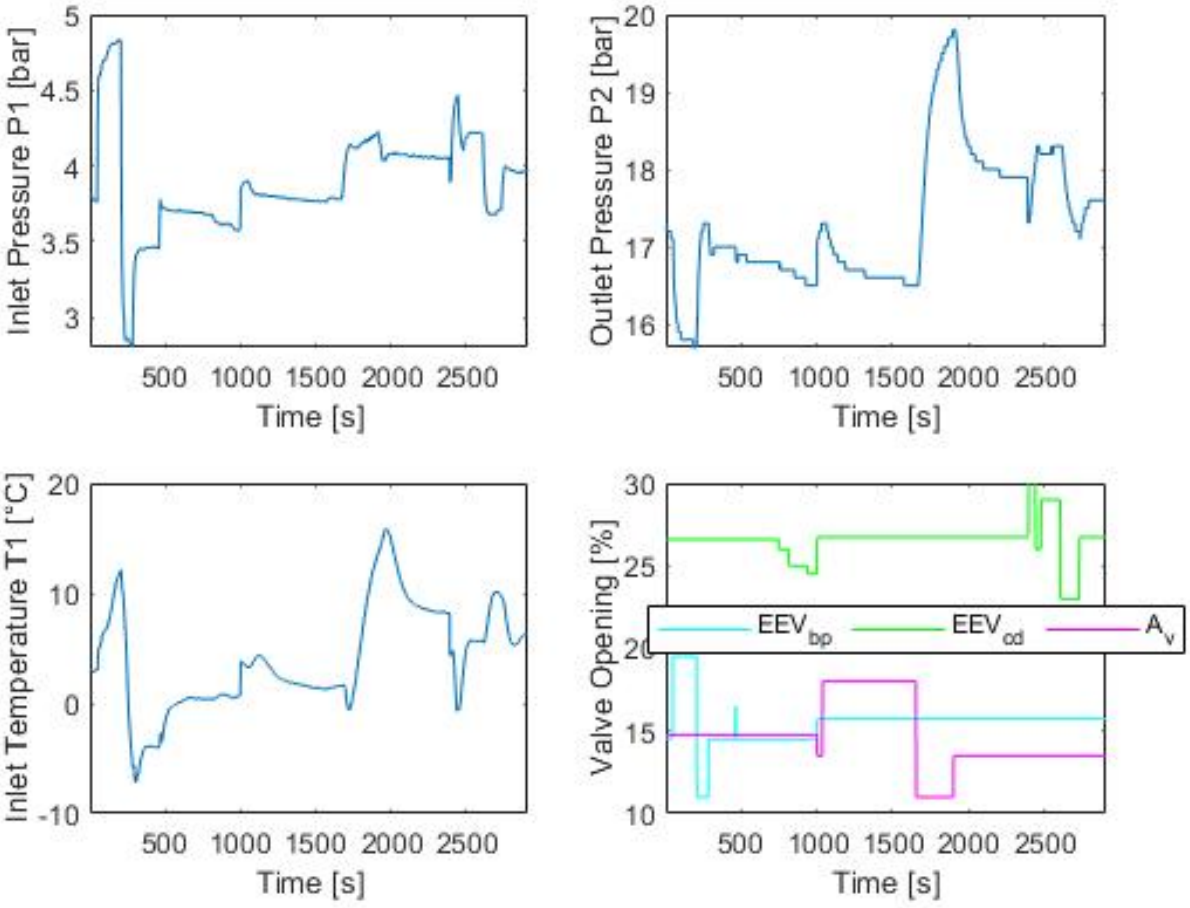

Figure 11.1: Test open loop on compressor YHV046 with R290 15T at 3600 rpm with nominal operating point (P_1 = 3.9 bar; P_2= 17.2 bar; T_1= 3.5 °C; T_2 = 78.2°C)

11.2 Appendix 2

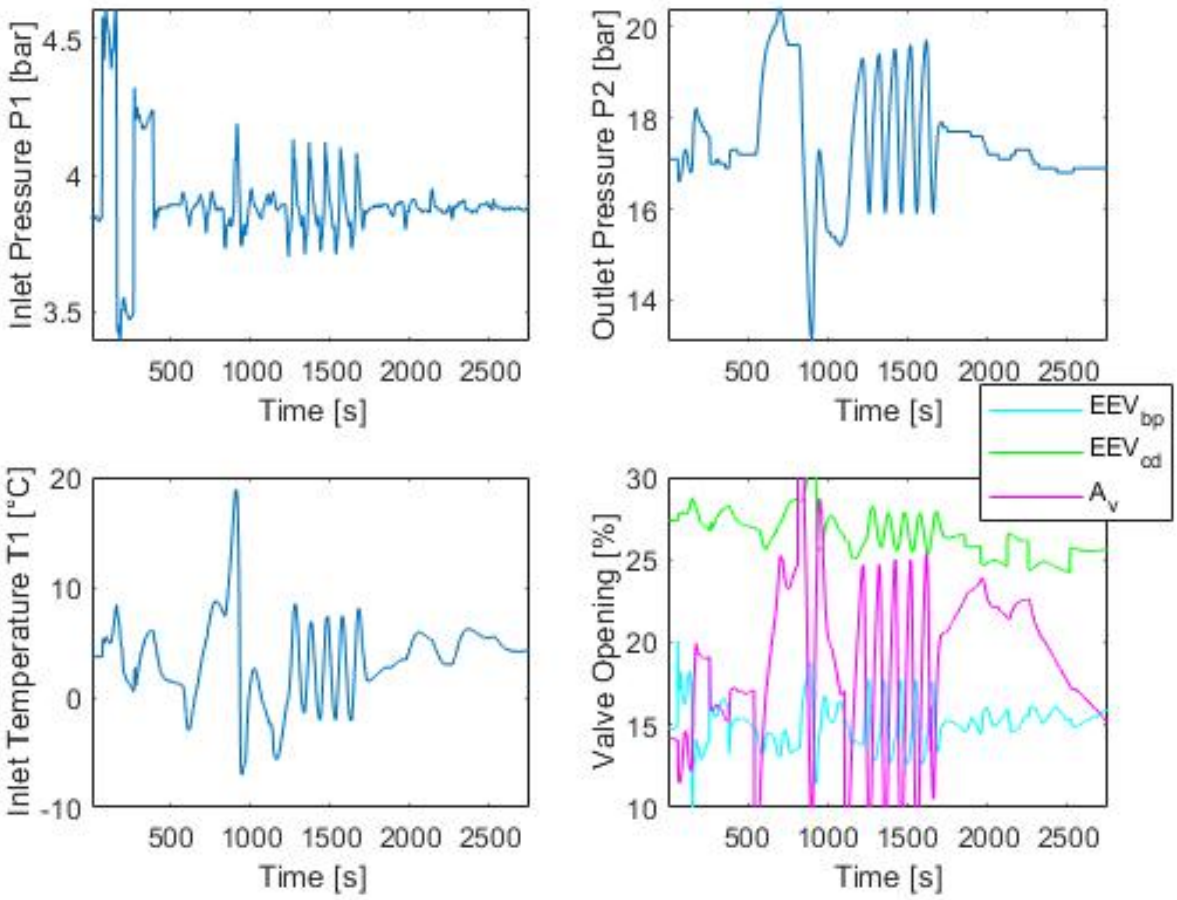

Figure 11.2: Test closed loop on compressor YHV046 with R290 15T at 3600 rpm with nominal operating point (P_1 = 3.9 bar; P_2= 17.2 bar; T_1= 3.5 °C; T_2 = 78.2°C)

11.3 Appendix 3

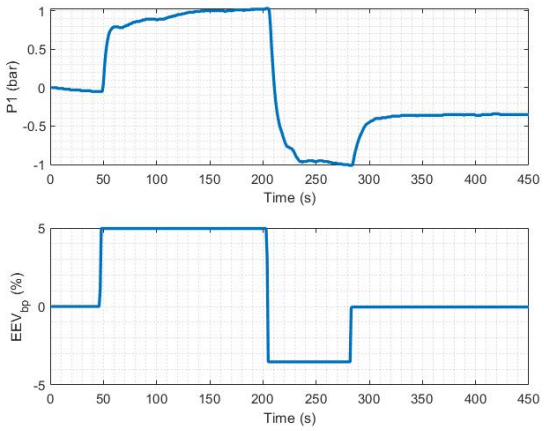

(a) Open loop Input-Output $EEV_{bp} - P_1$

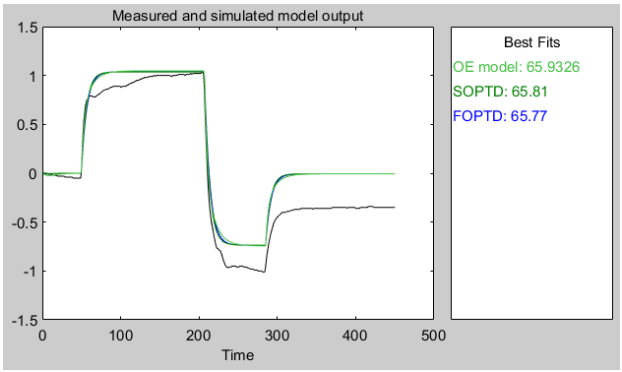

(b) Fitness of identified models with open loop data for validation

Figure 11.3: Input-Output $EEV_{bp} - P_1$
SISO FOPTD, SOPTD, Output-Error models identified and validated with open loop data

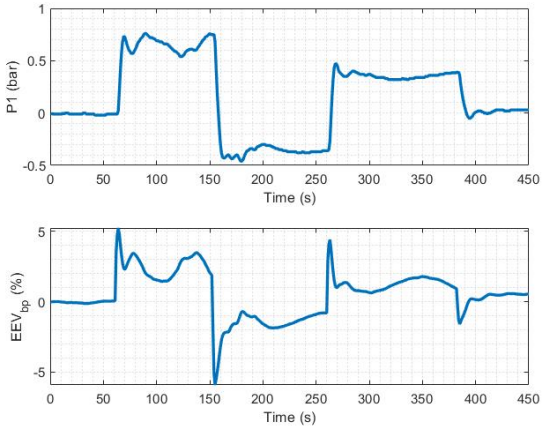

(a) Closed loop Input-Output $EEV_{bp} - P_1$

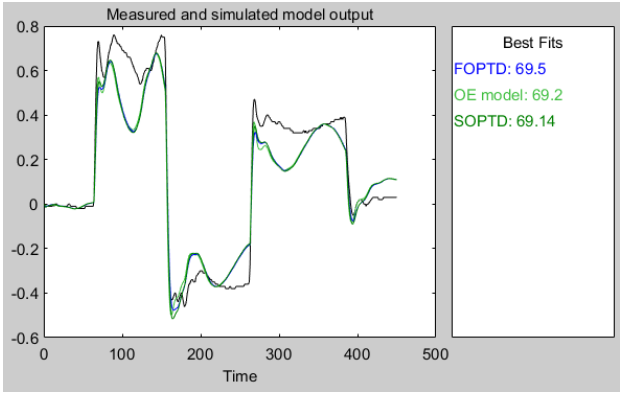

(b) Fitness of identified models with closed loop data for validation

Figure 11.4: Input-Output $EEV_{bp} - P_1$
SISO FOPTD, SOPTD, Output-Error models identified and validated with closed loop data

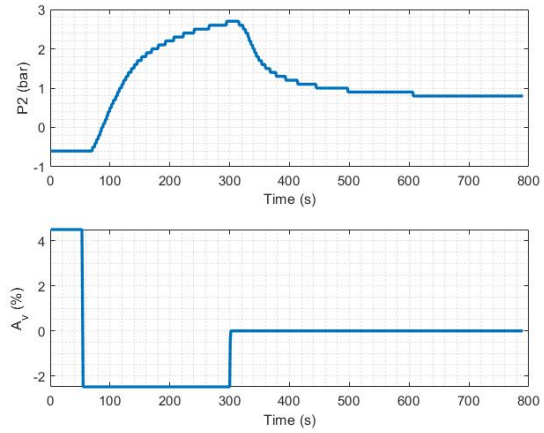

(a) Open loop Input-Output $A_v - P_2$

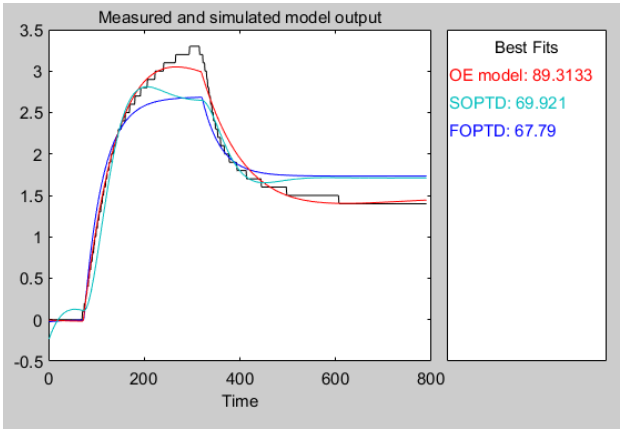

(b) Fitness of identified models with open loop data for validation

Figure 11.5: Input-Output $A_v - P_2$
SISO FOPTD, SOPTD, Output-Error models identified and validated with open loop data

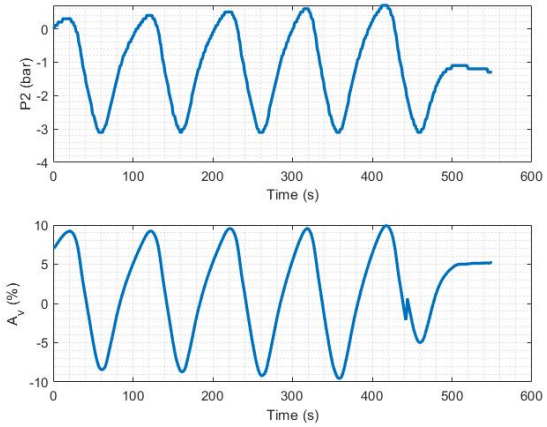

(a) Closed loop Input-Output $A_v - P_2$

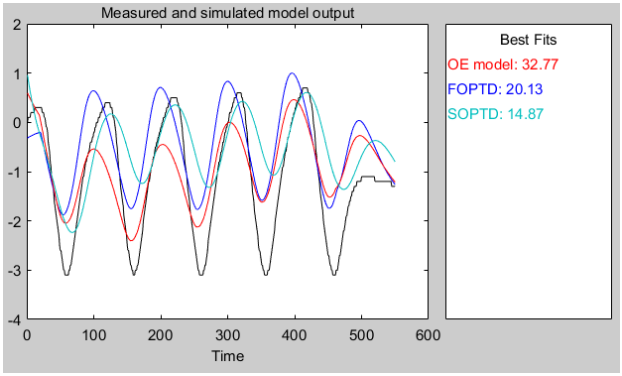

(b) Fitness of identified models with closed loop data for validation

Figure 11.6: Input-Output $A_v - P_2$
SISO FOPTD, SOPTD, Output-Error models identified and validated with closed loop data

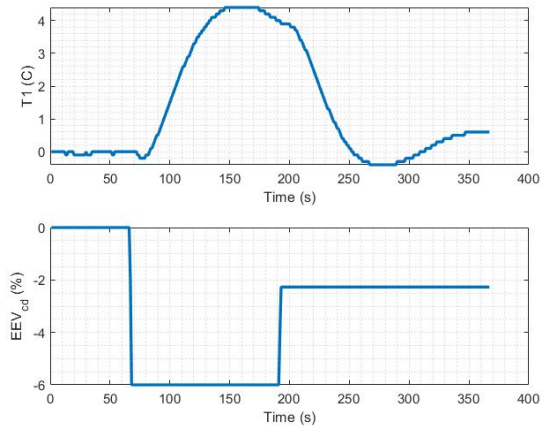

(a) Open loop Input-Output $EEV_{cd} - T_1$

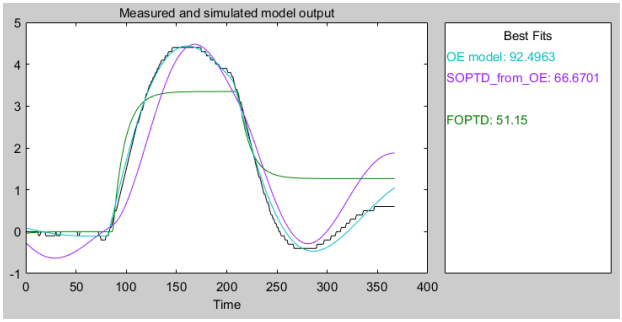

(b) Fitness of identified models with open loop data for validation

Figure 11.7: Input-Output $EEV_{cd} - T_1$
SISO FOPTD, SOPTD, Output-Error models identified and validated with open loop data

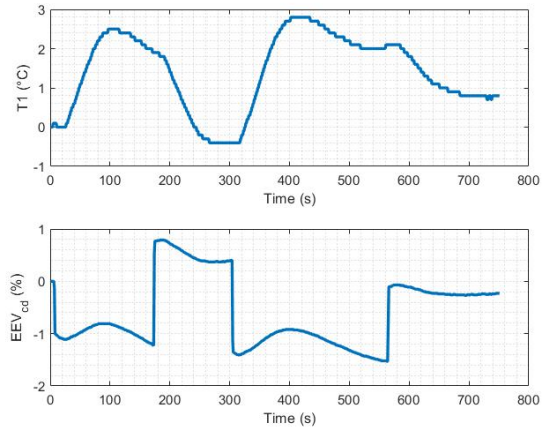

(a) Closed loop Input-Output $EEV_{cd} - T_1$

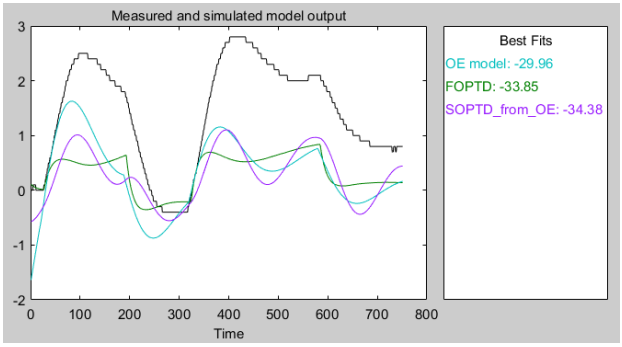

(b) Fitness of identified models with closed loop data for validation

Figure 11.8: Input-Output $EEV_{cd} - T_1$
SISO FOPTD, SOPTD, Output-Error models identified and validated with closed loop data